

South Dakota State University

## Open PRAIRIE: Open Public Research Access Institutional Repository and Information Exchange

---

Electronic Theses and Dissertations

---

2017

### Design, Synthesis and Biological Evaluation of Novel Estradiol-Triazole Analogs Targeting Epidermal Growth Factor Receptors in Colorectal Cancer

Faez Alotaibi  
South Dakota State University

Follow this and additional works at: <https://openprairie.sdstate.edu/etd>

 Part of the [Chemistry Commons](#)

---

#### Recommended Citation

Alotaibi, Faez, "Design, Synthesis and Biological Evaluation of Novel Estradiol-Triazole Analogs Targeting Epidermal Growth Factor Receptors in Colorectal Cancer" (2017). *Electronic Theses and Dissertations*. 1189.

<https://openprairie.sdstate.edu/etd/1189>

This Thesis - Open Access is brought to you for free and open access by Open PRAIRIE: Open Public Research Access Institutional Repository and Information Exchange. It has been accepted for inclusion in Electronic Theses and Dissertations by an authorized administrator of Open PRAIRIE: Open Public Research Access Institutional Repository and Information Exchange. For more information, please contact [michael.biondo@sdstate.edu](mailto:michael.biondo@sdstate.edu).

DESIGN, SYNTHESIS AND BIOLOGICAL EVALUATION OF NOVEL  
ESTRADIOL-TRIAZOLE ANALOGS TARGETING EPIDERMAL GROWTH  
FACTOR RECEPTORS IN COLORECTAL CANCER

BY

FAEZ ALOTAIBI

A thesis submitted in partial fulfillment of the requirements for the

Master of Science

Major in Chemistry

South Dakota State University

2017

DESIGN, SYNTHESIS AND BIOLOGICAL EVALUATION OF NOVEL  
ESTRADIOL-TRIAZOLE ANALOGS TARGETING EPIDERMAL GROWTH  
FACTOR RECEPTORS IN COLORECTAL CANCER

FAEZ ALOTAIBI

This thesis is approved as a creditable and independent investigation by a candidate for Master of Science in Chemistry degree and is acceptable for meeting the thesis requirements for this degree. Acceptance of this does not imply that the conclusions reached by the candidate are necessarily the conclusions of the major department.

Fathi T. Halaweish, Ph.D.  
Thesis Advisor

Date

Douglas Raynie, Ph.D.  
Head, Department of Chemistry  
and Biochemistry

Date

Dean, Graduate School

Date

To My Family, Friends, and Country.

## ACKNOWLEDGEMENTS

I would like to gratefully acknowledge many people in my life who have supported me in my pursuit of my higher education. First, I would like to thank my father and my mother for their support, patience, love and answered prayers. I would like to thank my two brothers, who have been supportive to my dreams and passion. I also would like to thank my lovely sister who always been a believer in me.

I would like to thank my advisor Dr. Fathi Halaweish for opportunity to work in his group. I would like to thank him for his patience, guidance and support to accomplish this project. I would like also to thank Dr. Halawesih's Group.

Many thanks to my advisory committee, Dr. Zhang Cheng, Dr. Michael Dianovsky, and Corey Shelsta for their support.

Finally, I would like to thank Qassim University, Saudi Arabia, for their academic support and financial support.

## CONTENTS

ABSTRACT.....	ix
CHAPTER ONE.....	1
General Introduction and Background.....	1
1.1. Natural Products as a Drug Discovery Tool.....	1
1.2. Click Chemistry as a New Tool in Organic Synthesis.....	2
1.2.1. Mechanism of Azide-Alkyne Cycloaddition Utilizing Copper as a Catalyst.....	4
1.2.2. Mechanism of Azide-Alkyne Cycloaddition Utilizing Ruthenium as A Catalyst.....	6
1.3. Azide-Alkyne Cycloaddition Conditions.....	7
1.3.1. Solvents.....	7
1.3.2. Catalyst.....	8
1.3.3. Azide and Alkyne Substrate.....	8
1.4. Utilization of Click Chemistry and Natural Pharmacophore in Drug Design and Modeling.....	9
1.5. Molecular Docking.....	11
1.5.1. Scoring Overview.....	12
1.5.2. Types of Scoring Functions.....	13
1.5.3. Docking Drawbacks.....	14
1.6. Role of The Epidermal Growth Factor Receptor in The Treatment Of CRC.....	15
1.7. Colorectal Cancer Diagnosis.....	17
1.7.1. Colorectal Cancer Stages and Treatment.....	17
1.7.1.1. 5-Fluorouracil Chemotherapy.....	19
1.7.1.2. Oxaliplatin.....	20
1.8. Examples of Biologically Active 1,2,3-Triazoles.....	21
1.8.1. Anti-Cancers.....	21
1.8.2. HIV Protease Inhibitors.....	22
1.8.3. Antituberculosis inhibitors.....	23
1.8.4. Antifungals and Antibacterials.....	24
1.9. References.....	25
Chapter Two.....	35

Design of 1.4-Disubstituted 1.2.3triazoles Targeting Epidermal Growth Factor Receptors (EGFRs) .....	35
2.1. Introduction .....	35
2.2. Molecular Modeling and Rational Design of 1,2,3-Triazol Bearing Inhibitors.....	37
2.2.1. Protein Kinases .....	37
2.2.1.1. Methods of Molecular Modeling .....	37
2.2.1.2. Molecular Modeling of 2-D and 3-D Structures .....	38
2.3. Utilization of OMEGA to Generate Structural Conformers.....	38
2.3.1. Utilization of FRED to Prepare the Receptors .....	39
2.3.2. Conducting Docking Using FRED .....	40
2.4. Results and Discussion.....	41
2.4.1. Result and Discussion of Molecular Modeling with EGFR .....	45
2.4.2. Result and Discussion of Molecular Modeling with RAF receptors.....	50
2.4.2.2. Result and Discussion of Molecular Modeling with 3OMV.....	52
2.4.3. Result and Discussion of Molecular Modeling with MEK.....	56
2.5. Summary of the mode of action in the selected receptors.....	58
2.6. Conclusion.....	60
2.7. References .....	60
Chapter Three.....	73
Design, Synthesis and biological evaluation of novel estrone -1.4-disubstituted triazoles analogs targeting colorectal cancer .....	73
3.1. Introduction .....	74
3.2. Material and methods .....	76
3.2.1. General material and methods.....	76
3.3. Result and discussion .....	77
3.3.1. Synthesis of 17 $\alpha$ alkynyl estradioils .....	77
3.3.2. Synthesis of organic azides .....	81
3.4. Conclusion .....	84
3.4.1. Future work and Recommendations .....	85
3.5 Experimental section.....	85
3.5.1. 3-OTBS protected estrone (2).....	85
3.5.2. 17 $\alpha$ ethynyl estradioil (3).....	86

3.5.3. Ethynyl estradiol-3-methyl ether (Mestranol) (4) .....	87
3.5.4. Ethynyl estradiol-3-methyl benzyl ether (5).....	88
3.5.5. ethynyl estradiol-3-acetate (6).....	88
3.5.6. 2-chloro-N-(4-methoxyphenyl)acetamide (7) .....	89
3.5.7. 2-chloro-N-(p-tolyl)acetamide (8).....	89
3.5.8. 2-chloro-N-phenylacetamide (9) .....	90
3.5.9. 2-chloro-1-morpholinoethan-1-one (10).....	91
3.5.10. 2-chloro-1-(piperidin-1-yl)ethan-1-one (11) .....	91
3.5.11. 2-chloro-1-(1H-indol-1-yl)ethan-1-one (12) .....	92
3.5.12. 2-azido-N-phenylacetamide (7b).....	93
3.5.13. 2-azido-N-(p-tolyl)acetamide (8b) .....	93
3.5.14. 2-azido-N-(4-methoxyphenyl)acetamide (9b)..	94
3.5.15. 2-azido-1-morpholinoethan-1-one (10b) .....	94
3.5.16 2-azido-1-(piperidin-1-yl)ethan-1-one (11b).....	95
3.5.17 2-azido-1-morpholinoethan-1-one (12b) .....	96
3.5.18. Estra-17-(1H-1,2,3-triazol-1-yl)-N-phenylacetamide)diol (13)(FZ60) .....	96
3.5.19. Estra-17-(1H-1,2,3-triazol-1-yl)-N-phenylacetamide)diol (14)(FZ300) .....	97
3.5.20. Estra-17-(1H-1,2,3-triazol-1-yl)-N-phenylacetamide)diol (15)(FZ313) .....	98
3.5.21. Estra-17-(1H-1,2,3-triazol-1-yl)-N-phenylacetamide)diol (16)(FZ518) .....	99
3.5.22. 3- Omethoxy estra-17-(1H-1,2,3-triazol-1-yl)-N-phenylacetamide)diol (17)(FZ 516) .....	100
3.5.23. 3-Oacetate estra-17-(1H-1,2,3-triazol-1-yl)-N-phenylacetamide)diol (18)(FZ514) .....	101
3.5.24. Estra-17 1H-1,2,3-triazol-1-yl)-1-(piperidin-1-yl)ethanone (29)(FZ600)..	102
3.5.25. 3-OAcetate estra-17 1H-1,2,3-triazol-1-yl)-1-(piperidin-1-yl)ethanone (20)(Fz550) .....	103
3.5.26. Estra-17 1H-1,2,3-triazol-1-yl)-1-(morpholen-1-yl)ethanone (26)(FZ100)	104
3.5.27. 3-Obenzyl Estra-17 (1H-1,2,3-triazol-1-yl)-N-phenylacetamide (22)(FZ57) .....	105
3.5.28. 3-Obenzyl Estra-17 (-1H-1,2,3-triazol-1-yl)-N-p-tolylacetamide (23)(FZ400) .....	106
3.5.29. 3-metoxy estra-17 1H-1,2,3-triazol-1-yl)-1-(piperidin-1-yl)ethanone (24)(FZ552) .....	107

3.5.30. 3-OAcetate estra-17 (1H-1,2,3-triazol-1-yl)-N-phenylacetamide (25)(FZ200) .....	108
3.5.31. 3-Obenzyl Estra-17 (-1H-1,2,3-triazol) (26) (FZ25) .....	109
3.6. References .....	110

## ABSTRACT

DESIGN, SYNTHESIS AND BIOLOGICAL EVALUATION OF NOVEL  
ESTRADIOL-TRIAZOLE ANALOGS TARGETING EPIDERMAL GROWTH  
FACTOR RECEPTORS IN COLORECTAL CANCER

FAEZ ALOTAIBI

2017

Colorectal cancer is a life threatening and second cause of death from cancer in the United States. Several proteins (molecular targets) are highly expressed in Colorectal cancer (CRC). Among these molecular targets is Epidermal Growth Factor Receptors (EGFRs) which are overexpressed in cancer cells. Targeting and blocking the downstream signaling could lead to cease cell proliferation and division and hence control the spread of the disease. Molecular modeling is a powerful tool in drug discovery, which has been utilized to design many drug candidates that exhibit biological effect in many disease including cancer. Additionally, pharmacophores such as 1,2,3-triazole showed potency towards many diseases including cancer. Therefore, incorporation of 1,2,3-triazole on a carrier such as estradiol could lead to novel analogs in drug discovery for treatment of cancer. A library of 800 compound containing 1,2,3-triazole-estradiol analogs were designed and virtually screened with seven molecular targets belong to EGFRs utilizing OpenEye® software. Among the designed candidates, fourteen of estradiol-triazole analogs were synthesized and biologically evaluated. Antiproliferation/cytotoxicity assay conducted on CRC cancer cell line (HT-29) showed that 5 out 14 analogs demonstrated potential antiproliferation activities ranging from 3.5  $\mu\text{M}$  to 30  $\mu\text{M}$  in comparison to a chemotherapeutic agent 5-flurouracil (5-FU) ( $\text{IC}_{50}$  17.3  $\mu\text{M}$ ) which is a standard drug for CRC.

## CHAPTER ONE

### General Introduction and Background

#### 1.1. Natural Products as a Drug Discovery Tool

Humans rely on natural sources for many purposes, such as energy sources, food and medicine. Particularly the natural sources for medicines had the greatest impact on humans lives and prosperity. Therefore, it kept the interest of humans growing and evolving until it has shaped a massive industry known today as pharmaceuticals. At the early ages of pharmaceutical companies, it was the standard procedure to use the crude extract to generate relatively crude therapeutic formulations until the mid-twentieth century when the separation techniques were developed and became of great help for purification of extracts [1-3]. In the realm of cancer and infections it is estimated that 60% and 70% respectively of the drugs discovered and marketed are isolated from natural sources.

The natural sources of drugs varies from plants, microorganisms, and animals, among of which the marine natural products, can be marine plants, microorganisms or animals, became the trend of drug discovery as the products isolated usually have enormous diversity and multiple functionality in addition to complexity. Natural products normally carry a group of atoms that are responsible of biological activity, this group of atoms called pharmacophores. Pharmacophores can react with molecular targets, such as receptors, utilizing multiple interactions and forces and hence cause certain biological response. Therefore, pharmacophores have been used as fingerprints for certain proteins utilizing qualitative and quantitative structure activity relationships as well as virtual

screening [4]. For example, one technique becoming popular in drug design is modeling of pharmacophore-based ligands with molecular targets under investigation to identify hits compounds that can be later optimized to become drug candidate. This technique is called ligand-based pharmacophore modeling [5]. Furthermore, pharmacophores significance can also be observed in another modeling technique, which called structure-based pharmacophore modeling, in which the modeling process deals with the 3D structure of the molecular target under investigation and/or the 3D structure of the molecular target complex with the ligand. This technique can map the interactions with the macromolecule and express these interactions as number of hydrogen bond acceptors, donors and hydrophobic interaction with the binding site of the macromolecule [4, 5]. To illustrate more, a pioneer study conducted by Zou et al., have established a map of all of the important interactions between Cyclin-dependent kinase CDK, a highly expressed protein in cancer, and 124 inhibitors and hence established a comprehensive pharmacophore for their CDK macromolecules under investigation [6].

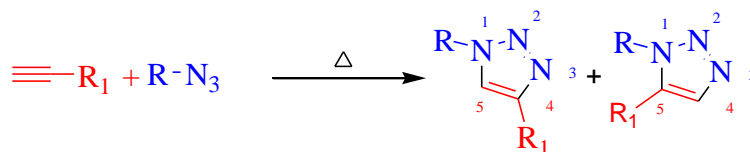
To sum it up, natural products pharmacophores became successful trend in drug discovery and contributed with tremendous effort toward the progress of the pharmacophore modeling techniques as well as chemoinformatics, which made it a powerful tool in drug discovery approaches today[5, 7].

## 1.2. Click Chemistry as a New Tool in Organic Synthesis

In 2001 K.B Sharpless reported a class of reactions that are rapid, wide in scope, easy to perform and high yielding. These reaction was named later as “click chemistry reactions” and the demanding pharmaceutical industry has triggered the grow of this class of reactions in a way that allow synthetic chemist to synthesize a library of compounds and

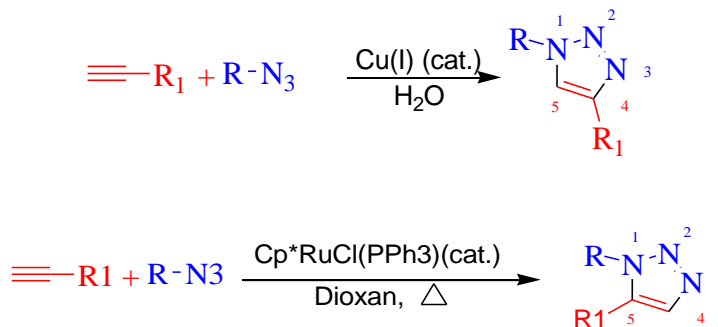
screen them on a macromolecule of interest as a reliable method for drug discovery. Although click chemistry can describe many reactions including nucleophilic ring opening, formation of heterocyclic compounds and hydrazones from ketones and reaction of aziridine and epoxides; however, thermal cycloaddition, especially Huisgen 1,3 dipolar reactions, have been widely investigated in click chemistry [8].

Huisgen reaction is classified as cycloaddition reaction that occur between a 1,3-dipolar and dipolarophile **Scheme 1.1**. The result of this reaction is a five-membered heterocyclic ring. In this reaction, there is a critical need for elevated temperature for the reaction to occur and the resulting compound lack regioselectivity [8].



**Scheme 1.1.** Huisgen 1,3-dipolar reaction lacks selectivity.

The lack of regioselectivity indicates that the reaction has different mechanism pathways that result in different products. To control the regioselectivity, K. B. Sharpless reported optimized conditions, most importantly, the catalyst in use significantly affect the product obtained from the cycloaddition. To illustrate more, the use of copper sulfate ( $\text{CuSO}_4$ ) or copper sulfate pentahydrate ( $\text{CuSO}_4 \cdot 5\text{H}_2\text{O}$ ) can direct the reaction to the pathway that result in 1,4-regioselectivity. On the other hand, ruthenium catalyzed click reactions direct the azide-alkyne cycloaddition to the 1,5-regioselectivity. Below **scheme 1.2** explains how the 1,3-dipolar cycloaddition became selective and efficient based on the condition used.



**Scheme 1.2.** The azide-alkyne cycloaddition exhibits regioselectivity based on the catalyst.

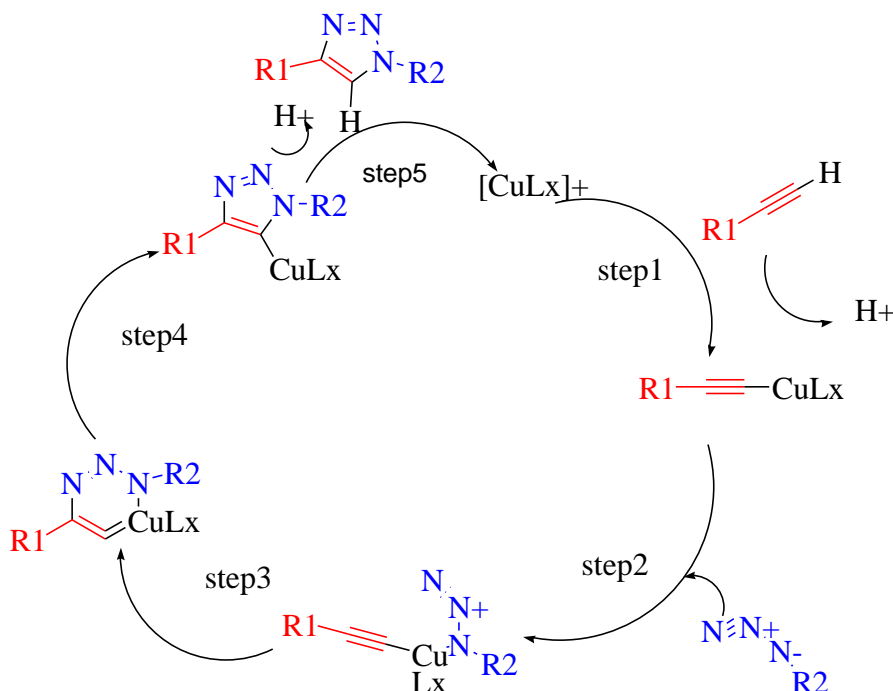
Besides the catalyst, the solvent in use gave the click chemistry a great advantage. Click reactions can be performed in a media of water in addition to an organic solvent in different ratio. In addition to the reaction conditions, in case of  $\text{Cu}^{2+}$  is used as a catalyst, a reducing agent must be used to allow copper to catalyze the reaction. In other words, the reducing agent convert  $\text{Cu}^{2+}$  to  $\text{Cu}^+$ , a necessary species to catalyzed the reaction. Click chemistry reactions are varies now in conditions since the outstanding efforts of K. B. Sharpless.

#### 1.2.1. Mechanism of Azide-Alkyne Cycloaddition Utilizing Copper as a Catalyst

In contrast to 1,3-dipolar cycloaddition, utilizing click chemistry reaction conditions, especially the catalyst, can accelerate the rate of the azide-alkyne cycloaddition [9]. The rate accelerated is measured in  $10^7$  to  $10^8$  unites. In addition, utilizing these conditions can tolerate many functional groups, wide range of pH and aqueous media. Evidence obtained from real-time monitoring of the cycloaddition between azide and alkyne utilizing heat-flow reaction calorimetry explicitly indicate that monomeric copper acetylide complexes does not appear to be reactive toward organic azides unless an exogenous copper in a catalyst form is added. Moreover, isotopically enriched exogenous

copper source experiments showed that the carbon–nitrogen bond-formation has a stepwise nature and the equivalence of the two copper atoms must be obtained to pursue the cycloaddition steps [9, 10]. Kinetic studies conducted by Fokin et al., 2013 show that the pKa of alkyne is lowered in the process of the alkyne coordination by 10 folds, which explains the deprotonation of the alkyne-Cu<sup>I</sup> intermediate without using any base but water itself, in aqueous medium conditions. [8, 9]. In addition, kinetic studies also indicate that the rate of the reaction is second order in presence of Cu<sup>I</sup> even at low concentration and formation of less reactive copper aggregates at higher concentrations [10].

The mechanism of the cycloaddition starts from the catalyst Cu<sup>+</sup> which can be generated from Cu<sup>2+</sup> salts using sodium ascorbate as reducing reagent, Cu<sup>+</sup> can be used directly, once Cu<sup>+</sup> is generated, a  $\sigma$ -bond copper acetylide is formed, and a  $\pi$ -bound copper to the azide moiety is formed as well [9, 10]. Consequently, an metallacycle constructed of six membered ring is formed. This step brings the azide and the alkyne together utilizing one copper atom and the  $\pi$ -bonded copper acts as stabilizing donor ligand. The following step is crucial as the aromaticity of triazolyl ring begins to form, triggered by ring contraction. Finally, the catalytic cycle is closed by the protonolysis which achieves the final 1,4-substituted triazole, **Scheme 1.3** explains in detail the mechanistic pathway of the 1,4- regioselective click reaction utilizing Copper as a catalyst [10].

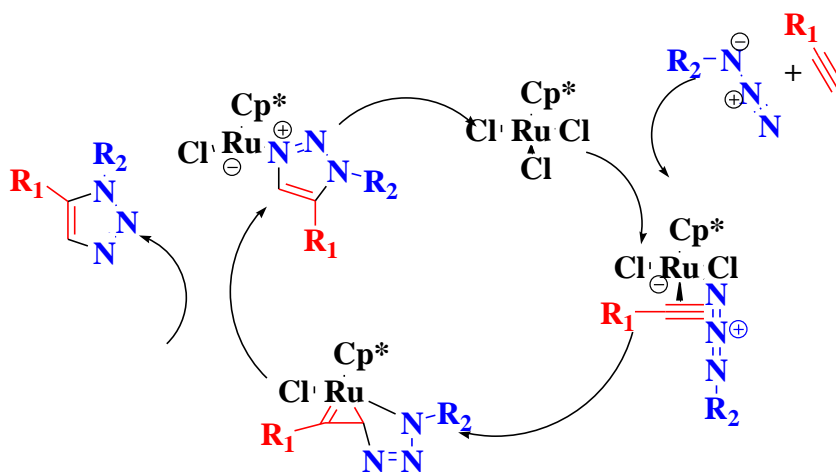


**Scheme 1.3.** The mechanistic route for the synthesis of 1,4-disubstituted triazole. the mechanistic route for the synthesis of 1,4-disubstituted triazole.

### 1.2.2. Mechanism of Azide-Alkyne Cycloaddition Utilizing Ruthenium as A Catalyst

The presence of ruthenium as a catalyst has significant effect on the formation of triazole product. It is regioselective only to one form of isomer, 1,5-substituted triazole, thus different pathway of the reaction mechanism must have been taken to offer this class of regioisomer. Studies suggest that first step of the mechanism of the reaction starts when the oxidative coupling between azide and alkyne occur to offer a six-membered ring where ruthenium is being placed next to the most electronegative carbon of the alkyne which allow the carbon to bond with the electrophilic nitrogen atom i.e. first nitrogen atom. followed by reductive elimination to form the desired regioselective product of triazole [10, 11]. Density functional theory (DFT) calculations suggest that the reductive

elimination step is the rate determining step of this mechanistic pathway. **Scheme 1.4** shows the mechanistic route for the synthesis of 1,5-disubstituted triazole [11].



**Scheme 1.4.** The mechanism of 1,5-disubstituted utilizing ruthenium as a catalyst.

It is worth to point out that the catalyst in use has impact the course of the reaction, however the rest of the reaction conditions are wide in scope.

### 1.3. Azide-Alkyne Cycloaddition Conditions

#### 1.3.1. Solvents

The most remarkable feature of Copper Alkyne-Azide Cycloaddition CuAAC is the variety of solvents used in the reaction. The solvent conditions are numerous including, polar solvents such as alcohols, acetone, acetonitrile, dimethyl sulfoxide DMSO, and dimethyl formamide DMF, non-coordinating solvents such as dichloromethane, chloroform, toluene, weakly coordinating solvents such as dioxane, tetrahydrofuran THF and pyridine, and aqueous solvents including mixtures of water with an organic solvent

such as alcohols. It is worth to mention that DMF is the most optimal solvent for CuAAC reactions especially when the  $\text{Cu}^{\text{I}}$  is introduced as CuBr without any additional ligand, as DMF cannot coordinate with  $\text{Cu}^{\text{I}}$ , hence will not lead to slow reaction or inert reaction [12, 13].

### 1.3.2. Catalyst

A wide ranges of Copper compounds were tested as catalysts and pre-catalysts including  $\text{Cu}^{2+}$ ,  $\text{Cu}^{1+}$  and  $\text{Cu}^0$ . In all cases  $\text{Cu}^{1+}$  must be generated to catalyze the CuAAC, if not began with, in addition,  $\text{Cu}^{1+}$  concentration must be in its highest to assist the progress of the reaction. Many pre-catalysts were used in the investigation of the catalyst of CuAAC, for example,  $\text{Cu}^{2+}$  salts were used and  $\text{CuSO}_4$  is the most popular form of  $\text{Cu}^{2+}$ . Furthermore,  $\text{Cu}^{1+}$  salts, commonly CuBr Or CuOAc, can be used directly in the reaction with amine ligand or a base to prevent the aerobic oxidation to  $\text{Cu}^{2+}$ . Finally,  $\text{Cu}^0$  can be used as a pre-catalyst in form of powder, wire and nanoparticles [10, 11, 13].

### 1.3.3. Azide and Alkyne Substrate

Generally, stereoelectronic effects can significantly impact the rate of reactions; However, in CuAAC reactions, the effect can be generalized fairly in terms of azide and alkyne substrates, to illustrate, Matyjaszewski has reported the impacts of electronic and steric effects on the reaction rate and conclude that the fastest rate was observed when the azide substrate has electron-withdrawing groups and has a minimum steric hindrance, on the other hand, alkynes with  $\alpha$ -carbonyl group was observed to have higher activity than alkynes with alkyl groups. Multiple azides on one substrate were also investigated for their reaction rates and were found that when the azides are held in proximity, the rate enhancement was disclosed unlike when multiple alkynes were held in proximity. It is

worth to mention that iodoalkynes were found to be more reactive than terminal alkynes [13, 14]

It is worth to state that the advances of click chemistry allowed chemists to design a variety of compounds libraries that are wide in scope, and then access the designed library by applying the synthetic approach established by K.B. Sharpless.

#### 1.4. Utilization of Click Chemistry and Natural Pharmacophore in Drug Design and Modeling

Estrogens as a natural product compounds are biologically synthesized by the human body through multiple processes starting from cholesterol as starting material [15]. Among of estrogen class of compounds are estrone and estradiol, which are identified pharmacophores for the estrogen receptors ER [16]. Furthermore, many investigations in the estrone-based designed drug candidates have shown potency towards cancer cells such as ovarian, prostate and breast cancer [17-19]. Among these investigations, a study conducted by Ahmad et al., 2014 established a pharmacophore of cucurbitacin D, a naturally occurring compound, on estrone as carrier skeleton for the side chain that is responsible for the biological activity [17]. Around these facts, a hypothesis was developed assuming that utilizing click chemistry to generate a triazole pharmacophore carried by a steroidal skeleton may lead to discovery of novel drug candidates. This assumption was backed by findings obtained by Solum et al., 2014, in tubulin polymerization inhibition utilizing and cytotoxic effect of estradiol-triazole moieties [19].

In the literature, many researchers used the same approach to discover new drug candidates; for example, a number of steroidal moieties bearing triazole pharmacophore were tested for the inhibition of human CYP17 targeting prostate cancer [20]. Another

example of utilizing the same approach is observed in incorporation of triazole pharmacophore on progesterone, another steroidal hormone, on position 11 by Dhyania et al., with uptakes ranging from  $5 \pm 0.6$ - $35 \pm 2.3$  % in MCF-7 and HT-29 cells (breast cancer cells)[21, 22]. Investigations on the triazole pharmacophore were done by many scientists; for example, Kharb et al., have reported the pharmacological profile of triazole derivatives with an updated research findings in the discovery of antifungal lead compounds within last ten years [22, 23]. On the other hand, Sheng and Zhang reported the structure–activity relationship (SAR) of antifungal lead compounds and possibility for future antifungal drug discovery [22, 24]. It is explicitly observed that 1,2,3-triazoles are more seen in comparison to 1,2,4-triazoles in medicinal chemistry field, including drug discovery utilizing computational methods, DNA labeling, bioconjugation, and selective modification of enzymes.

The reason relies behind these various applications is due to the fact that this sequence of nitrogen atoms is readily binds with molecular targets through hydrogen bonds and or dipole interactions, which lead to solubility. Another interesting feature of 1,2,3-triazoles is that they are staple to metabolic degradation which can ensure that the binding with molecular targets is affordable [22]. To sum it up, incorporation of triazole pharmacophore on the modified estradiol skeleton could lead to a drug candidate discovery.

The potential of pharmacophore screening in drug discovery encouraged scientists to utilize in-silico studies to design novel analogs. To illustrate this point, a summary of molecular modeling will be illustrated here.

### 1.5. Molecular Docking

Molecular docking is very broad topic in the process of drug discovery. Since the pharmaceutical industry is growing exponentially, the need of an accurate tool and a feasible approach is critical. Molecular modeling is used to predict the behavior and performance of every single atom and molecular target in order to anticipate the results of the synthetic strategies and conclude the mechanistic pathways by anticipation of transition state models. In addition, molecular modeling methods can be used to anticipate the behavioral characteristic of molecules toward receptors, enzymes and proteins under investigation to further enhance the efficacy of ligand-macromolecule binding which is reflected on the potentials of drug candidates [25-27]. Molecular docking is greatly appreciated as it is a powerful tool that can predict the physio-chemical parameters of ligand, such as absorption, distribution, metabolism, and toxicity utilizing many softwares and applications.

Computational approaches became of great help in drug discovery since 1980s. Popular computational methods including structure based drug design, ligand based drug design, structure activity relationship (SAR), quantitative structure activity relationship (QSAR) and protein binding sites determination are very crucial component in computational methodologies, in all of which, small molecule need to be docked to protein binding sites. this is simply referred to as molecular docking [27]. Docking can be utilized at different levels of drug discovery and when the crystallography of molecular target is well described, high-throughput docking can be used to identify hits for the molecular target. In that sense, the aim of docking is to predict and anticipate the binding affinity of a ligand with the active site of the molecular target. These binding affinities are based on

the arrangement, positions, and conformational structures of ligand on the binding pocket of the molecular target. Since docking can lead to a discovery of pharmacophore or a template for molecular targets, receptors for example, it is considered logical and affordable tool [26].

#### 1.5.1. Scoring Overview

There are three basic data representations of the receptor, surface, atomic and grid. They are representing the significance of protein-ligand interaction. Because of the computational complexity of atomic interaction calculations, the ranking procedures of atomic representation is utilized with promising energy function. In case of protein-protein docking, surface-based docking is used. In many docking programs, potential energy grids are used to calculate the energy. Grid-based methodologies utilize grid points to collect electrostatic potentials in addition to Van der Waals potentials [28]. The term search algorithms refer to the algorithm used to calculate the ligand flexibility and inferior quantity of receptor flexibility. Dealing with ligand flexibility is classified into 1) simulation methods 2) random, and 3) systematic. Simulation-based search methods are usually depending on the simulation of molecular dynamics. Since the main limitation of initiation of flexibility is the rely on higher energy barriers; the simulations will not pass the high-energy barriers in efficient time period. Therefore, protein flexibility is less efficient than ligand flexibility [27].

Alternatively, random-based search methods are simply make multiple alterations on the ligand to sample some degree of freedom. An example of random based-search methods is Monte Carlo & genetic algorithms. Lastly, systematic-based search methods are attempting to seek degree of freedom in molecule. Systematic search also can use rigid

structure that been pre-generated with diverse conformational poses (as openeye® employs). The computational expense in this method is reduced due to the performance of this method, in which the conformations are calculated first at once [28].

It is worth to point out that the advances of molecular modeling paved the way to use this technique in drug discovery.

### 1.5.2. Types of Scoring Functions

The aim of scoring functions is to effectively calculate and measure the  $\Delta G$  of the complex binding results from the interaction between the ligand and the receptor. These calculations and measurements are considered expensive, therefore, many speculations are made in sake of the completion of these calculation and measurement in a reasonable time manner [27]. Scoring function can be classified in three types, force field based, empirical based and lastly knowledge based [27, 29]. In the force field scoring, the molecular mechanics consider the sum of two energies. That means, the sum of the energy of receptor-ligand interactions, and the energy of internal ligand. In general, many of force field scoring functions are designed for single protein. for that reason, it is reasonable to remove the thermal protein energy calculations [26, 27, 29]. Force filed scoring functions are based on many parameters such as, MMFF94, AMBER, OPLS-AA and tripos force field. Van der Waals and electrical static energy can be used as well to describe the ligand-receptor interactions. Furthermore, Lennard-Jones potential function is used to describe Van der Waals energy. While coulombic formulations are used to describe the electrostatic terms. These coulombic formulations are usually with distance-dependent dielectric function, which limits the contribution resulting from charge-charge interactions [26, 27, 29].

Empirical scoring functions are based on the sum of many terms. Mainly, experimental data regarding the calculated value of binding affinities and the calculated value of binding energies, As well as the x-ray crystal structures are utilized to calculate the coefficients of these terms. Not only binding energy can be utilized in scoring functions, but also experimental 3-D structural databases can also be utilized too. In this sense using the simple potentials of atomic interactions, protein-ligand complex can be modeled [27].

Computational simplicity and efficacy are the most important feature of these scoring functions. These features particularly made screening of large numbers of analogs more efficient. However, because of the conclusion of scoring functions is based on the information obtained from the limited sets of protein-ligand structures, it is not accurate to assume that a single scoring function can fit for all types of interactions of the protein-ligand complexes. Therefore, combining the collected data from these different scores, which is known as consensus scoring is frequently used as consensus scoring balance the errors resulting from each single score. The advantage of consensus scoring is clearly observed in its ability to increase the percentage and ranking of the hit in comparison to the entire library in docking process [27, 29-32].

To sum up, modeling is a powerful tool that can be used to determine the potential analogs, which can be optimized to enhance the biological screening in order to evaluate the synthesized analogs.

### 1.5.3. Docking Drawbacks

Docking limitations basically come from the accuracy of the prediction of enthalpic and entropic effects. In addition, the conformational alterations during binding as well as the crystallography structure are playing major effects. Because of that, docking and

scoring are usually build up from many processing steps. Initially it begins with placing a molecule, ligand, into the binding pocket of the receptor. This placing must take in consideration the optimal interactions with the receptor, subsequently, the optimal interaction will be evaluated based on certain calculation, this process is known as scoring function, which is eventually tell the difference in terms of affinity of the library of ligands [31].

#### 1.6. Role of The Epidermal Growth Factor Receptor in The Treatment Of CRC

Epidermal growth factor receptor (EGFR) is a member of tyrosine kinase receptors family, which consists of EGFR (erbB1/Her1), Her2/neu (erbB2), Her3 (erbB3), and Her4 (erbB4). EGFRs have a natural ligand, which is the epidermal growth factor (EGF) [33]. EGFR consists of three domains, an extracellular ligand-binding domain, a cytoplasmic tyrosine kinase domain and lastly a single membrane-spanning region (Alroy and Yarden, 1997; Normanno et al., 2006) [34, 35]. The ligand, as a stimulating factor, binds specifically to the extracellular domain leading to receptor homo- or hetero-dimerization, which promotes conformational change of the intracellular phosphorylation components, which enables the downstream signaling [36]. The downstream signaling cascades has many pathways including RAS-RAF-MAP kinase pathway **Figure 1.1** [35], the phosphatidyl inositol 3-kinase (PI3K) and the Akt pathway (Burgering and Coffey, 1995) [37, 38]. These signaling pathways contribute in cell survival, activation, cycle, proliferation, and angiogenesis [39, 40].

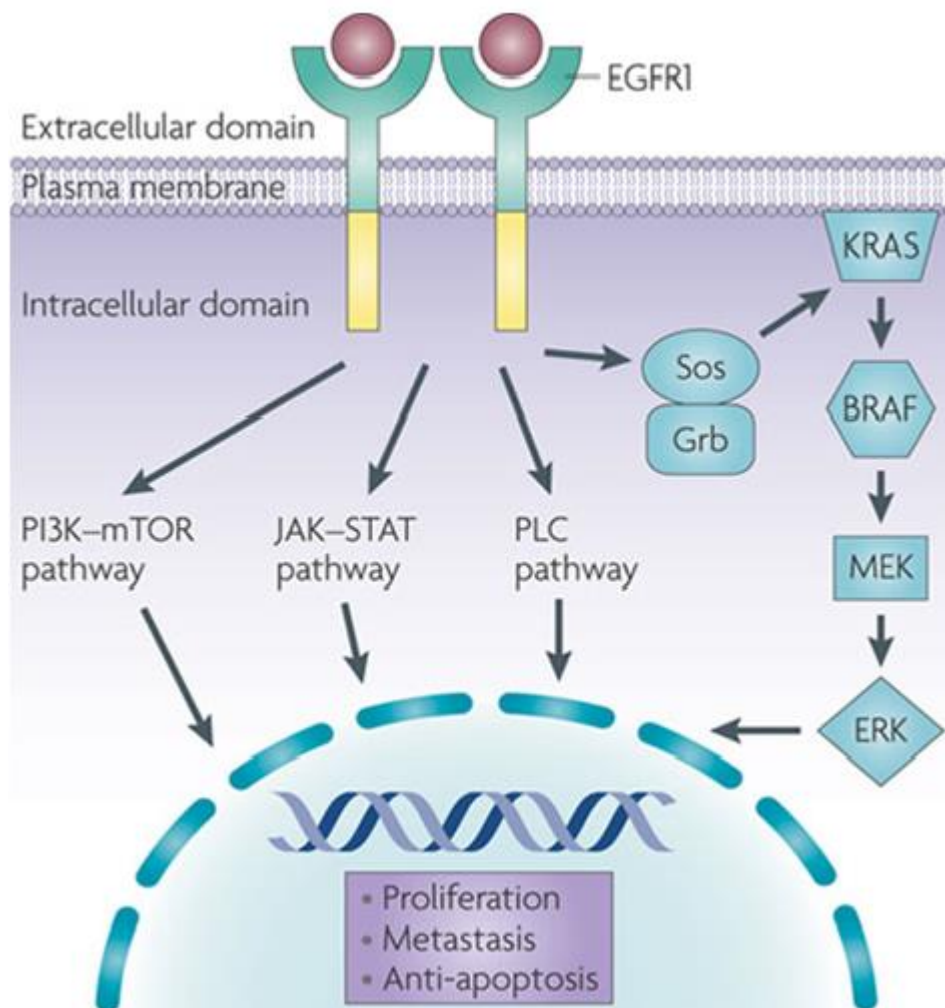


**Figure 1.1.** The EGFR signaling pathway overexpressed in CRC.

The significance of EGFRs stimulation pathways is relying behind the fact that it promotes tumor cell motility, metastasis and adhesion [41]. In that sense, there is no doubt that this led scientist to investigate more in EGFR inhibitors and come up with many EGFR inhibitors including cetuximab, panitumumab (both are FDA approved treatment for metastatic colorectal cancer (mCRC)), as well as erlotinib and gefitinib, which are another example of anti-EGFR tyrosine kinase inhibitors (TKIs) for the treatment of other malignancies [42].

## 1.7. Colorectal Cancer Diagnosis

Around the world, colorectal cancer detection is the main challenge that faces physicians. Therefore, many physicians recommend certain screening tests for people with no signs or symptoms of colorectal cancer, to ensure the health status of individuals. According to Sidney et al., these screening tests are of great advantage in diagnosis of colorectal cancer at early stages, which helps to treat the disease and to reduce the risk of dying [43]. Screening tests should be considered for the people at age 50 since it is the age of highest risk. While people of hereditary history of the disease should consider screening test sooner. In addition, African-American as well as native American should consider these tests at age 45 [43-45]. These screening test are primarily centered on colonoscopy, which is a flexible long slender tube attached to a camera that is inserted to the body to look at the colon and rectal areas as well [44]. It is important to notice that CRC diagnosis enable to classify CRC stage and consequently lead to determine therapy regimens.

### 1.7.1. Colorectal Cancer Stages and Treatment

Patients diagnosed with colorectal cancer will be asked to preform serval tests to show the extent of the cancer stage in a procedure known as stage diagnosis. Physicians use this staging diagnosis to decide which treatment is suitable with the disease. The process of staging diagnosis includes imaging techniques such as abdominal and chest CT scans [46]. According to tumor, node, metastasis system (TNM) colorectal cancer is classified into four stages. In stage I, cancer has grown through the mucosa of colon or rectum but did not spread out of this region. In this stage, the better treatment would be surgery, in which cancer tumor can be removed from the body. Stage II colorectal cancer means that the cancer cell has not spread to other lymph although it has spread and grew

through the colon or rectum walls. According to American Cancer Society (ACS) the treatment of the cancer at this stage would be also by a surgery and the physician would advise the patient to do more surgeries until the cancer tumor is removed from the polyp in addition to chemotherapy after surgery [47]. Stage III means that the cancer has spread through the rectum or colon walls and invade nearby lymph nodes but did not spread into different organs or other body compartments. At this stage, chemotherapy could be the better treatment in addition to surgery as well. As for chemotherapy, many physicians recommend FOLFOX, which is composed of leucovorin (Folinic Acid, chemo-protectant drug side effect and 5-FU) and oxaliplatin. alternatively, the physician could also recommend CapeOx, which is a regimen that consists of capecitabine and oxaliplatin [48]. Chemotherapy and surgery are not the only treatment of CRC stage III, radiation could also be utilized to kill cancer cells in case of the surgeons thought that some of the cancer tumor cannot be removed surgically [49, 50]. Lastly, stage IV CRC means that the cancer has spread to distant organs and affected the tissues of the new organs, which also known as metastasis [51]. It is worth to notice that CRC stage IV is commonly diagnosed as well with liver cancer [52]. **Figure 1.2** shows the chemical structure of CRC approved chemotherapy [48, 49, 53].

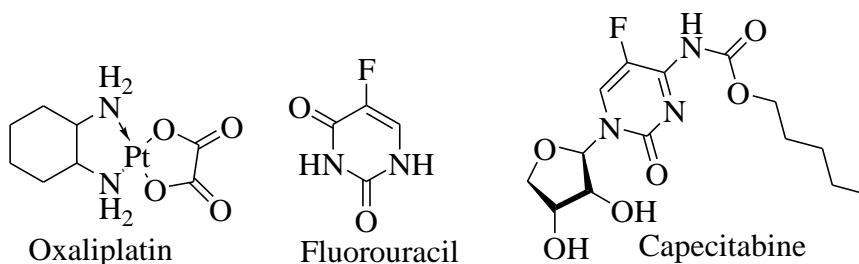


**Figure 1.2.** Commercially available and FDA-approved chemotherapy of CRC.

#### 1.7.1.1. 5-Fluorouracil Chemotherapy

5-fluorouracil (5-FU) is a fluoropyrimidine based compound that is widely used as chemotherapy for colorectal cancer as and breast cancer [49]. The anticancer activity of this drug comes from the inhibition of thymidylate synthase (TS) and incorporation of its metabolites into DNA and RNA [49, 54, 55]. Co-treatment with leucovorin and methotrexate as a modulation strategy of this drug have been utilized and showed a good profile of anticancer activity for 5-FU. The metabolic pathways of 5-FU have been studied and it was found that Dihydropyrimidine dehydrogenase (DPD) converted 5-FU to three active metabolites, fluorodeoxyuridine monophosphate (FdUMP), fluorodeoxyuridine triphosphate (FdUTP), and lastly fluorouridine triphosphate (FUTP). The activation of 5-FU is generated by the conversion of 5-FU into fluorouridine monophosphate (FUMP), which can be achieved by conjugation of phosphoribosyltransferase (OPRT) with cofactors such as phosphoribosyl pyrophosphate (PRPP), or indirectly by the subsequent action of uridine kinase (UK) and uridine phosphorylase (UP) [49].

Consequently, FUMP is further phosphorylated into fluorouridine diphosphate (FUDP). Similarly, FUDP can be further phosphorylated into fluorouridine triphosphate (FUTP), the active metabolite, or converted to another form of metabolite, fluorodeoxyuridine diphosphate (FdUDP), utilizing ribonucleotide reductase (RR). FdUDP fate in the body could be carried on for further phosphorylation to generate FdUTP. Alternatively, FdUDP could also dephosphorylated to generate FdUMP. Another pathway could occur involves the generation of fluorodeoxyuridine (FUDR) by the conversion of 5-FU utilizing the thymidine phosphorylase catalyzed conversion followed by phosphorylation by thymidine kinase (TK) to generate FdUMP. It is worth to notice that

the main side effect of 5-FU is reducing the white blood cells significantly, which may lead to infection, which put a significant need for new chemotherapy [49, 54, 56].

#### 1.7.1.2. Oxaliplatin

Oxaliplatin is one of the FDA approved drugs for CRC since 1996. Normally, oxaliplatin is used together with folinic acid and fluorouracil. Oxaliplatin has a 1,2-diaminocyclohexane (DACH) ring as a carrier ligand which gives the drug an efficacy in comparison to other carrier ligands especially in the cisplatin resistance [53]. In addition to that, DACH can guide the interaction of Pt with the DNA. There are three possible conformations for DACH carrier ligands trans L(R,R), trans-d(S,S) and cis(R,S). studies show that trans L(R,R) is the most affective conformation of DACH in cytotoxicity assays in comparison to the other two conformers. The logic explanation of this efficacy is possible considering the differential recognition of the isomer by damage processing complexes and/or damage recognition proteins [53, 57]. The mechanism of action of oxaliplatin is similar to cisplatin, a very well-known drug for ovarian cancer. The mechanism of action is mediated by formation of Pt-DNA adduct. Consequently, when the oxaliplatin penetrate the cell, it loses a chloride ligand to form a highly reactive monoaquamonochloro species, which rapidly reacts with the nitrogen on position 7(N7) of the guanine attached to DNA [53]. Similarly, the second chloride ligand dissociates to form multiple stable adducts mainly intrastrand adducts with DNA. It is important to highlight that oxaliplatin is not specific to the molecular target encoded as KRAS in the downstream signaling pathway of the EGFR [48, 53, 57-59].

## 1.8. Examples of Biologically Active 1,2,3-Triazoles

Although the number of molecules bearing 1,2,3-triazoles in the market are limited, needless to say in the advanced clinical trials; however, there are number of potential drugs including antibacterial, anticancer, HIV protease inhibitors, and anti-tuberculosis. Examples of these classes will be discussed in this section with details [22].

### 1.8.1. Anti-Cancers

Cancer is the major health concern in developing and developed countries. Therefore, it captures the interest of chemotherapeutic industry. There are several anti-cancer drugs in the market such as taxol, topotecan, irinotecan and vincristine. In addition, many anti-cancer drugs in the premarket stages such as flavopiridol, betulinic acid, roscovitine, and silvestrol. However, the realm of anti-cancer drugs may witness new candidates. Fray et al., reported hit compounds based on 6,7-dichloro-1,4-dihydro-(1H,4H)-quinoxaline-2,3-diones nucleus, where position 5 is substituted with heterocyclmethyl or 1(heterocyclyl)-1-propyl group [22]. Several novel hits contained 1,2,3-triazole ring, most recently potent compound a 6,7-dichloro-5-[1-(1,2,4triazol-4-yl)propyl]-1,4-dihydro-(1H,4H)-quinoxaline-2,3dione, which has remarkable brain penetration. Another example of anti-cancer candidates bearing 1,2,3-triazole is 4-aryl-1,2,3-triazoles, which is an inhibitor of human methionine aminopeptidase type 2 (hMetAP2) (Kallander et al.,). The inhibition mechanism of this candidates relies behind the ability of N1 and N2 to bind with the enzyme active site which results in the inhibition behavior of this drug [60].

Derivatives of available drugs were designed to bear 1,2,3-triazole moiety were also became of interst to chemotherapeutic industry, for example, resveratrol triazole

derivatives were synthesized by Pagliai et al., and many of these compounds showed antiproliferation activity [22, 61]. Another example shows the anti-cancer capability of 1,2,3-triazole is the work done by Lee et al., A series of 1,2,3-triazole-containing  $\alpha$ -GalCer analogues as agonistic antigen killer of T-cell receptor were prepared. The creativity of his work was achieved by the replacement of the amide of  $\alpha$ -GalCer by a triazole ring which increased the reactivity significantly [22, 62].

The work done by Pisaneschi et al., shows the tendency of 1,2,3-triazoles to bind with Epidermal Growth Factor Receptor (EGFR), which is a receptor that normally overexpressed in many cancers including ovarian, breast, and lung cancer [22, 63]. Pisaneschi et al., synthesized a small library of fluorine-containing compounds based on a 3-cyanoquinoline nucleus in order to discover an EGFR-specific imaging agent. [64] these derivatives were selected based on their high affinity for EGFR kinases ( $IC_{50}=(1.81\pm 0.18)$  nm), fair cellular potency ( $IC_{50}=(21.97\pm 9.06)$  nm), limited lipophilicity, and accepted metabolic stability. Among this library, the compound possesses 20-fluoroethyl-1,2,3-triazole was examined for radioligand activity and the result showed acceptable stability in vitro and the uptake was fourfold-higher in high EGFR-expressing A431 tumor xenografts relative to low EGFR-expressing HCT116 tumor xenografts [22, 63].

### 1.8.2. HIV Protease Inhibitors

Since 1981 AIDS results in death of 20 million people around the world. The control of this drug may rely behind the inhibition of the viral replication. HIV-1 protease (HIV-1Pr) became the molecular target to inhibit and hence control the disease and due to the increasing rate of the viral resistance, the need of wide spectrum of protease inhibitors has emerged [22]. One attempt to achieve this goal was done by Whiting et al., who has

built up a focused library of 1,4-disubstituted 1,2,3-triazole from multi functionalized alkynes [64]. Interestingly, the assembled triazoles exhibit a high binding affinity to human immunodeficiency virus type-1 protease. Furthermore, increasing the substitution degree on the triazole ring by functionalizing position 5 has led to increased binding affinity as well as low  $K_i$  values ( $K_i = 8$  nM). Finally, ribavirin is an anti HCV inhibitor which have been derivatized by Saito et al., with carbocyclic and phosphonocarbocyclic analogues and were evaluated against HCV and other viruses and exhibit fair  $IC_{50}$  against HIV-1 [22, 64].

### 1.8.3. Antituberculosis inhibitors

Tuberculosis (TB) is a major leading cause of mortality. World Health Organization (WHO) has approved a treatment for TB known as directly observed therapy short-course (DOTS), which comprises three or four drugs including, isoniazid, rifampin, pyrazinamide, and/or ethambutol for a minimum of six months of treatment. However, these first-generation remain useful in treating susceptible *Mycobacterium Tuberculosis* strains, therefore, a new multidrug-resistant tuberculosis are crucially wanted [22, 65].

Rationally designed nucleoside reported by Somu et al., and found to be a good inhibitor of *Mycobacterium Tuberculosis* that disrupts the siderophore biosynthesis [66]. The activity of this nucleoside was proven to be due to inhibition of the adenylateforming enzyme MbtA, which is an enzyme involved in the biosynthesis of the mycobactins [22, 66].

Costa et al., reported a two series of compounds that bear 1,2,3-triazole with antimycobacterial profile [65]. The *in vitro* screening of anti-tuberculosis of these series explains that the triazole-4-carbaldehyde derivatives were more effective than the 4-difluoromethyl derivatives; moreover, the importance of hydrogen-bond acceptor, and its

position in the aromatic ring, in addition to the planarity of triazole and phenyl rings were investigated by structure activity relationships studies (SAR) and showed an importance for the anti-tubercular activity [22, 65].

#### 1.8.4. Antifungals and Antibacterials

Continuous use of immunosuppressive drugs in addition to continuous use of wide spectrum antibiotics, have led to the spread of life-threatening fungal infections in the last two decades. Furthermore, the antifungal approved treatment present today in the market are either toxic or ineffective in the long use due to the resistant strains, which triggered the research of finding new drugs in new chemical classes. among these classes. Many classes including 1,2,3-triazoles were subjected to investigation.

A series of fluconazole/bile acid conjugates at C3 and C24 positions of bile acids were designed and synthesized by V.S Pore et al.,[67]. These new triazole- bearing molecules showed an excellent antifungal activity against *Candida* species. The MIC values of these compounds varies between 3.12 to 6.25 mg. mL<sup>-1</sup>. Studies suggest that the biological activity of this class was due to the bile acid moiety, which plays a drug carrier role, while the fluconazole moiety plays an inhibitory role. It is also noted that the functionalization of position 4 was clearly increasing the activity [22, 67].

The synthesis and biological evaluation of novel oxazolidinones bearing a 4-substituted 1,2,3-triazole moieties were reported by Reck et al., [68]. The access to this class of compounds was achieved by Vinylsulfone and tosylhydrazone reagents. The biological activity studies reveal that functionalized C 4 of the triazole ring with a small substituent bearing an sp or sp<sup>3</sup> center, were potent antibacterials against Gram-positive

bacteria. in addition, a number of these compounds were also found to be an excellent inhibitors of monoamine oxidase A (MAO-A) [22, 68, 69].

There is a tremendous amount of related data in the literature illustrates that 1,2,3-triazole ring is a potential pharmacophore for many diseases, and based on that a hypothesis was developed, by assembling a triazole pharmacophore on a carrier such as estradiol could enable targeting overexpressed macromolecules in colorectal cancer. To test this hypothesis, three objectives were formulated, 1) to design and virtually screen a library of triazole-based estradiol ligands on macromolecules expressed in CRC. 2) to synthesized the promising candidates of the designed ligands based on their consensus scoring in the docking study, and 3) to biologically test the synthesized ligand on different CRC cell lines.

#### 1.9. References

1. Mishra, B.B. and V.K. Tiwari, *Natural products: an evolving role in future drug discovery*. European journal of medicinal chemistry, 2011. **46**(10): p. 4769-4807.
2. Cragg, G.M. and D.J. Newman, *Natural products: a continuing source of novel drug leads*. Biochimica et Biophysica Acta (BBA)-General Subjects, 2013. **1830**(6): p. 3670-3695.
3. Harvey, A.L., *Natural products in drug discovery*. Drug discovery today, 2008. **13**(19): p. 894-901.
4. Mason, J., A. Good, and E. Martin, *3-D pharmacophores in drug discovery*. Current pharmaceutical design, 2001. **7**(7): p. 567-597.
5. Yang, S.-Y., *Pharmacophore modeling and applications in drug discovery: challenges and recent advances*. Drug discovery today, 2010. **15**(11): p. 444-450.

6. Zou, J., et al., *Towards more accurate pharmacophore modeling: Multicomplex-based comprehensive pharmacophore map and most-frequent-feature pharmacophore model of CDK2*. Journal of Molecular Graphics and Modelling, 2008. **27**(4): p. 430-438.
7. Brenk, R. and G. Klebe, *'Hot spot' analysis of protein-binding sites as a prerequisite for structure-based virtual screening and lead optimization*, in *Pharmacophores and pharmacophore searches*. 2006, Wiley-VCH. p. 171-192.
8. Rostovtsev, V.V., et al., *A stepwise Huisgen cycloaddition process: copper (I)-catalyzed regioselective "ligation" of azides and terminal alkynes*. Angewandte Chemie, 2002. **114**(14): p. 2708-2711.
9. Worrell, B., J. Malik, and V.V. Fokin, *Direct evidence of a dinuclear copper intermediate in Cu (I)-catalyzed azide-alkyne cycloadditions*. Science, 2013. **340**(6131): p. 457-460.
10. Liang, L. and D. Astruc, *The copper (I)-catalyzed alkyne-azide cycloaddition (CuAAC) "click" reaction and its applications. An overview*. Coordination Chemistry Reviews, 2011. **255**(23): p. 2933-2945.
11. Boren, B.C., et al., *Ruthenium-catalyzed azide-alkyne cycloaddition: Scope and mechanism*. Journal of the American Chemical Society, 2008. **130**(28): p. 8923-8930.
12. Cadelon, N., D. Lastòcou res, A. Khadri Diallo, J. Ruiz Aranzaes, D. Astruc, J.-M. Vincent. Chem. Commun, 2008. **7**: p. 41-43.

13. Kolb, H.C., M. Finn, and K.B. Sharpless, *Click chemistry: diverse chemical function from a few good reactions*. Angewandte Chemie International Edition, 2001. **40**(11): p. 2004-2021.
14. Tron, G.C., et al., *Click chemistry reactions in medicinal chemistry: Applications of the 1, 3-dipolar cycloaddition between azides and alkynes*. Medicinal research reviews, 2008. **28**(2): p. 278-308.
15. Miller, W.L. and R.J. Auchus, *The molecular biology, biochemistry, and physiology of human steroidogenesis and its disorders*. Endocrine reviews, 2010. **32**(1): p. 81-151.
16. Anstead, G.M., K.E. Carlson, and J.A. Katzenellenbogen, *The estradiol pharmacophore: ligand structure-estrogen receptor binding affinity relationships and a model for the receptor binding site*. Steroids, 1997. **62**(3): p. 268-303.
17. Ahmed, M.S., L.C. Kopel, and F.T. Halaweish, *Structural Optimization and Biological Screening of a Steroidal Scaffold Possessing Cucurbitacin-Like Functionalities as B-Raf Inhibitors*. ChemMedChem, 2014. **9**(7): p. 1361-1367.
18. Kopel, L.C., M.S. Ahmed, and F.T. Halaweish, *Synthesis of novel estrone analogs by incorporation of thiophenols via conjugate addition to an enone side chain*. Steroids, 2013. **78**(11): p. 1119-1125.
19. Solum, E.J., A. Vik, and T.V. Hansen, *Synthesis, cytotoxic effects and tubulin polymerization inhibition of 1, 4-disubstituted 1, 2, 3-triazole analogs of 2-methoxyestradiol*. Steroids, 2014. **87**: p. 46-53.

20. Clement, O.O., et al., *Three dimensional pharmacophore modeling of human CYP17 inhibitors. Potential agents for prostate cancer therapy*. Journal of medicinal chemistry, 2003. **46**(12): p. 2345-2351.
21. Dhyani, M.V., et al., *Preparation and preliminary bioevaluation of <sup>99m</sup>Tc (CO) 3-11 $\beta$ -progesterone derivative prepared via click chemistry route*. Nuclear medicine and biology, 2010. **37**(8): p. 997-1004.
22. Agalave, S.G., S.R. Maujan, and V.S. Pore, *Click Chemistry: 1, 2, 3-Triazoles as Pharmacophores*. Chemistry—An Asian Journal, 2011. **6**(10): p. 2696-2718.
23. Kharb, R., P.C. Sharma, and M.S. Yar, *Pharmacological significance of triazole scaffold*. Journal of enzyme inhibition and medicinal chemistry, 2011. **26**(1): p. 1-21.
24. Bohacek, R.S., C. McMartin, and W.C. Guida, *The art and practice of structure-based drug design: A molecular modeling perspective*. Medicinal research reviews, 1996. **16**(1): p. 3-50.
25. Csermely, P., et al., *Structure and dynamics of molecular networks: a novel paradigm of drug discovery: a comprehensive review*. Pharmacology & therapeutics, 2013. **138**(3): p. 333-408.
26. Ekins, S., J. Mestres, and B. Testa, *In silico pharmacology for drug discovery: applications to targets and beyond*. British journal of pharmacology, 2007. **152**(1): p. 21-37.
27. Kitchen, D.B., et al., *Docking and scoring in virtual screening for drug discovery: methods and applications*. Nature reviews Drug discovery, 2004. **3**(11): p. 935-949.

28. Kroemer, R.T., *Structure-based drug design: docking and scoring*. Current protein and peptide science, 2007. **8**(4): p. 312-328.
29. Charifson, P.S., et al., *Consensus scoring: A method for obtaining improved hit rates from docking databases of three-dimensional structures into proteins*. Journal of medicinal chemistry, 1999. **42**(25): p. 5100-5109.
30. Leach, A.R., *Ligand docking to proteins with discrete side-chain flexibility*. Journal of molecular biology, 1994. **235**(1): p. 345-356.
31. Brooijmans, N. and I.D. Kuntz, *Molecular recognition and docking algorithms*. Annual review of biophysics and biomolecular structure, 2003. **32**(1): p. 335-373.
32. Huang, S.-Y. and X. Zou, *Advances and challenges in protein-ligand docking*. International journal of molecular sciences, 2010. **11**(8): p. 3016-3034.
33. Cohen, S., *Isolation of a mouse submaxillary gland protein accelerating incisor eruption and eyelid opening in the new-born animal*. Journal of Biological Chemistry, 1962. **237**(5): p. 1555-1562.
34. Yarom, N. and D.J. Jonker, *The role of the epidermal growth factor receptor in the mechanism and treatment of colorectal cancer*. Discovery medicine, 2011. **11**(57): p. 95-105.
35. Alroy, I. and Y. Yarden, *The ErbB signaling network in embryogenesis and oncogenesis: signal diversification through combinatorial ligand-receptor interactions*. FEBS letters, 1997. **410**(1): p. 83-86.

36. Muthuswamy, S.K., M. Gilman, and J.S. Brugge, *Controlled dimerization of ErbB receptors provides evidence for differential signaling by homo- and heterodimers*. *Molecular and cellular biology*, 1999. **19**(10): p. 6845-6857.
37. Boudewijn, M. and P.J. Coffey, *Protein kinase B (c-Akt) in phosphatidylinositol-3-OH kinase signal transduction*. *Nature*, 1995. **376**(6541): p. 599.
38. Chan, T.O., S.E. Rittenhouse, and P.N. Tsichlis, *AKT/PKB and other D3 phosphoinositide-regulated kinases: kinase activation by phosphoinositide-dependent phosphorylation*. *Annual review of biochemistry*, 1999. **68**(1): p. 965-1014.
39. Petit, A., et al., *Neutralizing antibodies against epidermal growth factor and ErbB-2/neu receptor tyrosine kinases down-regulate vascular endothelial growth factor production by tumor cells in vitro and in vivo: angiogenic implications for signal transduction therapy of solid tumors*. *The American journal of pathology*, 1997. **151**(6): p. 1523.
40. Walther, A., et al., *Genetic prognostic and predictive markers in colorectal cancer*. *Nature Reviews Cancer*, 2009. **9**(7): p. 489-499.
41. Engebraaten, O., et al., *Effects of EGF, BFGF, NGF and PDGF (bb) on cell proliferative, migratory and invasive capacities of human brain-tumour biopsies In Vitro*. *International journal of cancer*, 1993. **53**(2): p. 209-214.
42. Douillard, J.-Y., et al., *Randomized, phase III trial of panitumumab with infusional fluorouracil, leucovorin, and oxaliplatin (FOLFOX4) versus FOLFOX4 alone as first-line treatment in patients with previously untreated metastatic colorectal cancer: the PRIME study*. *Journal of clinical oncology*, 2010. **28**(31): p. 4697-4705.

43. Kulkarni, S. and J.K. Savsaviya, *Study of a High-risk Group of Stage 2 Colon Cancer*.
44. Winawer, S., et al., *Colorectal cancer screening and surveillance: clinical guidelines and rationale—update based on new evidence*. *Gastroenterology*, 2003. **124**(2): p. 544-560.
45. Majumdar, S.R., R.H. Fletcher, and A.T. Evans, *How does colorectal cancer present? Symptoms, duration, and clues to location*. *The American journal of gastroenterology*, 1999. **94**(10): p. 3039-3045.
46. Popat, S., R. Hubner, and R. Houlston, *Systematic review of microsatellite instability and colorectal cancer prognosis*. *Journal of Clinical Oncology*, 2005. **23**(3): p. 609-618.
47. Figueredo, A., et al., *Adjuvant therapy for stage II colon cancer: a systematic review from the Cancer Care Ontario Program in evidence-based care's gastrointestinal cancer disease site group*. *Journal of clinical oncology*, 2004. **22**(16): p. 3395-3407.
48. Raymond, E., et al., *Oxaliplatin: a review of preclinical and clinical studies*. *Annals of Oncology*, 1998. **9**(10): p. 1053-1071.
49. Longley, D.B., D.P. Harkin, and P.G. Johnston, *5-fluorouracil: mechanisms of action and clinical strategies*. *Nature Reviews Cancer*, 2003. **3**(5): p. 330-338.
50. Twelves, C., et al., *Capecitabine as adjuvant treatment for stage III colon cancer*. *New England Journal of Medicine*, 2005. **352**(26): p. 2696-2704.

51. Scoggins, C.R., et al., *Nonoperative management of primary colorectal cancer in patients with stage IV disease*. *Annals of surgical oncology*, 1999. **6**(7): p. 651-657.
52. August, D.A., R.T. Ottow, and P.H. Sugarbaker, *Clinical perspective of human colorectal cancer metastasis*. *Cancer and metastasis reviews*, 1984. **3**(4): p. 303-324.
53. Graham, M.A., et al., *Clinical pharmacokinetics of oxaliplatin: a critical review*. *Clinical Cancer Research*, 2000. **6**(4): p. 1205-1218.
54. Salonga, D., et al., *Colorectal tumors responding to 5-fluorouracil have low gene expression levels of dihydropyrimidine dehydrogenase, thymidylate synthase, and thymidine phosphorylase*. *Clinical Cancer Research*, 2000. **6**(4): p. 1322-1327.
55. Hezel, A., et al., *Phase II study of gemcitabine, oxaliplatin in combination with panitumumab in KRAS wild-type unresectable or metastatic biliary tract and gallbladder cancer*. *British journal of cancer*, 2014. **111**(3): p. 430-436.
56. Heggie, G.D., et al., *Clinical pharmacokinetics of 5-fluorouracil and its metabolites in plasma, urine, and bile*. *Cancer research*, 1987. **47**(8): p. 2203-2206.
57. Raymond, E., et al. *Oxaliplatin: mechanism of action and antineoplastic activity*. in *Seminars in oncology*. 1998.
58. Woynarowski, J.M., et al., *Sequence-and region-specificity of oxaliplatin adducts in naked and cellular DNA*. *Molecular pharmacology*, 1998. **54**(5): p. 770-777.
59. Markman, B., et al., *EGFR and KRAS in colorectal cancer*. *Advances in clinical chemistry*, 2010. **51**: p. 72.

60. Kallander, L.S., et al., *4-Aryl-1, 2, 3-triazole: a novel template for a reversible methionine aminopeptidase 2 inhibitor, optimized to inhibit angiogenesis in vivo*. Journal of medicinal chemistry, 2005. **48**(18): p. 5644-5647.
61. Pagliai, F., et al., *Rapid synthesis of triazole-modified resveratrol analogues via click chemistry*. Journal of medicinal chemistry, 2006. **49**(2): p. 467-470.
62. Lee, T., et al., *Synthesis and evaluation of 1, 2, 3-triazole containing analogues of the immunostimulant  $\alpha$ -GalCer*. Journal of medicinal chemistry, 2007. **50**(3): p. 585-589.
63. Pisaneschi, F., et al., *Development of a new epidermal growth factor receptor positron emission tomography imaging agent based on the 3-cyanoquinoline core: synthesis and biological evaluation*. Bioorganic & medicinal chemistry, 2010. **18**(18): p. 6634-6645.
64. Whiting, M., et al., *Rapid discovery and structure– activity profiling of novel inhibitors of human immunodeficiency virus type 1 protease enabled by the copper (I)-catalyzed synthesis of 1, 2, 3-triazoles and their further functionalization*. Journal of medicinal chemistry, 2006. **49**(26): p. 7697-7710.
65. Costa, M.S., et al., *Synthesis, tuberculosis inhibitory activity, and SAR study of N-substituted-phenyl-1, 2, 3-triazole derivatives*. Bioorganic & medicinal chemistry, 2006. **14**(24): p. 8644-8653.
66. Somu, R.V., et al., *Rationally designed nucleoside antibiotics that inhibit siderophore biosynthesis of mycobacterium tuberculosis*. Journal of medicinal chemistry, 2006. **49**(1): p. 31-34.

67. Pore, V., *T etrahedron* 2006, 62, 11178–11186; b) NG Aher, VS Pore, NN Mishra, A. Kumar, PK Shukla, A. Sharma, MK Bhat. *Bioorg. Med. Chem. Lett*, 2009. **19**: p. 759-763.
68. Reck, F., et al., *Novel substituted (pyridin-3-yl) phenyloxazolidinones: antibacterial agents with reduced activity against monoamine oxidase A and increased solubility*. *Journal of medicinal chemistry*, 2007. **50**(20): p. 4868-4881.
69. Reck, F., et al., *Identification of 4-substituted 1, 2, 3-triazoles as novel oxazolidinone antibacterial agents with reduced activity against monoamine oxidase A*. *Journal of medicinal chemistry*, 2005. **48**(2): p. 499-506.

## CHAPTER TWO

### DESIGN OF 1,4-DISUBSTITUTED 1,2,3-TRIAZOLES TARGETING EPIDERMAL GROWTH FACTOR RECEPTORS (EGFRS)

#### 2.1. Introduction

1,2,3-triazoles are non-naturally occurring compounds that are synthesized in laboratories utilizing a well described reaction called click chemistry [8]. Furthermore, data gathered from multiple perspective concluded that 1,2,3-triazoles could be a possible inhibitors for many receptors signaling pathways as well as a pharmacophore for many diseases [22]. Among these diseases is cancer, the very same disease that considered a threat to many lives in the united states let alone the entire world. Since the inhibitory behavior of 1,2,3-triazoles for the epidermal growth factor receptors (EGFRs) is known, the aim of this part of the research is to investigate the binding affinity of estradiol-1,2,3-triazole analogs towards a selected EGFR signaling cascade, utilizing the modeling studies as well as the biological study [70, 71].

To achieve this goal, molecular modeling approaches including *in-silico* studies conducted on the downstream signaling cascade of EGFRs including MEK, ERK, RAF, and RAS. Estrogens are a naturally occurring hormone that is secreted by the ovary in the human body. they regulate and differentiate the growth of reproductive system; consequently, it influences the pathological development of hormone dependent cancer. In addition to that, it is known that estrogens can penetrate the cell and based on that were chosen to carry the 1,2,3-triazole fragment as potential inhibitors for EGFRs [72-74].

Epidermal growth factor receptors are overexpressed in many types of cancers including colorectal cancer. To illustrate more, types of cancer that utilized EGFRs can be classified into 4 groups. 1) endocrine gland cancers including adrenocortical carcinoma, ovarian cancer, pancreatic cancer and prostate and thyroid cancers. 2) breast and gynecologic cancers including cervical endometrial cancer and ovarian cancer. 3) lung carcinoma and finally. 4) digestive cancers which include colorectal cancer, esophageal cancer, liver cancer and pancreatic cancer. Based on these facts, estradiol-1,2,3-triazole analogs and epidermal growth factor receptors were the focus of the modeling in this research [74, 75].

Structural modification on various positions of estrone skeleton have been studied before, and showed an enhanced biological activity. Estrone modification can be classified into two distinct categories 1) adding different moieties to the estron skeleton in different positions and 2) adding a heteroatom to the steroidal ring system or by ring expansion of one of the estradiol tetra cyclic system as shown in **Figure2.1**. Due to the complexity of the latter, it is reasonable to conclude that based on the current literature the first category of modifications is the most popular method used to enhance the biological activity [76, 77].

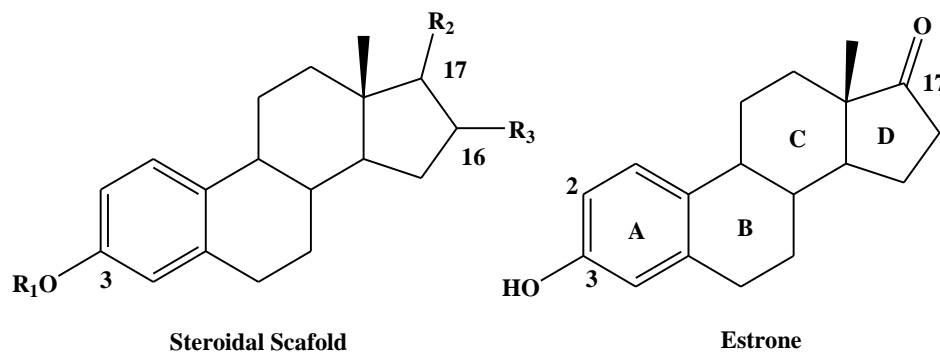


**Figure 2.1.** distinct positions of estrone and steroidal skeleton that been extensively modified and proven to enhance biological activity.

Modification on position 2 of the estrone skeleton by introducing sulfamate group has significantly reduced the estrogen undesired side effects as well as increasing the anti-proliferative activity in breast cancer cell [78]. Triazolyl functionalization on position 3 utilizing propargyl azide-cycloaddition has resulted in enhanced anti-cancer proliferation with  $IC_{50}=0.3-0.9\mu\text{M}$  Bodnar et al., [79]. Not only position 2 and 3 were investigated but also position 17 was subjected to several investigations too. For example, Ahmad et al., 2014 proved that acquiring a cucurbitacin side chain on position 17 have led to a potency in the inhibitory activity to the MAPK signaling pathway toward the treatment of melanoma [17].

## 2.2. Molecular Modeling and Rational Design of 1,2,3-Triazol Bearing Inhibitors.

### 2.2.1. Protein Kinases

#### 2.2.1.1. Methods of Molecular Modeling

All the computer-based experiments were conducted on a Gateway Computer with Windows XP operating system.

#### 2.2.1.2. Molecular Modeling of 2-D and 3-D Structures

A virtual library of 800 compounds bearing estradiol-1,2,3-triazole analogs were assembled on position 17 of the steroidal skeleton. Additionally, a selection of known inhibitors to the EGFR as well as known chemotherapeutics for CRC were used as standards in the docking process. The virtual library including the standards were assembled and energy minimized using Chemoffice 2012, utilizing MMFF94 calculation for energy minimization purposes. The energy minimization calculations were aim to obtain a similar structural confirmation mimic to the natural 3-D structure for each compound designed.

#### 2.3. Utilization of OMEGA to Generate Structural Conformers

All the compounds that been energy-minimized were converted into pdb formats. consequently, all the generated pdb files were gathered in one pdb file containing all the minimized compounds including standards. The purpose of this step is to use this pdb file as an input parameter for OMEGA calculations. OMEGA calculations include creation of multiple and different conformers of each designed compound in the virtual library utilizing the MMFF94 calculations in order to perform ligand-protein flexible docking. Multiple modifications on the default setting of OMEGA were conducted. These modifications include reject conformers that possess an energy different to the global minimum of  $>5.0$  kcal/mol (GP\_ENERGY\_WINDOW). Additionally, maximizing the number of output of conformers to 400 (GP\_NUM\_OUTPUT\_CONFS) and finally, selection of the low energy of conformers from the final ensembled compounds

(GP\_SELECT\_RANDOM false) taking in considerations the root-mean square deviation (RMSD) cut-off of 0.8 Å (GP\_RMS\_CUTOFF). additionally, increasing the rotatable bonds in the designed molecules to 30 for each conformer (GP\_MAX\_ROTORS) the purpose of these modifications is to generate conformers for all of the designed ligands in the data obtained from the virtual library [73].

### 2.3.1. Utilization of FRED to Prepare the Receptors

Protein data bank was the only source of all the receptors under investigation. All the receptors were downloaded as PDB files. The receptors under investigation were known for their high expression as well as they consistent in their pathway toward the signaling that lead to the cell proliferation. The following receptors were chosen (PDB ID in parentheses) to conduct the docking study, epidermal growth factor with tyrosine kinase domain (PDB ID:1M17), RAS (4DST), RAF (PDB ID: 3OMV, 3PRF), MEK1 (PDB ID: 3PP1), ERK2 (PDB IDs:1TVO & 2OJJ), and CDK (PDB ID: 3QL8) **Figure 2.2.** FRED-make receptor, a software that OpenEye® offers, was utilized to prepare all the receptors. A part of FRED-make receptors software is the graphical visualization which was utilized to prepare the receptors. FRED-make receptor consists of three components, mode selection, control and 3D visualization window. FRED-make receptor process in receptors preparation can be summarized in three steps, FRED-make receptor is used to open the PDB file of the receptor then convert it into a 3D view of the whole receptor including the receptor's binding pocket, ligand and cofactors. Consequently, utilizing the binding pocket of the receptor, which usually coexisted with a bounded ligand, in the mode selection window to generate the grid box in a specific size (less than 60.000 Å°).

It is worth to mention that in case of larger grid sizes were needed, the grid box must be split into two parts. This step is crucial as the docking process will not proceed properly otherwise. Finally, mode selection window will generate a final shape of the binding pocket, as FRED will guide the docking process to the specific site and shape of the prepared receptor with their inner

and outer shells. Conducting these three steps in a chronological manner will ensure that the receptor is ready to execute the docking on [80].

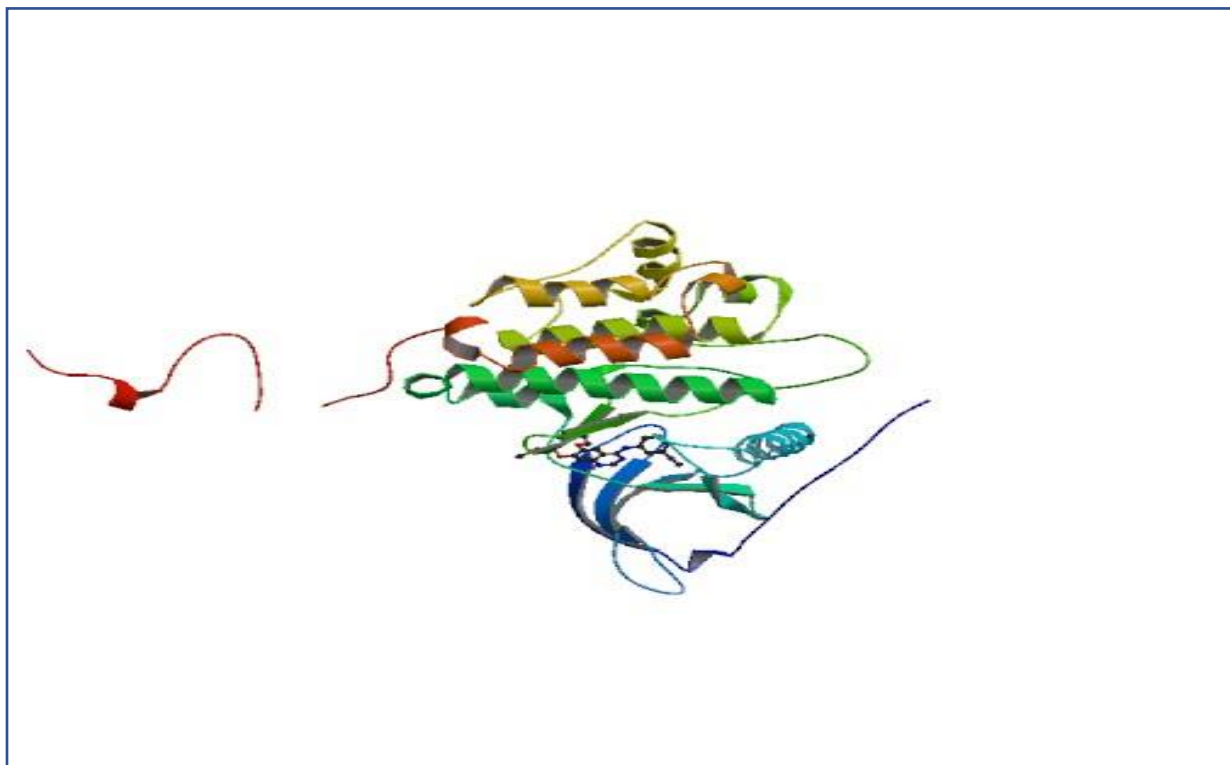


**Figure 2.2.** Epidermal Growth Factor Receptor Tyrosine Kinase domain with 4-anilinoquinazoline inhibitor erlotinib. (PDB ID: 1M17)

### 2.3.2. Conducting Docking Using FRED

FRED generates a fit-shapes in a shape fitting step, in which FRED locates the three dimensional area where the algorithmic search is preformed, this particular step allows

FRED to recognize the possible shapes for the calculations and hence the docking [80]. The shape fitting step ensure that the three dimensional-shaped area is located properly for the ligand and the best binding pocket will ensure to avoid the unnecessary binding with other sites of the receptor, in addition to simultaneously flipping the area of binding to ensure the optimum interactions occur in the pocket. Lastly, the PDB file of the combined library, including standards, as well as the prepared receptors were collected by FRED to perform the docking process. There are multiple optimization steps for the scoring functions, including rigid skeleton optimization, torsion optimization and -OH groups rotamer optimization [81].

Consensus score can be obtained utilizing multiple scoring functions when the docking process reaches the final steps. These scoring functions that shape the consensus score, in a chronological manner, includes, shapegauss, chemgauss3, oechemscore, screenscore and finally PLP. More information regarding each scoring function can be obtained from OpenEye® FRED website [www.eyesopen.com/products](http://www.eyesopen.com/products). Additionally, the three-dimensional conformers for each ligand and receptor can be visualized by OpenEye® VIDA and from which all the figures (in the result and discussion section) were taken from [81].

#### 2.4. Results and Discussion

The virtual library of estradiol-1,2,3-triazole analogs as well as three standards including FDA-approved and commercialized drugs were docked on six different receptors starting from the overexpressed receptor extracellular domain (1M17), and ending to the downstream signaling cascade including Raf, Ras, ERK and MEK. The novel estradiol-1,2,3-triazole analogs were designed in systematic manner by 1) functionalization of position 17 of the estradiol by the triazolyl moieties including 1,4-disubstituted triazole and 1,4,5-

trisubstituted triazole, where C 5' of the triazole ring is functionalized with phenyl and carbinol groups. 2) Functionalization of position 3 of the estradiol with the following groups: -OH, -Me, -AcO, -SO<sub>2</sub>NH<sub>2</sub>, -(CH<sub>3</sub>)<sub>3</sub>CCO, -Bn and -CH<sub>2</sub>C<sub>6</sub>H<sub>5</sub>X, where X= F,Cl,Br,I, CH<sub>3</sub> and OCH<sub>3</sub> on para, ortho, and meta positions. Lastly functionalization of position 16 and 17 by introducing double bond, which results in a significant change of the conformation of the triazole ring in addition to removing an OH group which is possible hydrogen acceptor. An average of 114 analogs showed better binding affinity to the receptors (**appendix 1**). These binding affinities expressed as a lower consensus scores than the known inhibitors such as erlotinib 5-Fu, capecitabine oxaliplatin, **Figure 2.3** illustrates numerous examples of the library.

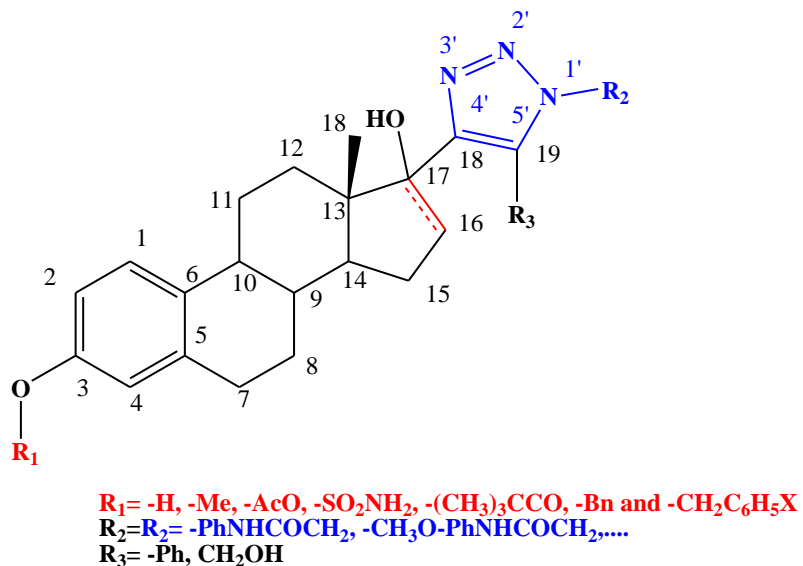


**Figure 2.3.** The variety of functionalization of the estrone-triazole analogs. The functionalization took place on C3, C16, C17, C18 and N1.

To sum it up, the virtual library can be divided into three groups based on the substitution of the triazole ring.

Group 1, where is no substitution on position 5' of the triazole ring, and it is the majority of the hits in EGFR. Group 2, where the substitution on position 5' of the triazole ring is carbinol group and Finally, Group 3, where the substitution of position 5 is a phenyl ring, and interestingly enough, even though the phenyl ring can offer a hydrophobic feature and hence, become the mode of action in hydrophobic pockets, however most of the trends in hydrophobic pockets is the mild polarity that the triazole ring possess. To put it differently, lack of substitution on position 5' in addition to bearing a hydrophobic group on R<sub>2</sub> of the triazole is the trending mode of action. **Figure 2.4** shows the selected compounds for the synthesis.

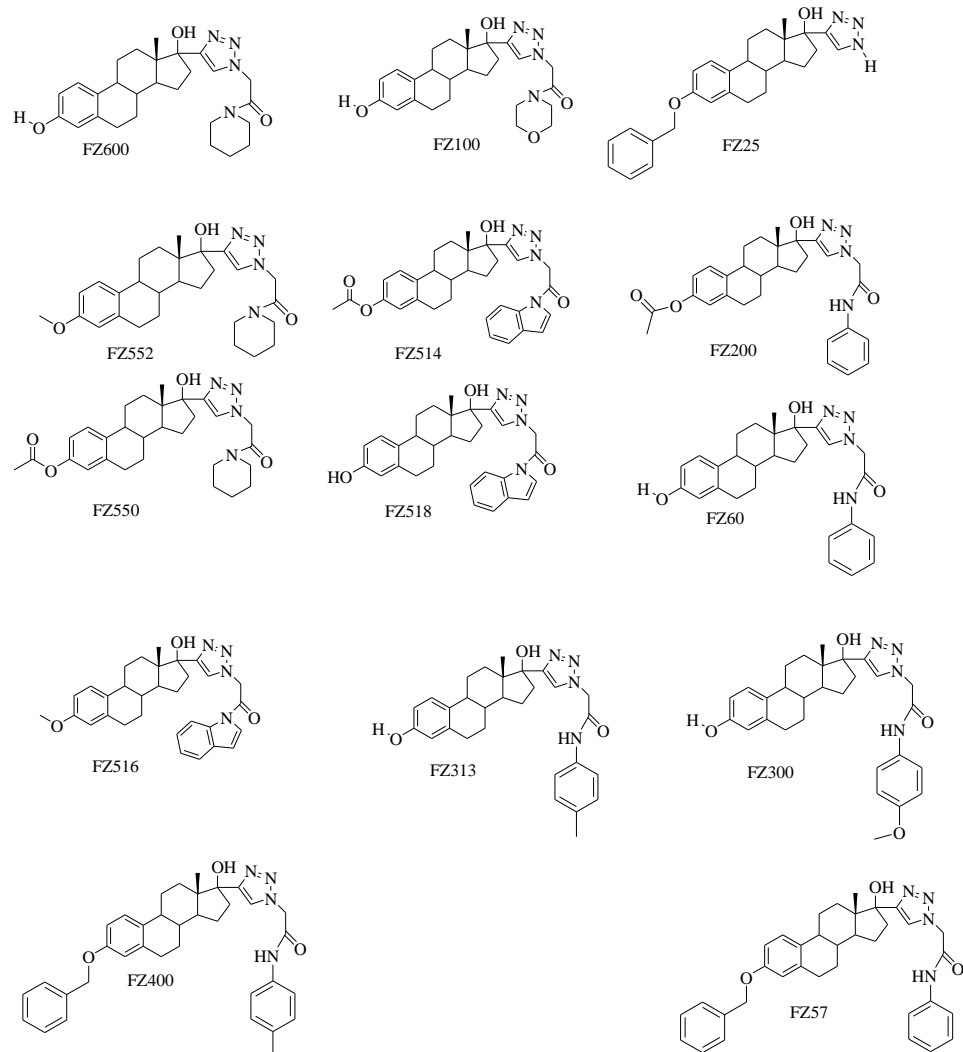


**Figure 2.4.** Group 1 trending compounds, all the compounds in this group lack functionalization in C18 (C5' in the triazole ring)

### 2.4.1. Result and Discussion of Molecular Modeling with EGFR

The docking study conducted on epidermal growth factor receptor tyrosine kinase domain (1M17) showed an interesting binding mode. The trending mode of action was the following: functionalization of position 3 of estradiol with hydrophobic groups such as benzyl group or methyl group and lack of substitution on position 5' of the triazole ring was dominant. In addition, the group that the triazole ring bears at position 1' (N1) was fairly polar. Examples of the substituents at position 1 are 1-N-acetylindole, N-acetylaniline, N-acetylmethoxybenzene, N-acetylmorphiline and N-acetylpipridine. The previous trend was founded in the following compounds: FZ 600, FZ 100, FZ514, FZ 516, FZ 518, FZ 560, FZ 313, FZ560, FZ 100. **Figure 2.7** shows the presence of indole nucleus is important in the binding of the ligands to the pocket. This binding is through the N2 and N3 of the triazole ring.

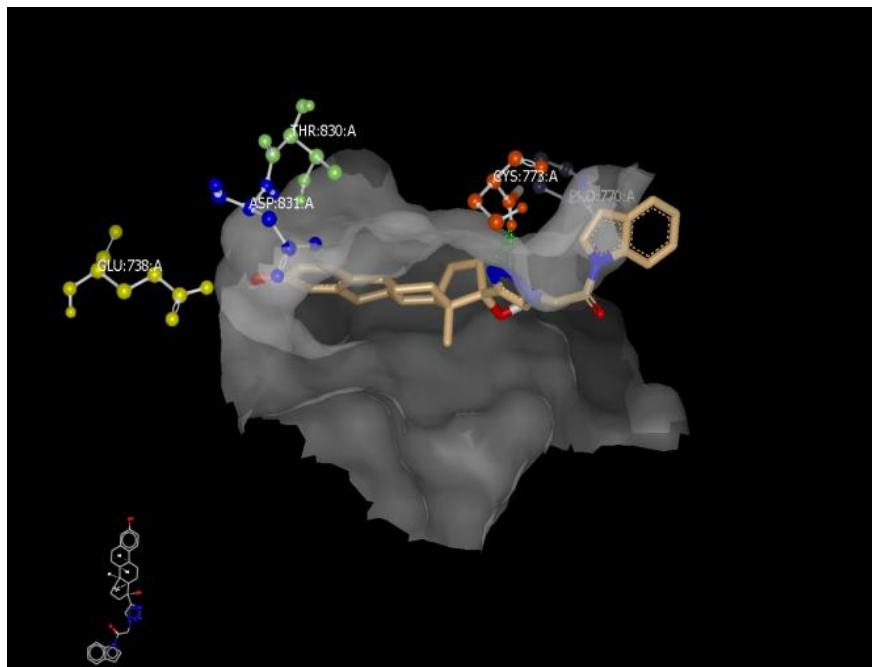


**Figure 2.7.** FZ 518 and 5-FU as a standard which binds with GLU783 A and ASP831 A and THR 830A via three hydrogen bonds.

It appears that the indole ring can deliver the ligand closer to the pocket and into the space that is required to form the hydrogen bond. This trend is noted in FZ 514, FZ 516 and FZ 518. On the contrary, the absence of an indole ring changed the trending to a hydrophobic interaction when the substituent on N1' of the triazole ring bore an aromatic amine. **Figures 2.8.** show the aromatic amines effect on the binding mode. It is noted that the aromatic amine is occupying a space out of the binding pocket. This mode of action is observed in the following compounds: FZ57, FZ60, FZ 200, FZ 300, FZ 313 and FZ 400. An exception is FZ 313, where the OH group at position 3 has a hydrogen bond with PRO 770 A.

Overall, this mode of action differs due to the presence of a highly hydrophobic group attached to the amine, which is causing a hydrophobic interaction that orients the hydrophobic group outside the binding pocket. Additionally, hydrogen binding took place in only one instance, by increasing the hydrophobicity on the amine side and having mild polarity on position 3 (FZ 313). Table 2.1 sums up the functionality responsible for the binding.

Similarly, replacing R<sub>3</sub> with slightly polar heterocyclic amino groups, such as morpholine and Piperidine nucleuses (**Figure 2.9 A&B**), have the same implications for the binding mode, which is clearly observed in the following ligands: FZ 100, FZ 552, FZ 556, and FZ 600. **Table 2.2** summarizes the mode of action of the last group.

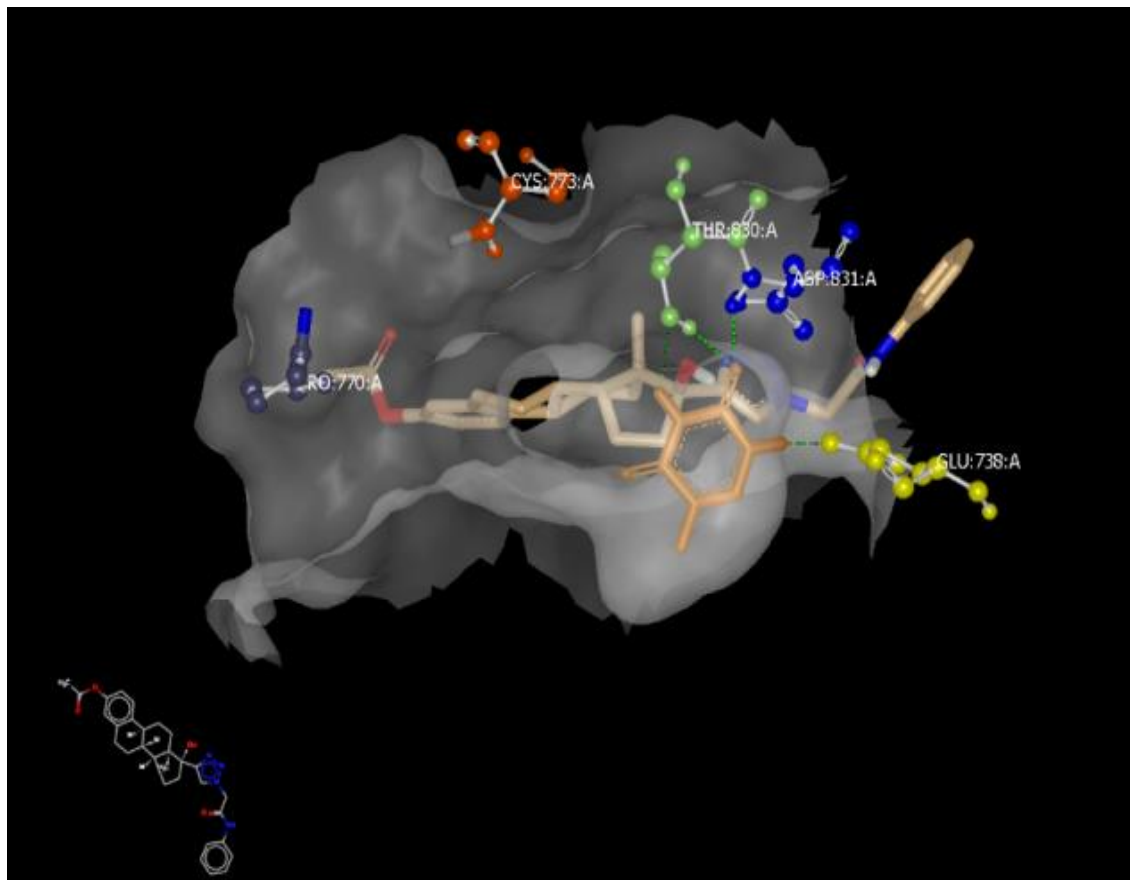


**Figure 2.8.** FZ 200 and 5-FU, the latter binds with GLU783 A and ASP 831 A and THR 830 A via three hydrogen bonds.

**Table 2.1:** Summary of the binding mode of actions of hydrophobic aromatic analogs.

Compound	R1	R2	Mode of Action	Aromatic Ring Orientation
FZ 25	OBn	H	Hydrophobic interaction	No aromatic ring present.
FZ57	OBn	PhNHCOCH <sub>2</sub> -	Hydrophobic interaction	Out of the pocket
FZ 60	OH	PhNHCOCH <sub>2</sub> -	Hydrophobic interaction	Out of the pocket
FZ 200	OAC	PhNHCOCH <sub>2</sub> -	Hydrophobic interaction	Out of the pocket
FZ 300	OH	CH <sub>3</sub> OPhNHCOCH <sub>2</sub> -	Hydrogen bonding/ PRO 770 A	Out of the pocket
FZ313	OH	CH <sub>3</sub> PhNHCOCH <sub>2</sub> -	Hydrophobic interaction	Out of the pocket
FZ 400	OBn	CH <sub>3</sub> PhNHCOCH <sub>2</sub> -	Hydrophobic interaction	Out of the pocket

**Table2.2:** Summary of the mode of actions in compounds that exhibit an orientation of the heterocyclic ring outside the binding pocket.

Compound	R1	R2	Mode of Action	Heterocyclic amine Ring Orientation
FZ 100	OH	C <sub>4</sub> H <sub>8</sub> ONCOCH <sub>2</sub> -	Hydrogen Bonding/ PRO 770 A	Out of the pocket
FZ 552	OMe	C <sub>5</sub> H <sub>10</sub> NCOCH <sub>2</sub> -	Hydrophobic interaction	Out of the pocket
FZ 556	OAC	C <sub>5</sub> H <sub>10</sub> NCOCH <sub>2</sub> -	Hydrophobic interaction	Out of the pocket
FZ 600	OH	C <sub>5</sub> H <sub>10</sub> NCOCH <sub>2</sub> -	Hydrophobic interaction	Out of the pocket

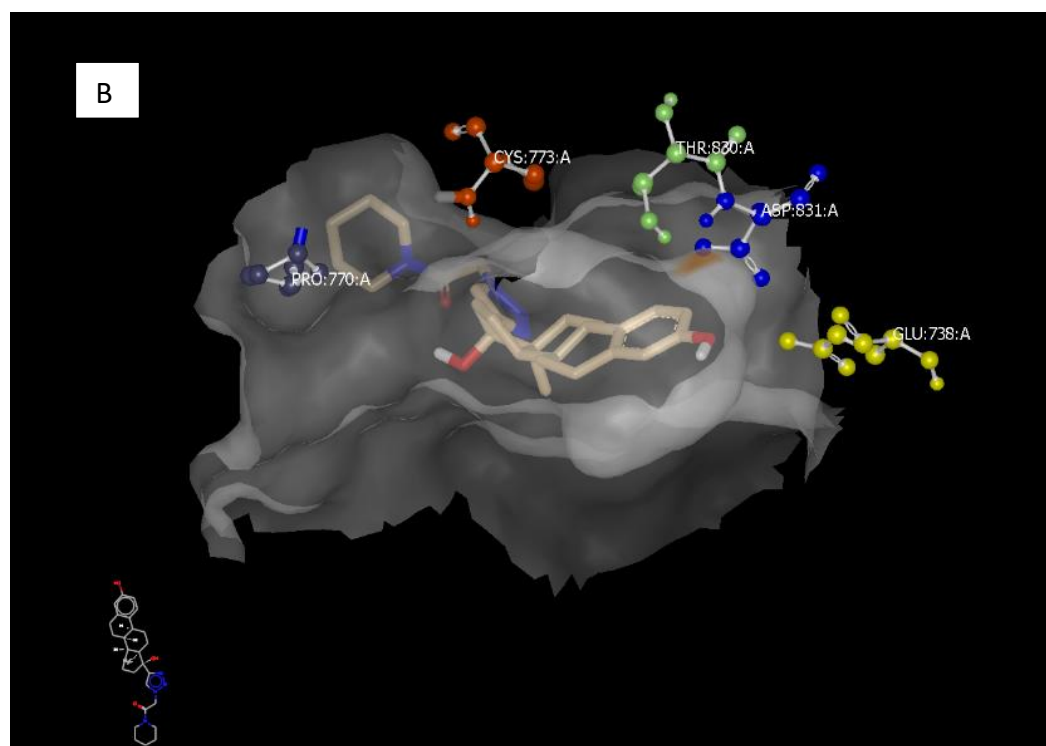
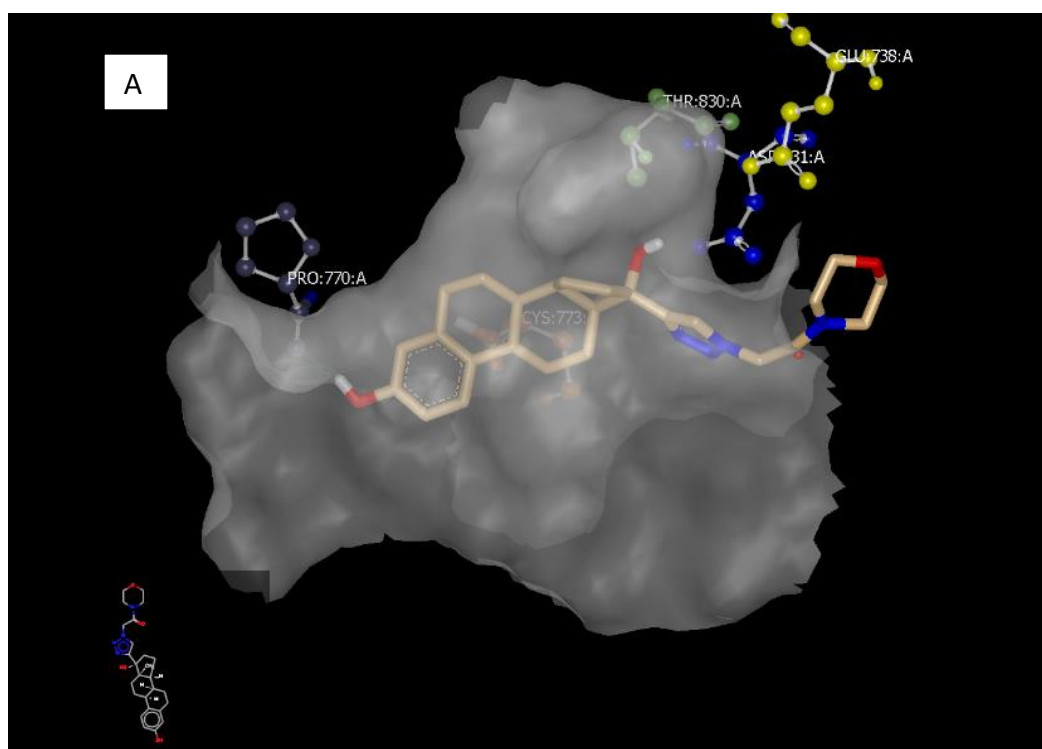


**Figure 2.9.** (A) both rings are outside of the pocket. However, FZ 100 shows hydrogen binding with PRO 770 A. FZ 100 containing morpholine ring (B) FZ 600 containing Piperidine ring in the binding pocket.

## 2.4.2. Result and Discussion of Molecular Modeling with RAF receptors

### 2.4.2.1 Result and Discussion of Molecular Modeling with 3PRF

The result of the docking study conducted on the B-Raf Kinase Domain (3prf) showed similar results in comparison to 1M17. The presence of an indole nucleus showed hydrophobic interaction; however, there were no hydrogen bonds involved in the binding (**Figure 2.10**). On the contrary, both ligands, 5-FU and capecitabine, bind with two amino acids present in the binding pocket.

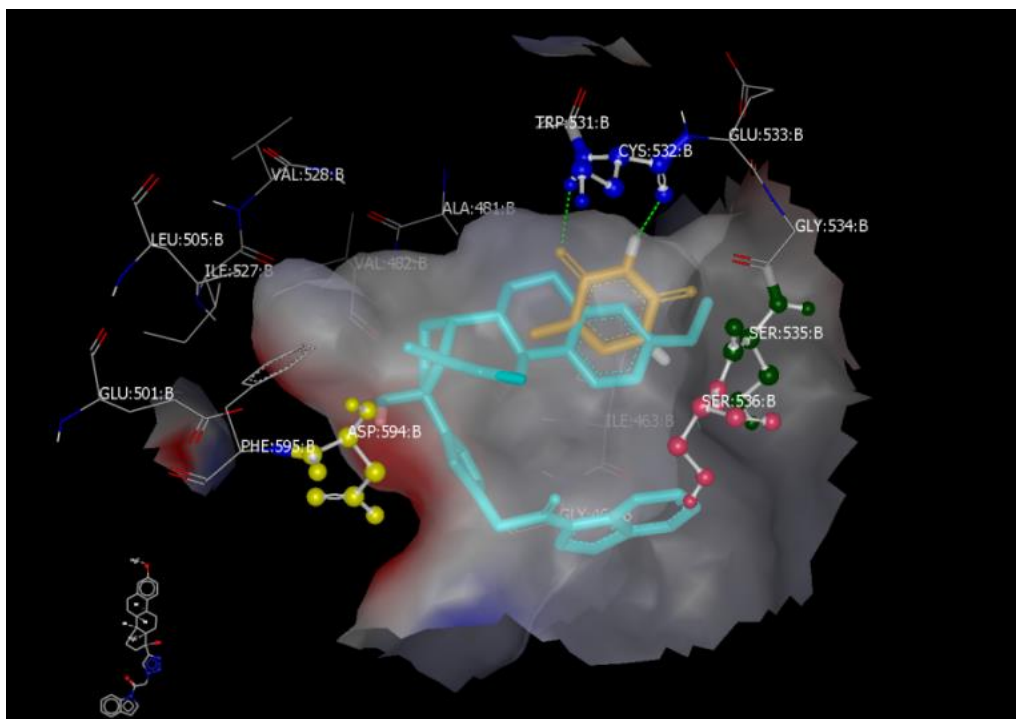


**Figure 2.10.** FZ 516 containing indole ring (light-blue), 5FU (gold) which fits the binding pocket with hydrogen bonding with CYS 531B and CYS 532B

Similarly, an aromatic amine containing triazoles exhibits hydrophobic interactions, except with the mild polarity on position 3, which results in hydrogen binding

with CYS532 B. This mode of action is noticed in FZ57, FZ60, FZ 200, FZ 300, FZ 313 and FZ 400. **Figure 2.12** shows the binding affinity modes in this set of ligands.

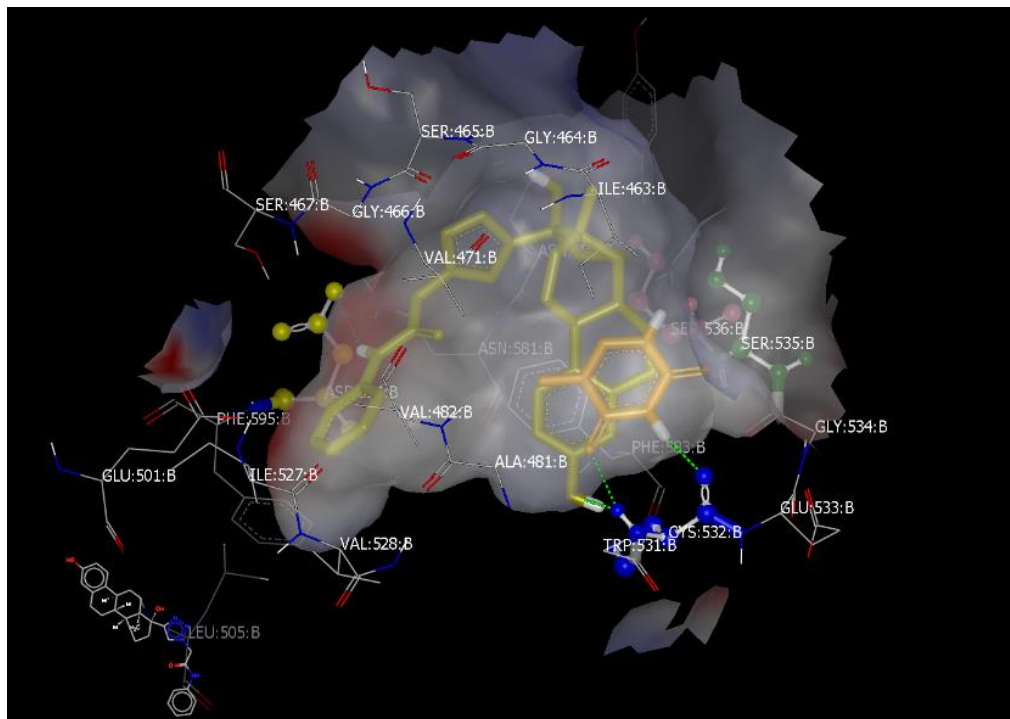


**Figure 2.12.** FZ 60 (Yellow) and 5-FU (Gold) which bears two hydrogen bonds, and CYS 532 B and TRP 531 B as the design ligand.

Alternatively, the last set of compounds (3compounds) have a different mode of action. The piperidine nucleus-containing compound binds with SER 535 B (the same amino acids bind with capecitabine) through the OH existing on position 17 (FZ 552, FZ 600 and FZ 556). On the other hand, the morpholine-containing triazole binds with a different amino acid (SER 536 B) utilizing N2 on the triazole ring. Figure 2.13 A-F shows the visual representation of these binding affinities. **Table 2.3** summarizes the binding mode of action from many perspectives.

**Table 2.3:** Summary of the binding modes of action of the last set of compounds in three perspectives.

Type of amine attached to triazole	Type of interaction	Orientation of Amine
Indole bearing triazole.	Hydrophobic.	Inside the pocket.
aromatic bearing triazole.	Hydrophobic, except OH on C3.	Inside the pocket.
Aliphatic bearing triazole.	Hydrogen bonding utilizing OH on C17, except with morpholine bearing triazole binds with N2.	Inside the pocket.

#### 2.4.2.2. Result and Discussion of Molecular Modeling with 3OMV.

The binding affinities of RAF-1 (3OMV) are different than the binding affinities in B-RAF Kinase Domain (3prf). The presence of an indole ring attached to the triazole fragment establishes a hydrogen bond with the hydroxyl group present in position 17 with GLY 426 (**Figure 2.14 A**). On the other hand, 5-Fu binds in the same pocket with CYS 424 A with one hydrogen bond (**Figure 2.14 B**). Lastly, capecitabine binds with LYS 431 A utilizing one bond (**Figure 2.14 C**).

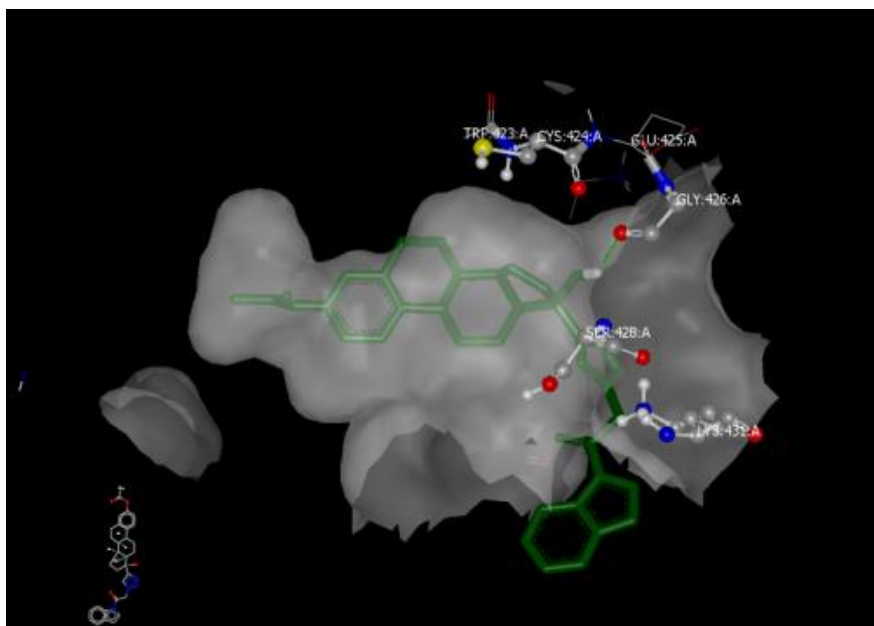


**Figure 2.14A.** FZ 514 (green) binds with GLY 426 A through the hydroxyl group in position 17.

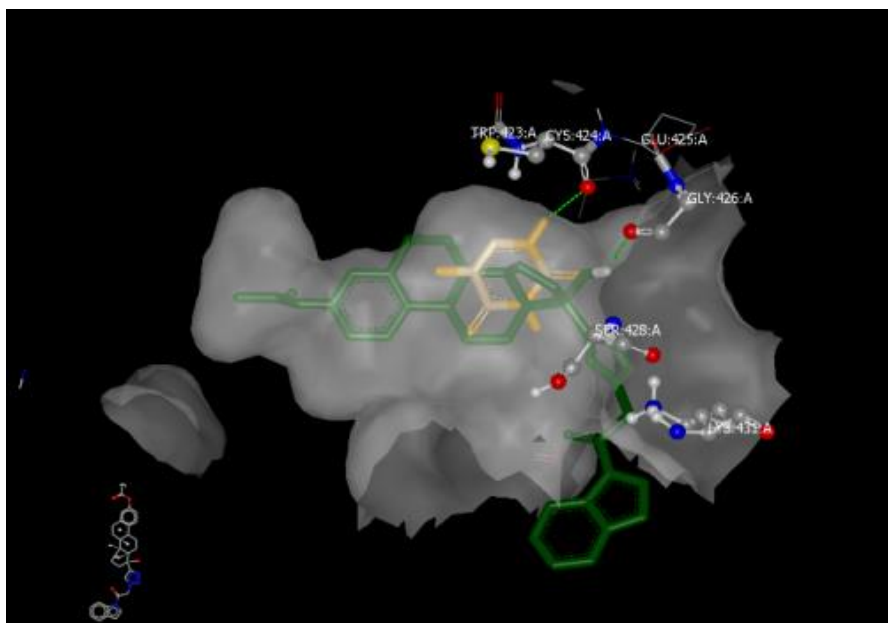


**Figure 2.14B.** FZ 514 (green) Vs. capecitabine (gold) which binds with LYS 431 A.

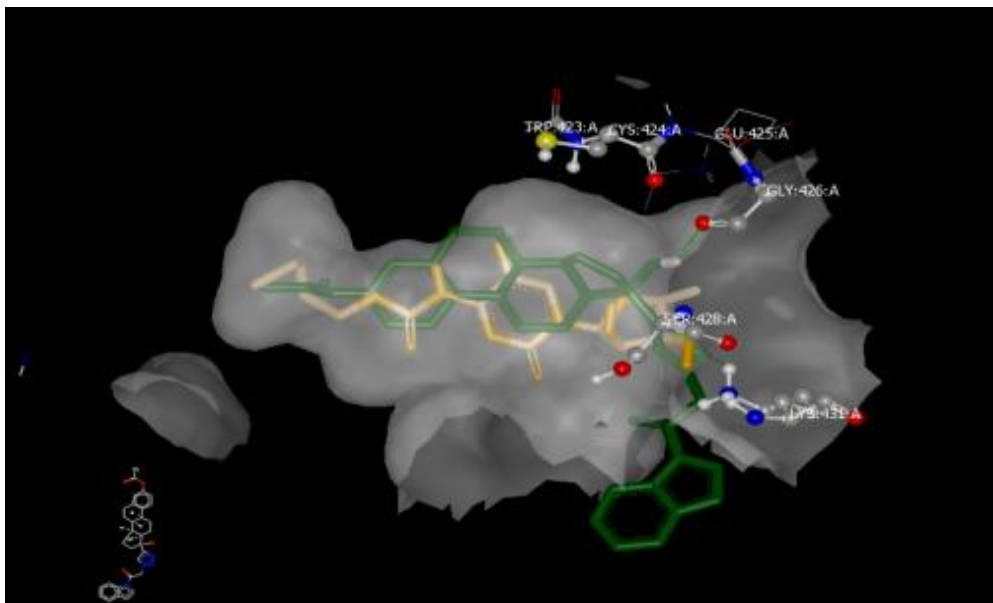


**Figure 2.14 C.** FZ 514 (green) Vs. 5-FU (gold) which binds with CYS 424A.

The second set of compounds, triazole containing aromatic amines, exhibited general binding affinities involving the hydroxy group on position 17, as well as N3 of the triazole ring. In addition, a hydrophobic interaction took place when position 3 was substituted with OBn. This trend is the mode of action noticed in FZ 25, FZ 57, FZ 200, FZ 300, FZ 313 and FZ 400. **Figures 2.15 A-C** represent the binding affinities of this class of compounds.

Similarly, the binding affinity of the last set of ligands is different than the aromatic amines attached to the triazole ring. The last set of ligands bears either piperidine or morpholine, with differing functionality on position 3. In general, the morpholine moiety containing a ligand has better binding affinity with two different hydrogen bonds involving CYS 424 A through the hydroxy group on position 17 and N3 of the triazole ring on SER

428 A. While the piperidine containing ligands are not interacting with amino acids in the binding pocket through hydrogen bonding, they do bind through the hydrophobic interaction.

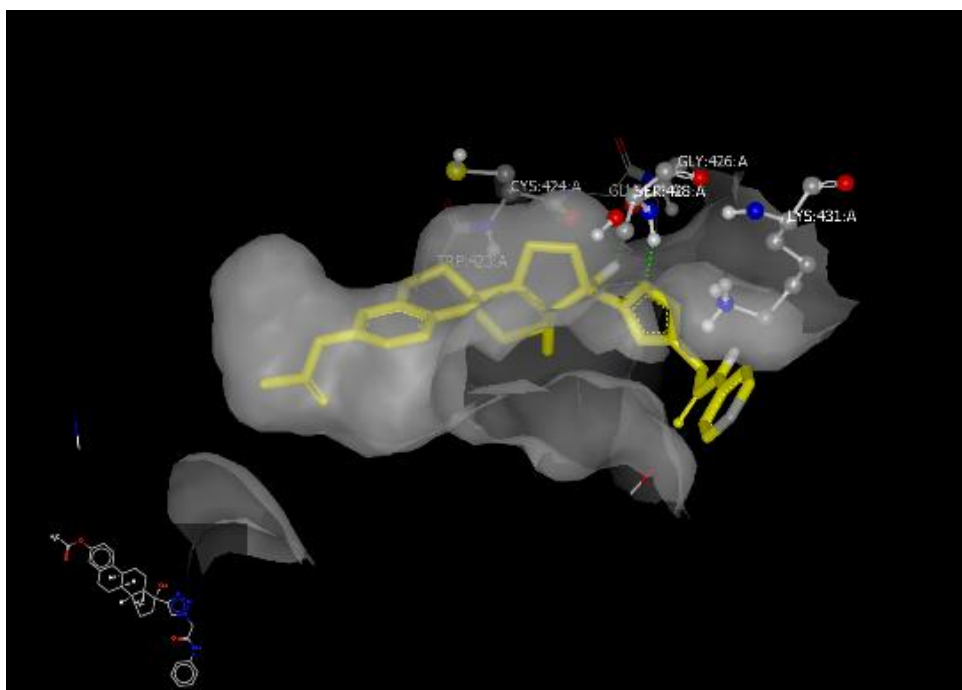


**Figure 2.15 A.** FZ 200 (yellow), which binds with SER 428 A with two hydrogen bonds utilizing OH present on position 17 as well as N2 of the triazole ring.

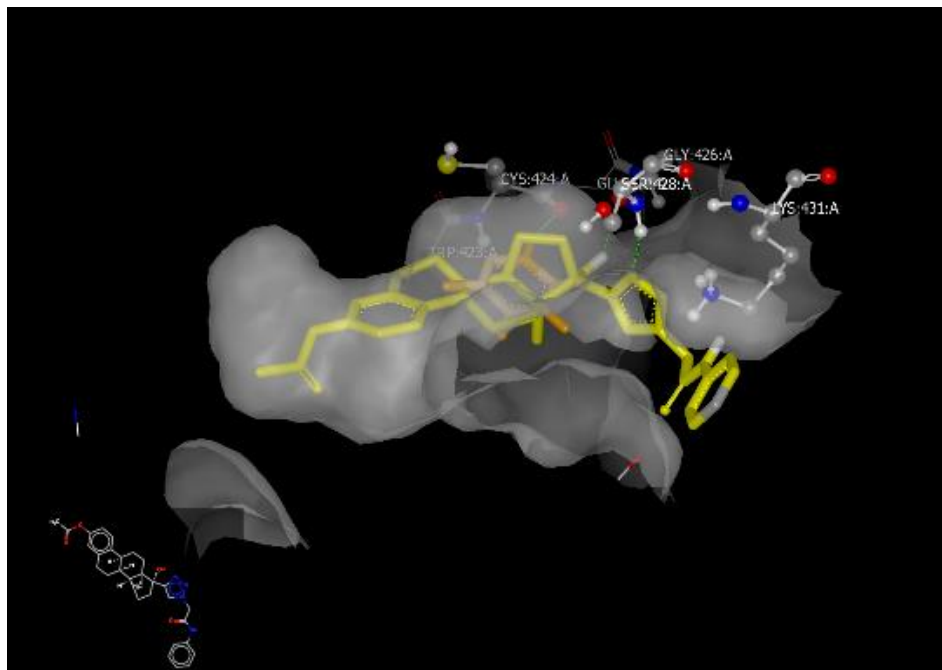


**Figure 2.15 B.** FZ 200 (yellow) VS 5-FU(gold), which binds CYS 424A utilizing one hydrogen bond.

#### 2.4.3. Result and Discussion of Molecular Modeling with MEK

The result of the molecular docking conducted on the human mitogen-activated protein kinase MEK1 receptor (3PP1) was different than that seen with the RAF receptors. In the case of a heterocyclic amine attached to the triazole ring, the estrone part of the ligand pumped out of the pocket, while the triazole part was oriented inside the pocket. This indicates that only the triazole ring will react with the binding pocket. **Figure 2.16** shows the orientation of the indole containing ligands in the MEK receptor. On the contrary, ligands containing aromatic amines attached to the triazole ring, as well as the Piperidine and morpholine containing triazoles, fit in the pocket with different binding modes. **Figure 2.18A-B** represents the binding modes of action in the MEK pocket

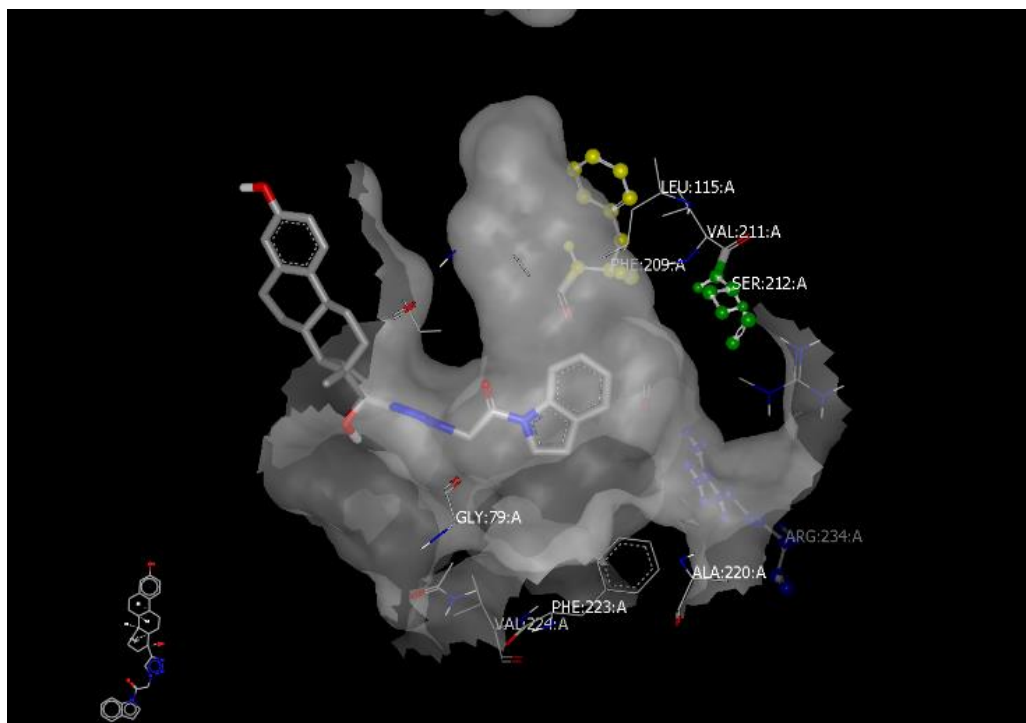


**Figure 2.17.** FZ 518 inside the MEK receptor. The estrone part is oriented outside of the pocket.

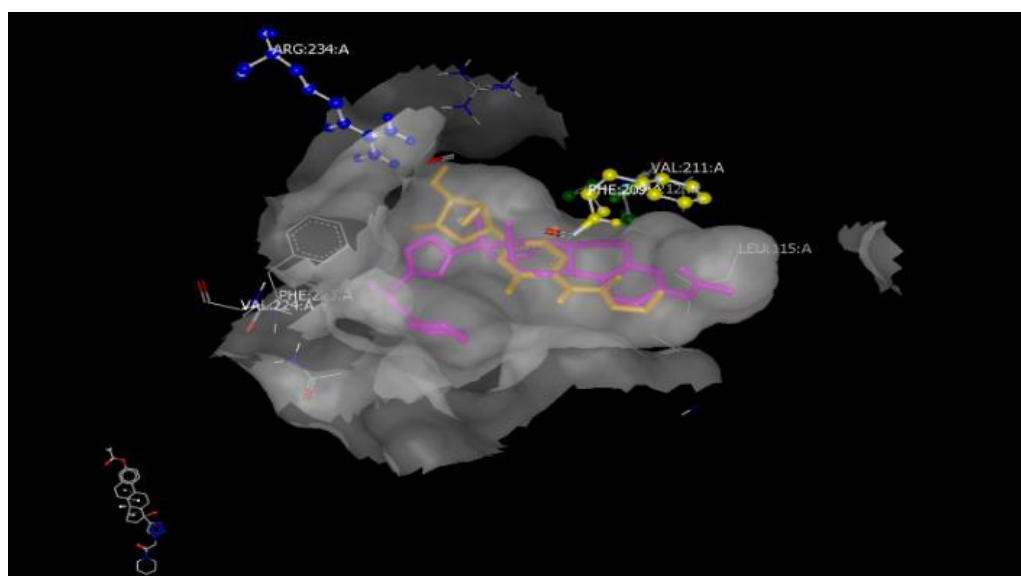


**Figure 2.18 A.** FZ 550 (pink) Vs. capecitabine (gold) which binds through VAL 211 A and PHE 209 A utilizing two hydrogen bonds.

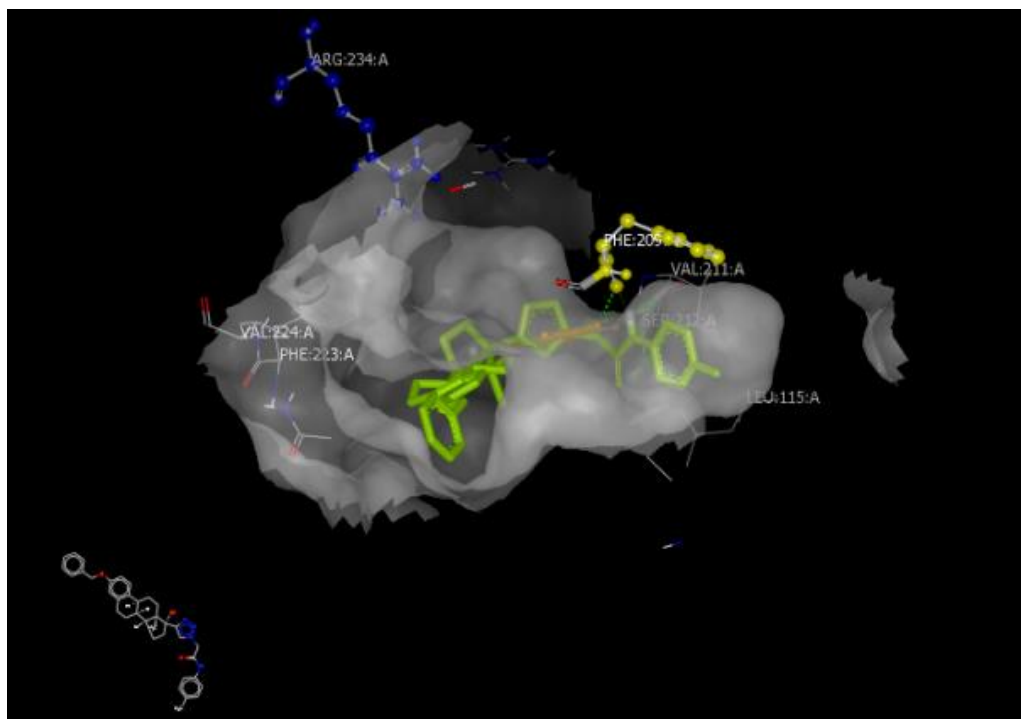


**Figure 2.18 B.** FZ 400 (green) Vs. 5-FU (gold) which binds through ARG 234 A utilizing one hydrogen bond through PHE 209 A. The same amino acid binds with the designed ligand.

## 2.5. Summary of the mode of action in the selected receptors

The binding modes in EGFR (1m17) show that the presence of an indole nucleus is important in the binding of the ligands to the pocket. This binding is through N2 and N3 of the triazole ring. It appears that the indole ring can deliver the ligand closer to the pocket, to a space that is necessary to form the hydrogen bond. On the contrary, the absence of an indole ring changes the trending to a hydrophobic interaction, when the substituent on N1 of the triazole ring is bearing an aromatic amine.

Binding modes in the B-Raf Kinase Domain (3prf) showed similar results in comparison to 1M17. The presence of an indole nucleus showed a hydrophobic interaction; however, there were no hydrogen bonds involved in the binding. Similarly, an aromatic amine containing triazoles exhibits a hydrophobic interaction, except in the case of a mild polarity on position 3, which results in hydrogen binding with CYS532 B. Alternatively, the last set of compounds (3compounds) have a different mode of action. The piperidine nucleus-containing compound binds with SER 535 B (the same amino acids bind with capecitabine) through the OH existing on position 17 (FZ 552, FZ 600 and FZ 556), while the morpholine containing triazole binds with a different amino acid (SER 536 B) utilizing N2 on the triazole ring.

The binding affinities of RAF-1 (3OMV) are different than the binding affinities in the B-RAF Kinase Domain (3prf). The presence of an indole ring attached to the triazole fragment establishes a hydrogen bond with the hydroxyl group present in position 17 with GLY 426 A. The triazole containing aromatic amines, exhibiting general binding affinities, involve the hydroxy group on position 17, N3 of the triazole ring, and a hydrophobic interaction when position 3 is substituted with OBn.

The last set of ligands bears either piperidine or morpholine, with different functionality on position 3. In general, the morpholine moiety-containing ligand has a better binding affinity with two different hydrogen bonds involving CYS 424 A through the hydroxy group on position 17 and N3 of the triazole ring SER 428 A. While the piperidine-containing ligands are not interacting with amino acids in the binding pocket through hydrogen bonding, they do bind through the hydrophobic interaction.

The result of the molecular docking conducted on human mitogen-activated protein kinase MEK1 receptor (3PP1) was different than that seen with the RAF receptors. In the presence of a heterocyclic amine attached to the triazole ring, the estrone part of the ligand pump is out of the pocket while the triazole part is oriented inside the pocket. This indicates that only the triazole ring reacts with the binding pocket.

## 2.6. Conclusion

The molecular docking process proved its feasibility in terms of drug discovery methodologies. In addition, it saves tremendous amounts of time and money on the drug discovery process. This process can speculate on the binding affinity energy and express it as a consensus score, which eventually represents the small molecule behavior in the biological system and the interaction of ligands with molecular targets. In this work, molecular modeling was used under consideration of the possibility of pharmacophore presence through the 1.2.3-triazole ring utilizing the estrone main skeleton to deliver the triazole-bearing ligand to the receptor *in silico*. The molecular modeling also took into consideration the EGFRs starting from upstream and ending with downstream as a known overexpression in many cancer diseases, including colorectal cancer (CRC). The whole process aimed to discover and synthesize a possible drug that can be used to inhibit the signaling pathway observed in CRC.

## 2.7. References

1. Mishra, B.B. and V.K. Tiwari, Natural products: an evolving role in future drug discovery. *European journal of medicinal chemistry*, 2011. 46(10): p. 4769-4807.

2. Cragg, G.M. and D.J. Newman, Natural products: a continuing source of novel drug leads. *Biochimica et Biophysica Acta (BBA)-General Subjects*, 2013. 1830(6): p. 3670-3695.
3. Harvey, A.L., Natural products in drug discovery. *Drug discovery today*, 2008. 13(19): p. 894-901.
4. Mason, J., A. Good, and E. Martin, 3-D pharmacophores in drug discovery. *Current pharmaceutical design*, 2001. 7(7): p. 567-597.
5. Yang, S.-Y., Pharmacophore modeling and applications in drug discovery: challenges and recent advances. *Drug discovery today*, 2010. 15(11): p. 444-450.
6. Zou, J., et al., Towards more accurate pharmacophore modeling: Multicomplex-based comprehensive pharmacophore map and most-frequent-feature pharmacophore model of CDK2. *Journal of Molecular Graphics and Modelling*, 2008. 27(4): p. 430-438.
7. Brenk, R. and G. Klebe, 'Hot spot' analysis of protein-binding sites as a prerequisite for structure-based virtual screening and lead optimization, in *Pharmacophores and pharmacophore searches*. 2006, Wiley–VCH. p. 171-192.
8. Rostovtsev, V.V., et al., A stepwise Huisgen cycloaddition process: copper (I)-catalyzed regioselective "ligation" of azides and terminal alkynes. *Angewandte Chemie*, 2002. 114(14): p. 2708-2711.

9. Worrell, B., J. Malik, and V.V. Fokin, Direct evidence of a dinuclear copper intermediate in Cu (I)-catalyzed azide-alkyne cycloadditions. *Science*, 2013. 340(6131): p. 457-460.
10. Liang, L. and D. Astruc, The copper (I)-catalyzed alkyne-azide cycloaddition (CuAAC)“click” reaction and its applications. An overview. *Coordination Chemistry Reviews*, 2011. 255(23): p. 2933-2945.
11. Boren, B.C., et al., Ruthenium-catalyzed azide– alkyne cycloaddition: Scope and mechanism. *Journal of the American Chemical Society*, 2008. 130(28): p. 8923-8930.
12. Cadelon, N., D. LastØcou res, A. Khadri Diallo, J. Ruiz Aranzaes, D. Astruc, J.-M. Vincent. *Chem. Commun*, 2008. 7: p. 41-43.
13. Kolb, H.C., M. Finn, and K.B. Sharpless, Click chemistry: diverse chemical function from a few good reactions. *Angewandte Chemie International Edition*, 2001. 40(11): p. 2004-2021.
14. Tron, G.C., et al., Click chemistry reactions in medicinal chemistry: Applications of the 1, 3-dipolar cycloaddition between azides and alkynes. *Medicinal research reviews*, 2008. 28(2): p. 278-308.
15. Miller, W.L. and R.J. Auchus, The molecular biology, biochemistry, and physiology of human steroidogenesis and its disorders. *Endocrine reviews*, 2010. 32(1): p. 81-151.

16. Anstead, G.M., K.E. Carlson, and J.A. Katzenellenbogen, The estradiol pharmacophore: ligand structure-estrogen receptor binding affinity relationships and a model for the receptor binding site. *Steroids*, 1997. 62(3): p. 268-303.
17. Ahmed, M.S., L.C. Kopel, and F.T. Halaweish, Structural Optimization and Biological Screening of a Steroidal Scaffold Possessing Cucurbitacin-Like Functionalities as B-Raf Inhibitors. *ChemMedChem*, 2014. 9(7): p. 1361-1367.
18. Kopel, L.C., M.S. Ahmed, and F.T. Halaweish, Synthesis of novel estrone analogs by incorporation of thiophenols via conjugate addition to an enone side chain. *Steroids*, 2013. 78(11): p. 1119-1125.
19. Solum, E.J., A. Vik, and T.V. Hansen, Synthesis, cytotoxic effects and tubulin polymerization inhibition of 1, 4-disubstituted 1, 2, 3-triazole analogs of 2-methoxyestradiol. *Steroids*, 2014. 87: p. 46-53.
20. Clement, O.O., et al., Three dimensional pharmacophore modeling of human CYP17 inhibitors. Potential agents for prostate cancer therapy. *Journal of medicinal chemistry*, 2003. 46(12): p. 2345-2351.
21. Dhyani, M.V., et al., Preparation and preliminary bioevaluation of  $^{99m}\text{Tc}$  (CO) 3-11 $\beta$ -progesterone derivative prepared via click chemistry route. *Nuclear medicine and biology*, 2010. 37(8): p. 997-1004.
22. Agalave, S.G., S.R. Maujan, and V.S. Pore, Click Chemistry: 1, 2, 3-Triazoles as Pharmacophores. *Chemistry—An Asian Journal*, 2011. 6(10): p. 2696-2718.

23. Kharb, R., P.C. Sharma, and M.S. Yar, Pharmacological significance of triazole scaffold. *Journal of enzyme inhibition and medicinal chemistry*, 2011. 26(1): p. 1-21.
24. Bohacek, R.S., C. McMartin, and W.C. Guida, The art and practice of structure-based drug design: A molecular modeling perspective. *Medicinal research reviews*, 1996. 16(1): p. 3-50.
25. Csermely, P., et al., Structure and dynamics of molecular networks: a novel paradigm of drug discovery: a comprehensive review. *Pharmacology & therapeutics*, 2013. 138(3): p. 333-408.
26. Ekins, S., J. Mestres, and B. Testa, In silico pharmacology for drug discovery: applications to targets and beyond. *British journal of pharmacology*, 2007. 152(1): p. 21-37.
27. Kitchen, D.B., et al., Docking and scoring in virtual screening for drug discovery: methods and applications. *Nature reviews Drug discovery*, 2004. 3(11): p. 935-949.
28. Charifson, P.S., et al., Consensus scoring: A method for obtaining improved hit rates from docking databases of three-dimensional structures into proteins. *Journal of medicinal chemistry*, 1999. 42(25): p. 5100-5109.
29. Leach, A.R., Ligand docking to proteins with discrete side-chain flexibility. *Journal of molecular biology*, 1994. 235(1): p. 345-356.

30. Brooijmans, N. and I.D. Kuntz, Molecular recognition and docking algorithms. *Annual review of biophysics and biomolecular structure*, 2003. 32(1): p. 335-373.
31. Huang, S.-Y. and X. Zou, Advances and challenges in protein-ligand docking. *International journal of molecular sciences*, 2010. 11(8): p. 3016-3034.
32. Kroemer, R.T., Structure-based drug design: docking and scoring. *Current protein and peptide science*, 2007. 8(4): p. 312-328.
33. Kulkarni, S. and J.K. Savsaviya, Study of a High-risk Group of Stage 2 Colon Cancer.
34. Siegel, R.L., K.D. Miller, and A. Jemal, Cancer statistics, 2016. *CA: a cancer journal for clinicians*, 2016. 66(1): p. 7-30.
35. Majumdar, S.R., R.H. Fletcher, and A.T. Evans, How does colorectal cancer present? Symptoms, duration, and clues to location. *The American journal of gastroenterology*, 1999. 94(10): p. 3039-3045.
36. Cohen, S., Isolation of a mouse submaxillary gland protein accelerating incisor eruption and eyelid opening in the new-born animal. *Journal of Biological Chemistry*, 1962. 237(5): p. 1555-1562.
37. Yarom, N. and D.J. Jonker, The role of the epidermal growth factor receptor in the mechanism and treatment of colorectal cancer. *Discovery medicine*, 2011. 11(57): p. 95-105.

38. Alroy, I. and Y. Yarden, The ErbB signaling network in embryogenesis and oncogenesis: signal diversification through combinatorial ligand-receptor interactions. *FEBS letters*, 1997. 410(1): p. 83-86.
39. Muthuswamy, S.K., M. Gilman, and J.S. Brugge, Controlled dimerization of ErbB receptors provides evidence for differential signaling by homo- and heterodimers. *Molecular and cellular biology*, 1999. 19(10): p. 6845-6857.
40. Boudewijn, M. and P.J. Coffey, Protein kinase B (c-Akt) in phosphatidylinositol-3-OH kinase signal transduction. *Nature*, 1995. 376(6541): p. 599.
41. Chan, T.O., S.E. Rittenhouse, and P.N. Tsichlis, AKT/PKB and other D3 phosphoinositide-regulated kinases: kinase activation by phosphoinositide-dependent phosphorylation. *Annual review of biochemistry*, 1999. 68(1): p. 965-1014.
42. Petit, A., et al., Neutralizing antibodies against epidermal growth factor and ErbB-2/neu receptor tyrosine kinases down-regulate vascular endothelial growth factor production by tumor cells in vitro and in vivo: angiogenic implications for signal transduction therapy of solid tumors. *The American journal of pathology*, 1997. 151(6): p. 1523.
43. Engebraaten, O., et al., Effects of EGF, BFGF, NGF and PDGF (bb) on cell proliferative, migratory and invasive capacities of human brain-tumour biopsies *In Vitro*. *International journal of cancer*, 1993. 53(2): p. 209-214.
44. Douillard, J.-Y., et al., Randomized, phase III trial of panitumumab with infusional fluorouracil, leucovorin, and oxaliplatin (FOLFOX4) versus FOLFOX4 alone

as first-line treatment in patients with previously untreated metastatic colorectal cancer: the PRIME study. *Journal of clinical oncology*, 2010. 28(31): p. 4697-4705.

45. Winawer, S., et al., Colorectal cancer screening and surveillance: clinical guidelines and rationale—update based on new evidence. *Gastroenterology*, 2003. 124(2): p. 544-560.

46. Popat, S., R. Hubner, and R. Houlston, Systematic review of microsatellite instability and colorectal cancer prognosis. *Journal of Clinical Oncology*, 2005. 23(3): p. 609-618.

47. Renehan, A.G., et al., Impact on survival of intensive follow up after curative resection for colorectal cancer: systematic review and meta-analysis of randomised trials. *Bmj*, 2002. 324(7341): p. 813.

48. Figueredo, A., et al., Adjuvant therapy for stage II colon cancer: a systematic review from the Cancer Care Ontario Program in evidence-based care's gastrointestinal cancer disease site group. *Journal of clinical oncology*, 2004. 22(16): p. 3395-3407.

49. Raymond, E., et al., Oxaliplatin: a review of preclinical and clinical studies. *Annals of Oncology*, 1998. 9(10): p. 1053-1071.

50. Longley, D.B., D.P. Harkin, and P.G. Johnston, 5-fluorouracil: mechanisms of action and clinical strategies. *Nature Reviews Cancer*, 2003. 3(5): p. 330-338.

51. Twelves, C., et al., Capecitabine as adjuvant treatment for stage III colon cancer. *New England Journal of Medicine*, 2005. 352(26): p. 2696-2704.

52. Scoggins, C.R., et al., Nonoperative management of primary colorectal cancer in patients with stage IV disease. *Annals of surgical oncology*, 1999. 6(7): p. 651-657.
53. August, D.A., R.T. Ottow, and P.H. Sugarbaker, Clinical perspective of human colorectal cancer metastasis. *Cancer and metastasis reviews*, 1984. 3(4): p. 303-324.
54. Graham, M.A., et al., Clinical pharmacokinetics of oxaliplatin: a critical review. *Clinical Cancer Research*, 2000. 6(4): p. 1205-1218.
55. Salonga, D., et al., Colorectal tumors responding to 5-fluorouracil have low gene expression levels of dihydropyrimidine dehydrogenase, thymidylate synthase, and thymidine phosphorylase. *Clinical Cancer Research*, 2000. 6(4): p. 1322-1327.
56. Hezel, A., et al., Phase II study of gemcitabine, oxaliplatin in combination with panitumumab in KRAS wild-type unresectable or metastatic biliary tract and gallbladder cancer. *British journal of cancer*, 2014. 111(3): p. 430-436.
57. Heggie, G.D., et al., Clinical pharmacokinetics of 5-fluorouracil and its metabolites in plasma, urine, and bile. *Cancer research*, 1987. 47(8): p. 2203-2206.
58. Raymond, E., et al. Oxaliplatin: mechanism of action and antineoplastic activity. in *Seminars in oncology*. 1998.
59. Woynarowski, J.M., et al., Sequence-and region-specificity of oxaliplatin adducts in naked and cellular DNA. *Molecular pharmacology*, 1998. 54(5): p. 770-777.

60. Markman, B., et al., EGFR and KRAS in colorectal cancer. *Advances in clinical chemistry*, 2010. 51: p. 72.
61. Kallander, L.S., et al., 4-Aryl-1, 2, 3-triazole: a novel template for a reversible methionine aminopeptidase 2 inhibitor, optimized to inhibit angiogenesis in vivo. *Journal of medicinal chemistry*, 2005. 48(18): p. 5644-5647.
62. Pagliai, F., et al., Rapid synthesis of triazole-modified resveratrol analogues via click chemistry. *Journal of medicinal chemistry*, 2006. 49(2): p. 467-470.
63. Lee, T., et al., Synthesis and evaluation of 1, 2, 3-triazole containing analogues of the immunostimulant  $\alpha$ -GalCer. *Journal of medicinal chemistry*, 2007. 50(3): p. 585-589.
64. Pisaneschi, F., et al., Development of a new epidermal growth factor receptor positron emission tomography imaging agent based on the 3-cyanoquinoline core: synthesis and biological evaluation. *Bioorganic & medicinal chemistry*, 2010. 18(18): p. 6634-6645.
65. Whiting, M., et al., Rapid discovery and structure- activity profiling of novel inhibitors of human immunodeficiency virus type 1 protease enabled by the copper (I)-catalyzed synthesis of 1, 2, 3-triazoles and their further functionalization. *Journal of medicinal chemistry*, 2006. 49(26): p. 7697-7710.
66. Costa, M.S., et al., Synthesis, tuberculosis inhibitory activity, and SAR study of N-substituted-phenyl-1, 2, 3-triazole derivatives. *Bioorganic & medicinal chemistry*, 2006. 14(24): p. 8644-8653.

67. Somu, R.V., et al., Rationally designed nucleoside antibiotics that inhibit siderophore biosynthesis of mycobacterium tuberculosis. *Journal of medicinal chemistry*, 2006. 49(1): p. 31-34.
68. Pore, V., *Tetrahedron* 2006, 62, 11178–11186; b) NG Aher, VS Pore, NN Mishra, A. Kumar, PK Shukla, A. Sharma, MK Bhat. *Bioorg. Med. Chem. Lett*, 2009. 19: p. 759-763.
69. Reck, F., et al., Novel substituted (pyridin-3-yl) phenyloxazolidinones: antibacterial agents with reduced activity against monoamine oxidase A and increased solubility. *Journal of medicinal chemistry*, 2007. 50(20): p. 4868-4881.
70. Reck, F., et al., Identification of 4-substituted 1, 2, 3-triazoles as novel oxazolidinone antibacterial agents with reduced activity against monoamine oxidase A. *Journal of medicinal chemistry*, 2005. 48(2): p. 499-506.
71. Sequist, L.V., et al., Genotypic and histological evolution of lung cancers acquiring resistance to EGFR inhibitors. *Science translational medicine*, 2011. 3(75): p. 75ra26-75ra26.
72. Sartore-Bianchi, A., et al., PIK3CA mutations in colorectal cancer are associated with clinical resistance to EGFR-targeted monoclonal antibodies. *Cancer research*, 2009. 69(5): p. 1851-1857.
73. Ryan, K.J., Biochemistry of aromatase: significance to female reproductive physiology. *Cancer research*, 1982. 42(8 Supplement): p. 3342s-3344s.

74. Ejembi, D.O., Comparative Study of the Effects of Aqueous Extracts of Moringa Oleifera and Vernonia Amygdalina Leaves on Some Biochemical Indices in Albino Rats. 2014, UNIVERSITY OF NIGERIA NSUKKA.
75. Chen, G.G., Q. Zeng, and G.M. Tse, Estrogen and its receptors in cancer. Medicinal research reviews, 2008. 28(6): p. 954-974.
76. Heldring, N., et al., Estrogen receptors: how do they signal and what are their targets. Physiological reviews, 2007. 87(3): p. 905-931.
77. Yeung, Y.-Y., R.-J. Chein, and E. Corey, Conversion of Torgov's synthesis of estrone into a highly enantioselective and efficient process. Journal of the American Chemical Society, 2007. 129(34): p. 10346-10347.
78. Ibrahim-Ouali, M., Recent advances in oxasteroids chemistry. Steroids, 2007. 72(6): p. 475-508.
79. Leese, M.P., et al., A-ring-substituted estrogen-3-O-sulfamates: potent multitargeted anticancer agents. Journal of medicinal chemistry, 2005. 48(16): p. 5243-5256.
80. Bodnár, B., et al., Synthesis and Biological Evaluation of Triazolyl 13 $\alpha$ -Estrone–Nucleoside Bioconjugates. Molecules, 2016. 21(9): p. 1212.
81. McGann, M., FRED pose prediction and virtual screening accuracy. Journal of chemical information and modeling, 2011. 51(3): p. 578-596.

82. Schulz-Gasch, T. and M. Stahl, Binding site characteristics in structure-based virtual screening: evaluation of current docking tools. *Journal of Molecular Modeling*, 2003. 9(1): p. 47-57.
83. de la Torre, M.C., et al., The Reversible Nicholas Reaction in the Synthesis of Highly Symmetric Natural-Product-Based Macrocycles. *European Journal of Organic Chemistry*, 2015. 2015(5): p. 1054-1067.
84. Boivin, R.P., et al., Structure– Activity Relationships of 17 $\alpha$ -Derivatives of Estradiol as Inhibitors of Steroid Sulfatase. *Journal of medicinal chemistry*, 2000. 43(23): p. 4465-4478.
85. Kasiotis, K.M., et al., High affinity 17 $\alpha$ -substituted estradiol derivatives: Synthesis and evaluation of estrogen receptor agonist activity. *Steroids*, 2006. 71(3): p. 249-255.

## Chapter Three

### Design, Synthesis and biological evaluation of novel estrone -1,4-disubstituted triazoles analogs targeting colorectal cancer

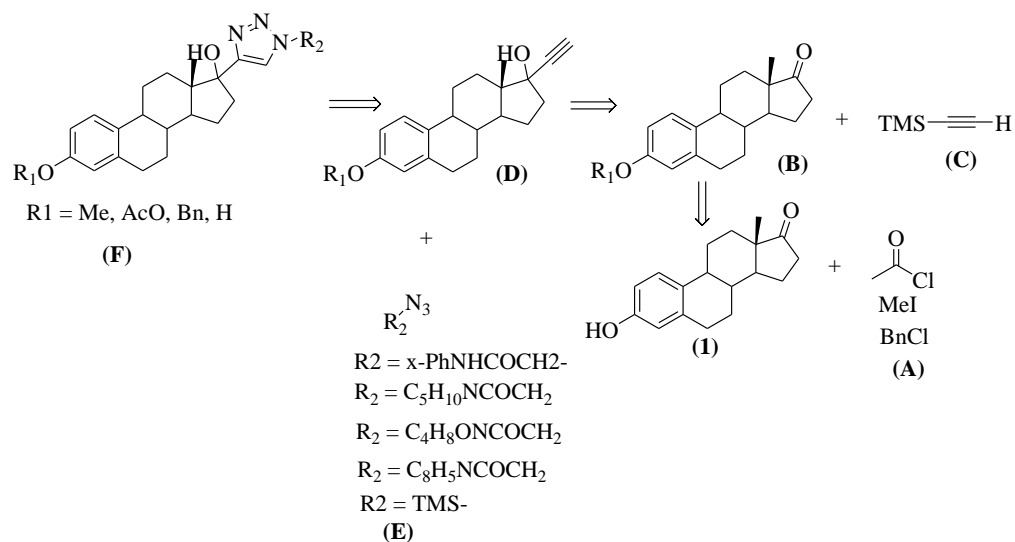
#### ABSTRACT

Colorectal cancer is the second death causing disease in the United States when men and women considered collectively. Epidermal Growth Factor Receptors (EGFRs) are over expressed in cancer cells. Targeting and blocking the downstream signaling could lead to cease cell proliferation and division and hence control the spread of the disease. 1,2,3-Disubstituted triazole as a pharmacophore showed a potency towards many diseases including cancer. Estradiols are a class of estrogen naturally occurring compounds and they are known for their penetration of the cell, therefore, incorporation of 1,2,3-triazole on a carrier such as estradiol could lead to drug discovery. A library of 1,2,3-triazole-estradiol-based analogs were designed and virtually screened with EGFRs utilizing OpenEye® as docking software. Among the designed candidates, fourteen 1,4-disubstituted triazole analogs of 3-functionalized estradiol were synthesized and biologically evaluated. MTT assay conducted on CRC cancer cell line shows cytotoxicity behavior for 5 compounds ranging from 3.5  $\mu\text{M}$  for FZ60 to 30  $\mu\text{M}$  for FZ518.

### 3.1. Introduction

Colorectal cancer is the second death causing disease in the United States when men and women considered collectively. Estrogens as a natural product compounds are biologically synthesized by the human body through multiple processes starting from cholesterol as starting material [15]. Among estrogen class of compounds are estrone and estradiol, which are identified pharmacophores for the estrogen receptors ER [16]. Furthermore, many investigations in the estrone-based drug design, have found candidates with a high potency and specificity towards cancer cells such as ovarian, prostate and breast cancer [17-19]. Among these investigations, Ahmad et al., 2014 assembled the pharmacophore that is responsible for the cytotoxicity of cucurbitacin D on estrone as carrier skeleton [17]. Around these facts, a hypothesis was developed assuming that utilizing click chemistry to generate a triazole pharmacophore carried by a steroidal skeleton may lead to novel drug candidates for CRC. This hypothesis was backed by finding from other data obtained from Solum et al., 2014, in tubulin polymerization inhibition as well as cytotoxicity activity utilizing estradiol-triazole moieties [19].

Many researchers used the same approach to discover new drug candidates; for example, a number of steroidal moieties bearing triazole pharmacophore to inhibit human CYP17 targeting prostate cancer with  $IC_{50}$  ranging from 50-12000 nM [20]. Another example of utilizing the same approach is observed in incorporation of triazole pharmacophore on progesterone, another steroidal hormone, on position 11 by Dhyania et al., [21, 22]. Molecular docking data described in chapter 2 was used to determine the binding modes of the designed library of 800 compounds. The



**Scheme 3.1.** The retrosynthetic analysis of the designed triazole bearing inhibitors.

A library was virtually screened with Epidermal Growth Factor Receptors (EGFRs) starting from extracellular domain to downstream signaling pathway. A library of hits ranked based on their consensus scoring was obtained and the mode of actions of these hits is described in section **2.4.1-2.4.3**. The aim of this study is to design, synthesize and biologically evaluate a novel estrone-based triazoles targeting colorectal cancer.

**Scheme 3.1** shows the retrosynthetic route of the designed drug candidates. Where reaction of estrone (**1**) with alkylation agents (**A**) to afford different functionality groups at C-3(**B**). Consequently, reaction with ethynyltrimethylsilane (**C**) to afford the alkyne (**D**) necessary to react with organic azides (**E**) to generate the triazole-estradiol final hits (**F**).

## 3.2. Material and methods

### 3.2.1. General material and methods

$^1\text{H}$  and  $^{13}\text{C}$  NMR spectra were acquired on a Bruker AVANCE-400 MHz NMR spectrometer, in deuterated solvents such as  $\text{CDCl}_3$  using solvent residual peak as the internal standard for  $^1\text{H}$  NMR ( $\delta=7.24$  ppm) and  $\text{CDCl}_3$  ( $\delta = 77.16$  ppm) for  $^{13}\text{C}$  NMR, with the reporting of coupling constants in Hz and the signal multiplicities are reported as singlet (s), doublet (d), triplet (t), quartet (q), doublet of doublets (dd), doublet of triplets (dt), multiplet (m), or broad (br). HRMS data was obtained using EI ionization on a ThermoFinnigan MAT 95 XL mass spectrometer. TLC analysis was performed using pre-coated silica gel PE sheets. Products were purified via column chromatography using silica gel 40–63  $\mu\text{m}$  (230–400 mesh), normal phase preparative TLC plates. TLC plates were visualized by ultraviolet at 254 nm. TLC plates were stained by Iodine, Vanillin, and Ceric Ammonium Molybdate (CAM) stain. All reagents and solvents were obtained from commercial suppliers and used as received. All chemical reactions requiring anhydrous conditions were performed with oven-dried glassware under an atmosphere of nitrogen.

### 3.2.2 Cytotoxicity Assay:

The colon cancer cells line HT<sub>29</sub> were seeded in 96-well plate as  $5 \times 10^4$  cells/mL (100  $\mu\text{L}$ /well). A serial dilution of compounds was added after overnight incubation of the cells at 37°C and 5%  $\text{CO}_2$ . DMSO was used as a control (0.1 %). The cells were incubated with the synthesized compounds for 48 hrs. After that 15  $\mu\text{L}$  of 3-(4,5-dimethylthiazol-2-yl)-2,5-diphenyl tetrazolium bromide (MTT) (5 mg/mL PBS) were added to each well and

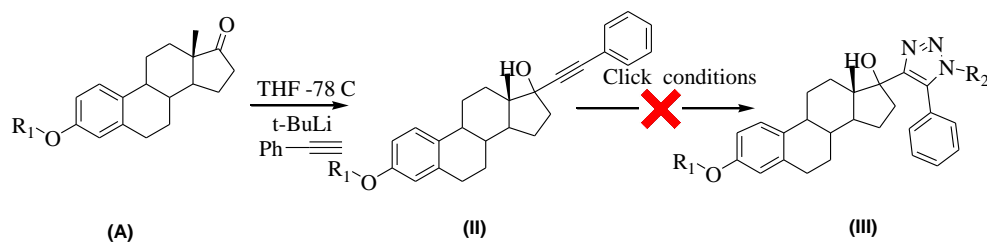
the plates were incubated for another 4 hrs. The formazan crystals were solubilized by 100  $\mu$ L acidified SDS solution (10% SDS/0.01 N HCl). The absorbance was measured after 14 hrs of incubation at 37°C and 5% CO<sub>2</sub> at 570 nm by Biotech plate reader.

### 3.3. Result and discussion

The final selected strategy for acquiring the 1,2,3-triazole ring on position 17 of the estrone was designed through assembling an alkyne group on the desired position, **Scheme 3.1**. [82]. Typically, this reaction is classified as addition reaction to a carbonyl group, which requires a harsh condition to achieve. Many alkyne moieties were incorporated to the desired position, including propargyl alcohol and phenyl acetylene moieties [83, 84]. Additionally, the protection step was aimed to ease the separation step as the tert-butyl dimethylsilyl ethers (OTBS) group increases the lipophilicity of the titled compound **(2)** **section 3.5.1**. Formation of organic azides was conducted under high caution, as organic azides are usually explosive and photosensitive [85].

#### 3.3.1. Synthesis of 17 $\alpha$ alkynyl estradiols

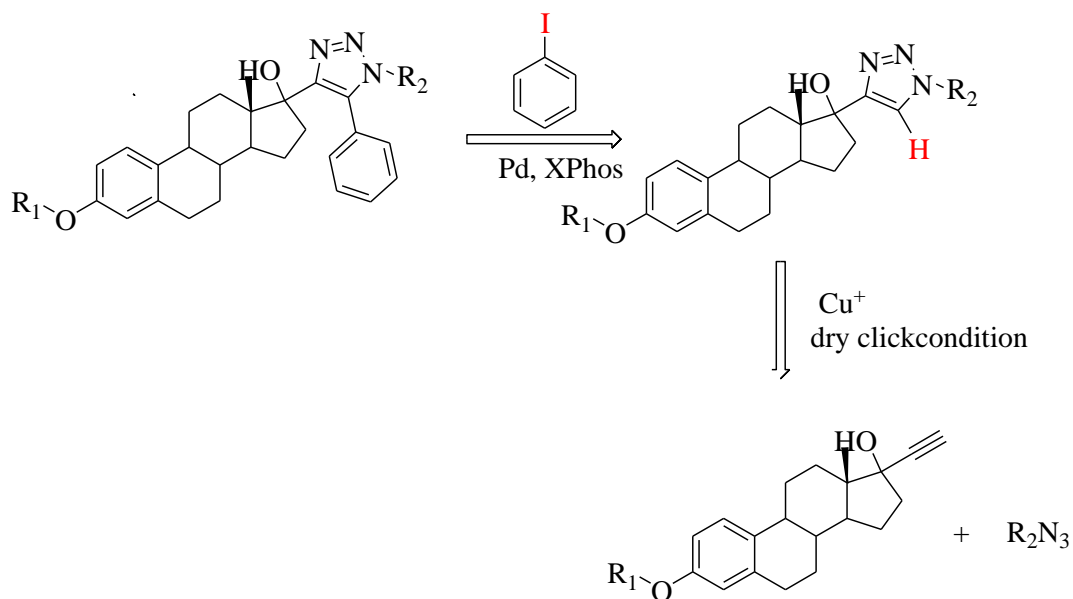
It is worth to point out that click chemistry reactions only can be conducted on terminal alkynes to result in 1,4-disubstituted triazoles. However, 1,4,5-trisubstituted triazoles were designed as if the click reaction on internal alkynes (phenyl acetylene and propargyl alcohol reactions) proceeds; in other words, the design of the phenyl-triazole derivatives was performed as compound **(III)** can be obtained from the click reaction on **(II)** (**scheme 3.2**); however, this is not possible and hence a proposed retrosynthetic scheme was formed **Scheme 3.3A-B**.



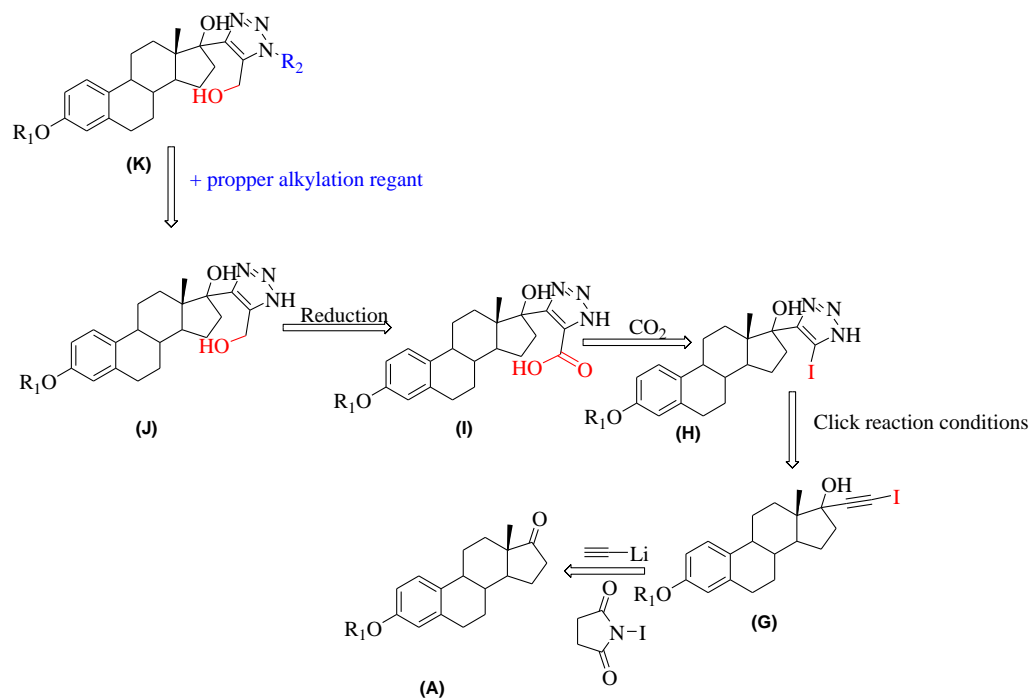
**Scheme 3.2.** the click reaction cannot proceed on internal alkynes; however, the result of the inert reaction was considered in the design of novel inhibitors and alternative proposed scheme was designed.

Although the majority of the library hits showed that the 1,4-disubstituted triazoles have higher binding scoring. However, attempts to synthesize phenyl-triazole derivatives were conducted utilizing one pot reaction, by first, generating the 1,4-disubstituted triazole in situ and subsequently reaction with phenyl substituent to occupy position five of the triazole ring utilizing Pd as a catalyst. **Scheme 3.3A.**

Generation of 1,4-disubstituted triazoles was started with the reaction of estrone (1) with TBSCl to afford the protected estrone (2), which subsequently was subjected to alkyne addition to generate and then cleavage of protecting groups to result in 17 $\alpha$  substituted estradiols (3) **section 3.4. 2.** [82-84]. On the other hand, the aromatic amines and heterocyclic amines were subjected to acylation reaction utilizing chloroacetyl chloride and subsequently convert the resulting  $\alpha$ -chloro amides to  $\alpha$ -azido amides by the reaction with sodium azide.



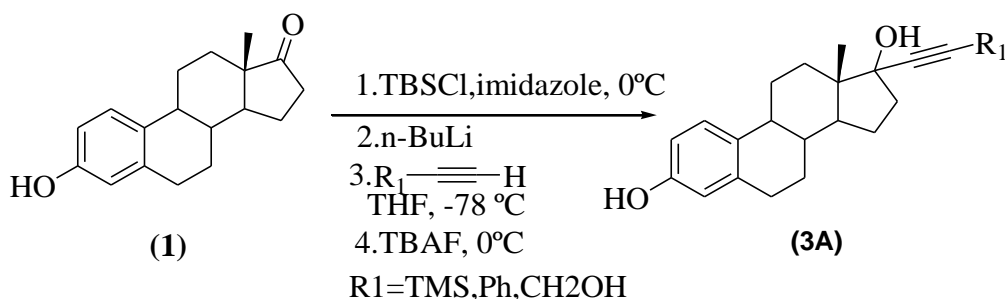
**Scheme 3.3A.** The retrosynthetic analysis of one pot reaction to afford 1,2,3-trisubstituted triazole.

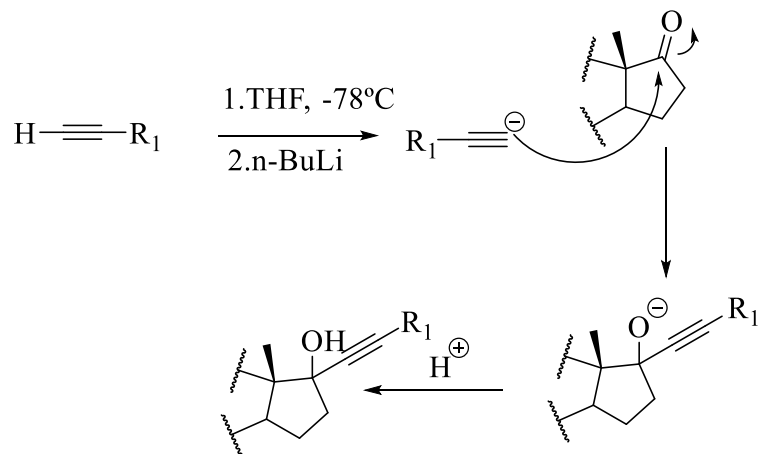


**Scheme 3.3B.** The retrosynthetic analysis of preparation of C5' carbinol triazole.

The proposed scheme for the fully substituted triazole is presented below in Scheme 3.3A-B where the substitution with phenyl group can be obtained by the one pot reaction [86]. On the other hand, the carbinolic group can be introduced by generation of iodoalkyne (**G**) and then subsequent reaction in a click reaction manner to generate 5-iodo-1,4-disubstituted triazole (**H**) and subsequently introduce a carboxyl group to generate compound (**I**) by reaction with CO<sub>2</sub> and finally reduce the carboxyl group with proper reducing agent to the corresponding alcohol (**J**) [87-90]. The strategy for the carbinol bearing triazoles must take in consideration the assembly of the N1' substituent later after

assembling the triazole ring with functionalized C5', to put it differently it must take in consideration alkylation of N1' of triazole after reducing the carboxyl group to avoid reduction of amide [91].



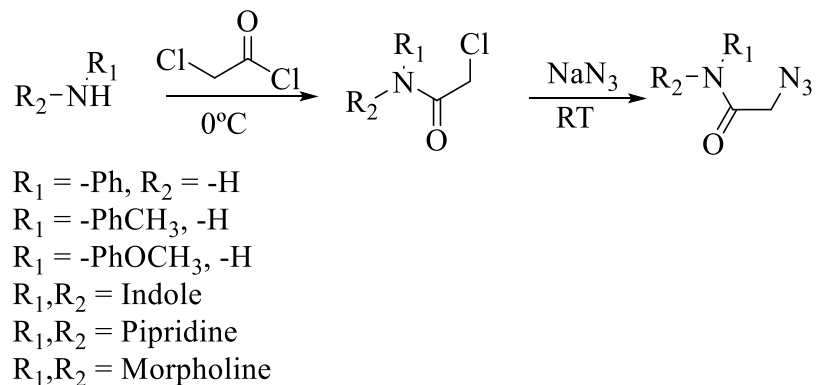


**Scheme 3.3:** Mechanism of nucleophilic addition to carbonyl group.

### 3.3.2. Synthesis of organic azides

Molecular modeling design showed diversity in the azides attached to different amines. Therefore, a general scheme for the azide preparation starts from the chloroacylation of amines and subsequent azidation utilizing  $\text{S}_{\text{N}}2$  reaction mechanism.

**Scheme 3.4** shows the general method for preparation of organic azide. chloroacylation of aromatic heterocyclic amines (indole 33%) was obtained in low yield as comparison to aromatic amines (e.g. aniline 95%) due to the resonance of the lone pair on the nitrogen atom of indole. The chloroacylation of aliphatic heterocyclic amines (morpholine and piperidine) was obtained in high yield in comparison to indole, since the lone pair is not in resonance in the heterocyclic ring.



**Scheme 3.4:** General method of preparation of organic azides.

### 3.3.3. Cytotoxicity results

The synthesized compounds showed variable cytotoxic behavior in comparison to the standard 5-FU ( $\text{IC}_{50}$  17.3  $\mu\text{M}$ ). Functionalization of position 3 of the steroidal skeleton with non-polar groups (Me, Bn) show no toxicity. On the contrary, polar functional groups at C-3 showed ant proliferative cytotoxicity toward HT-29 cell line. In case of the presence of OH group in addition to aromatic amine attached to the triazole, the cytotoxicity was as follow: FZ60  $\text{IC}_{50}$  3.5  $\mu\text{M}$ , FZ300  $\text{IC}_{50}$  18  $\mu\text{M}$ , FZ 313  $\text{IC}_{50}$  25  $\mu\text{M}$ , and FZ 518  $\text{IC}_{50}$  30  $\mu\text{M}$ . alternatively, in presence of OAC group, for example, FZ 200, showed  $\text{IC}_{50}$  13  $\mu\text{M}$ .

It is clear that the polarity of position 3 of the steroidal skeleton as well as the ring orientation of the aromatic amine attached to the triazole ring at position 17 are contributing factors in the cytotoxicity behavior. **Table 3.1** shows the  $\text{IC}_{50}$  values in

comparison to 5-FU in the HT-29 cell line. **Figure 3.1** shows FZ 60 in 3MOV binding pocket with all hydrogen bonds involved in the binding.

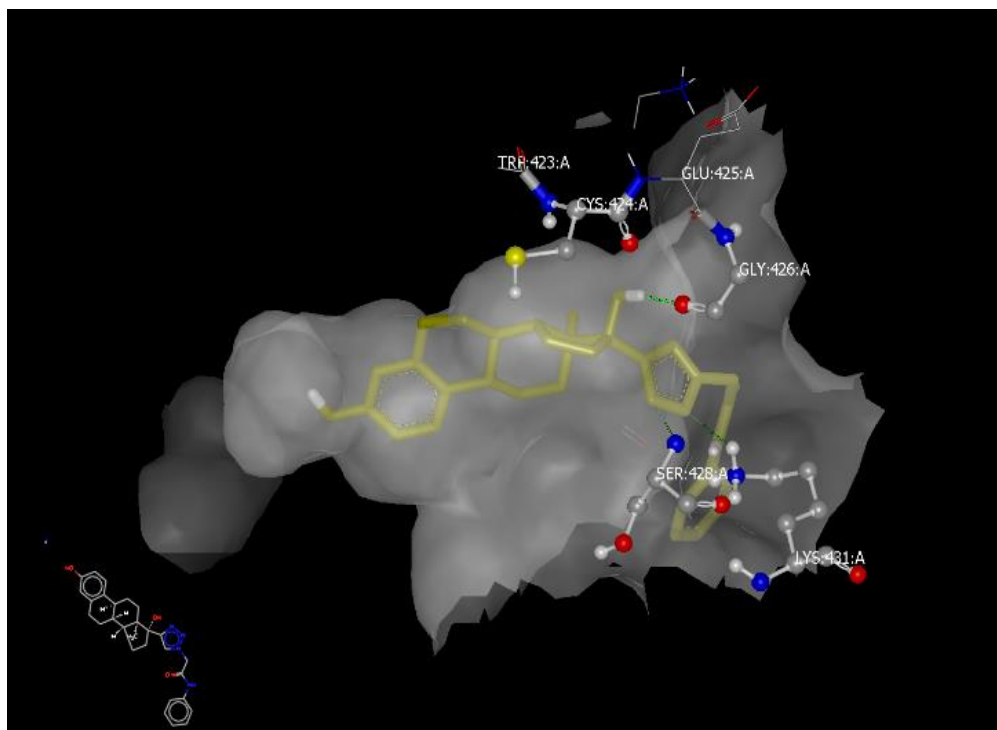


**Figure 3.1.** FZ60 binds with GLY426A utilizing OH group at C17. Another hydrogen bonding by utilizing N2 and N3 of the triazole ring with LYS431A and SER428A respectively.

**Table 3.1:** The IC<sub>50</sub> values in HT-29 of the designed estradiol-triazole derivatives in comparison to 5-FU.

no	Compound	IC <sub>50</sub>	C-3 functionality	Group attached to triazole
1	FZ60	3.5 μM	OH	aniline
2	FZ200	10 μM	OAC	aniline
3	FZ300	18 μM	OH	p-Anisidine
4	FZ313	25 μM	OH	p-toludine
5	F3518	30 μM	OH	indole
6	FZ400	No cytotoxicity	Bn	p-toludine
7	FZ57	No cytotoxicity	Bn	aniline
8	FZ516	No cytotoxicity	Me	indole
9	FZ514	No cytotoxicity	AC	indole
10	FZ25	No cytotoxicity	Bn	No group attached
11	FZ552	No cytotoxicity	Me	pipridine
12	FZ100	No cytotoxicity	OH	morpholine
13	FZ600	No cytotoxicity	OH	pipridine
14	FZ550	No cytotoxicity	AC	pipridine
15	5-FU	17.3 μM	-	-

### 3.4. Conclusion

Fourteen analogs bearing 1.2.3-triazole were chosen for synthesis based on their consensus scores. The synthetic strategy of modifications of the steroidal skeleton starts from the generation of 17 $\alpha$  ethynyl estradiol to obtain an alkyne functionality that can be utilized in the click chemistry subsequently through azide coupling. Functionality in C5' of the triazole ring could be achieved by three components click reaction catalyzed

by Cu/Pd to obtain a C5' functionalized with a phenyl ring, or could be achieved by assembling 5-iodotriazole and converting the C5' iodotriazole to carbinol, by carboxylation then reduction respectively. Estrone was chosen for the modification for two reasons mainly, first: estrone is recognized by the human body and can penetrate the cell; consequently, it can deliver the triazole pharmacophore to targeted receptors and secondly, modification of estrone leads to a dramatical change in the biological activity, which opens the door for drug discovery. Biological evaluation was conducted on the novel compounds and showed a fair cytotoxicity in CRC cell lines by MTT assay.

#### 3.4.1. Future work and Recommendations

Our study demonstrated the potential of design and synthesis of 1,4-disubstituted triazole targeting colorectal cancer. Optimization of triazole analogs ring in C5' has the potential to produce and enhance the biological activities, which is highly correlated to the polarity and lipophilicity. This can clearly control the orientation of the drug inside the binding pocket, which is a contributing factor in the biological activity. Further optimization of the biological activity is necessary and would be beneficial to start by optimizing the novel analogs FZ60 to enhance the anticancer activity. Focusing on the most active analogs at this point is the best strategy and line up with all recent approaches in drug design.

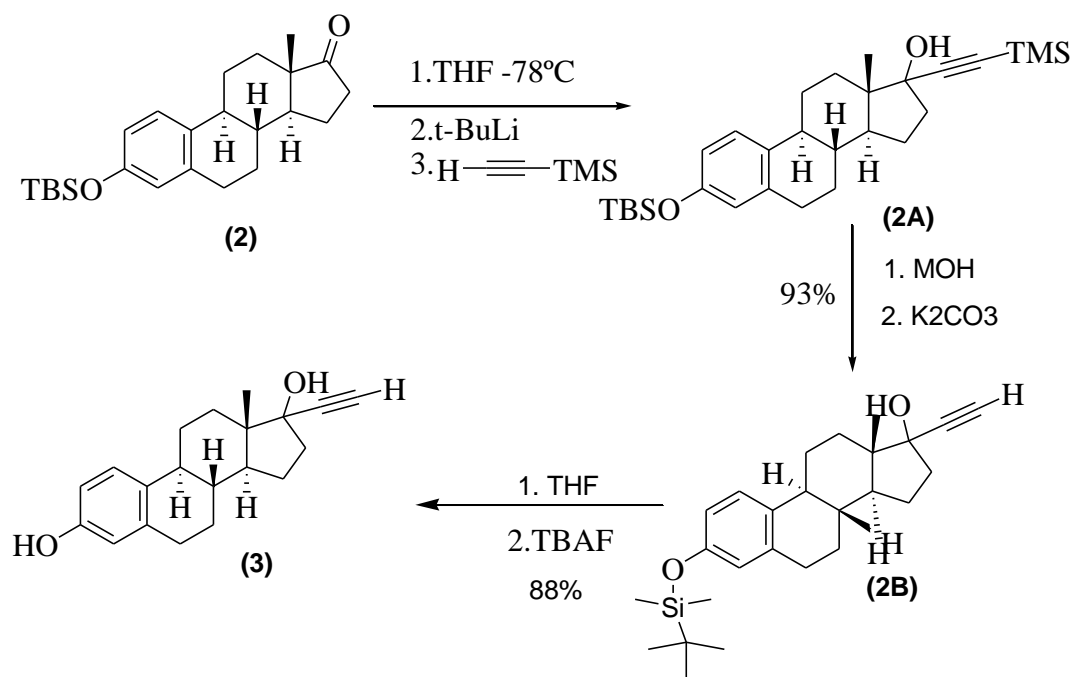
### 3.5 Experimental section

#### 3.5.1. 3-OTBS protected estrone (2)



To a serried solution of Estrone (1.0g, 3.7 mmol) in DMF 18 ml 3.9 eq of imidazole and TBSCl 1.5 eq were added. The reaction was left overnight and then quenched with ammonium chloride and extracted with ethylacetate 3x. The organic layers were collected evaporated and flash column was used to purify the resulting compound using hexane: ethylacetate 9:1 yeilded 100% of compound (1).

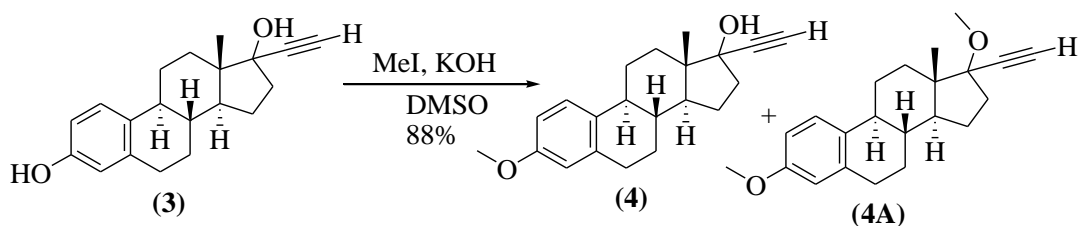
### 3.5.2. 17 $\alpha$ ethynyl estradioil (3)



To a serried solution of ethynyltrimethylsilane (27.75 mmol) in dry THF (150 ml) t-BuLi (27.75 mmol) was added drop wise at -78 °C under Nitrogen. The reaction was

stirred for 2hrs under this condition and allowed to reach 0°C. Then 5.55 mmol of estrone (2) in 50 mL THF was added drop wise. The reaction was allowed to reach room temperature and after the completion of the reaction it was quenched with saturated ammonium chloride at 0°C. The resulting mixture was extracted with ethylacetate 3x . The organic layer was combined and washed with brine, dried over Na<sub>2</sub>SO<sub>4</sub> and reduced under *vaccum*. The crude compound (2A) dissolved in 25 mL MeOH and was moved to the next step without purification. K<sub>2</sub>CO<sub>3</sub> (50 mmole) was added in one portion to (2A) for 2h to generate (2B) in 93% yield the product was purified by silica gel chromatography hexane/ethyl acetate 9:1 – 8:2. Finally (2B) was subjected to the reaction with 2eq of TBAF for 8h and after completion of the reaction, the reaction was quenched with ammonium chloride at 0°C purified through silica gel chromatography hexane/ethyl acetate 9:1 – 8:2 yielding 93% of the titled compound (3). The product was proved by <sup>1</sup>H-<sup>13</sup>C NMR.

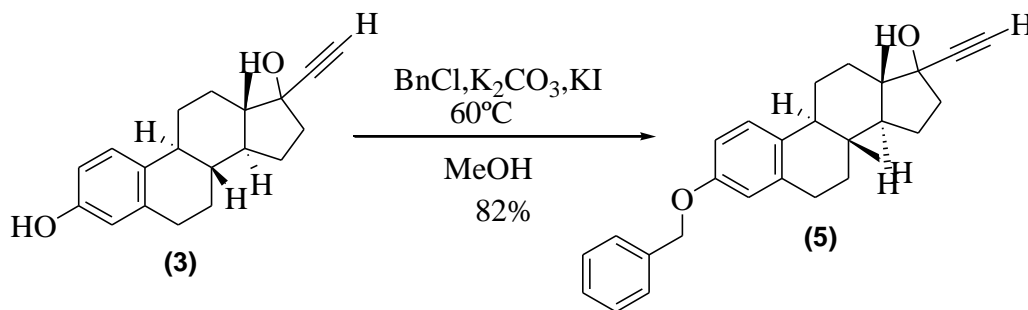
### 3.5.3. Ethynyl estradiol-3-methyl ether (Mestranol) (4)



To a stirred solution of (3) (1.61 mmol) in DMSO (6.5 ml), 6.44 mmol of KOH was added followed by addition of 1.61 mmol of MeI. The reaction was stirred for 2h under nitrogen. After the reaction completion, it was extracted with DCM 3x, washed with brine and dried over Na<sub>2</sub>SO<sub>4</sub>. The organic solvent was reduced under *vaccum*. Silica

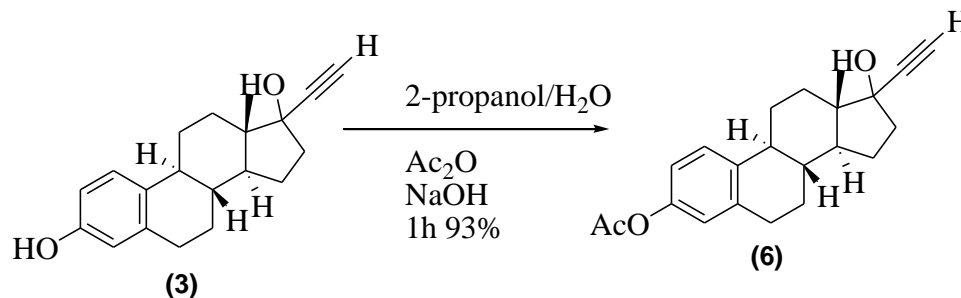
gel column chromatography (hexane/EtOAc 8:2) was used to purify the mixture to yield compound (**4**) 88%. The product was proved by  $^1\text{H}$ - $^{13}\text{C}$  NMR.

#### 3.5.4. Ethynyl estradiol-3-methyl benzyl ether (**5**)



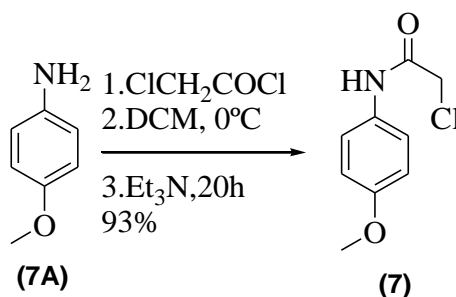
To a stirred solution of (**3**) (1.08 mmol) in dry  $\text{MeOH}$  (0.5 ml) and 6.44 mmol  $\text{K}_2\text{CO}_3$  (1.18mmol) was added as one portion followed by addition of 1.18 mmol of  $\text{KI}$ . The reaction was stirred for 30 min under reflux at  $50^\circ\text{C}$ . After the reaction completion, the reaction was extracted with  $\text{DCM}$  3x, washed with brine and dried over  $\text{Na}_2\text{SO}_4$ . The organic solvent was reduced under *vacuum* and silica gel column chromatography (hexane/ $\text{EtOAc}$  8:2) was used to purify the mixture to yield compound (**5**) 82%. The product was proved by  $^1\text{H}$ - $^{13}\text{C}$  NMR.

#### 3.5.5. ethynyl estradiol-3-acetate (**6**)



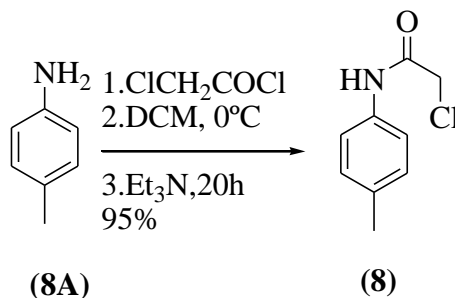
1.7 mmol of compound **(3)** dissolved in isopropanol 12.5 mL containing 0.185 g of NaOH dissolved in 2.5 mL H<sub>2</sub>O was stirred and 0.5 mL of acetic anhydride was added gradually. After the reaction completion, the reaction was extracted with DCM 3x, washed with brine and dried over Na<sub>2</sub>SO<sub>4</sub>. The organic solvent was reduced under *vaccum* and silica gel column chromatography (hexane/EtOAc 8:2) was used to purify the mixture to yield compound **(6)** 82%. The product was proved by <sup>1</sup>H-<sup>13</sup>C NMR.

### 3.5.6. 2-chloro-N-(4-methoxyphenyl)acetamide (**7**)



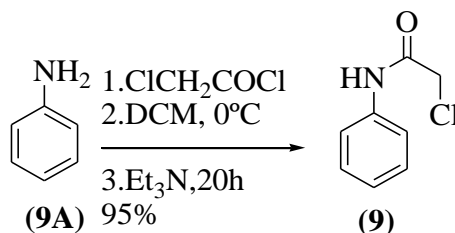
To a solution of p-anisidine (**7A**)(5.4 mmol) in 10 ml dichloromethane and triethylamine (10.75 mmol, 1.5 ml) chloroacetyl chloride (1 mmol ,0.44 ml) was added dropwise at 0°C under nitrogen atmosphere and vigorous stirring. The reaction was then allowed to reach room temperature for 20h. After the reaction completion the reaction was quenched with ammonium chloride and washed with 20 ml ethyl acetate 3X. the organic layers were combined and washed with saturated sodium chloride and dried over sodium sulfate anhydrous. The product was purified using silica gel column chromatography hexane: ethyl acetate 9:1 to yield 2-chloro-N-phenylacetamide (**7**) 93%. The product was proved by <sup>1</sup>H-<sup>13</sup>C NMR.

### 3.5.7. 2-chloro-N-(p-tolyl)acetamide (**8**)



To a solution of p-toluidine (5.4 mmol) (**8A**) in 10 ml dichloromethane and triethylamine (10.75 mmol, 1.5 ml) chloroacetyl chloride (1 mmol, 0.44 ml) was added dropwise at 0°C under nitrogen atmosphere and vigorous stirring. The reaction was then allowed to reach room temperature for 20h. after the reaction completion the reaction was quenched with ammonium chloride and washed with 20 ml ethyl acetate 3X. the organic layers were combined and washed with saturated sodium chloride and dried over sodium sulfate anhydrous. The product was purified using silica gel column chromatography hexane: ethyl acetate 9:1 to yield 2-chloro-N-phenylacetamide (**8**) 95%. The product was proved by  $^1\text{H}$ - $^{13}\text{C}$  NMR.

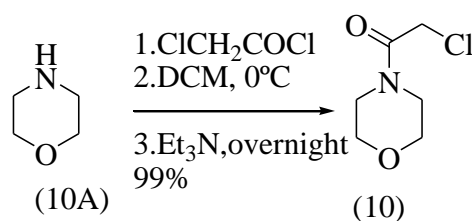
### 3.5.8. 2-chloro-N-phenylacetamide (**9**)



To a solution of aniline (**9A**) (51 mmol, 2ml) in 56 ml dichloromethane and triethylamine (102 mmol, 14.2 ml) chloroacetyl chloride (1.5 mmol, 6.1ml) was added dropwise at 0°C under nitrogen atmosphere and vigorous stirring. The reaction was then allowed to reach room temperature for 20h. after the reaction completion the reaction was

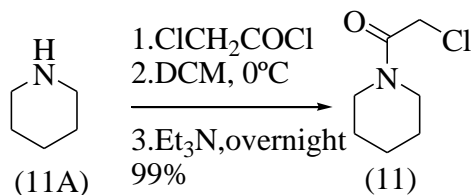
quenched with ammonium chloride and washed with 20 ml ethyl acetate 3X. the organic layers were combined and washed with saturated sodium chloride and dried over sodium sulfate anhydrous. The product was purified using silica gel column chromatography hexane: ethyl acetate 9:1 to yield 2-chloro-N-phenylacetamide (**9**) 98%. The product was proved by  $^1\text{H}$ - $^{13}\text{C}$  NMR.

### 3.5.9. 2-chloro-1-morpholinoethan-1-one (10)



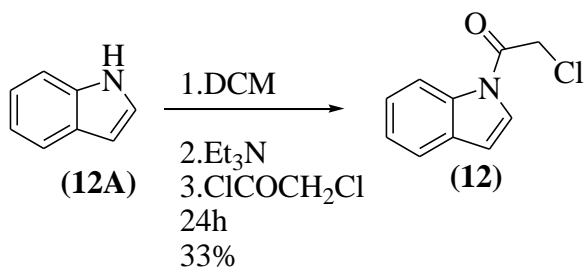
To a solution of morpholine (**10A**) (6.4 mmol, 0.5 ml) dissolved 10 ml dichloromethane and triethylamine (1.3 mmol, 1.7 ml) chloroacetyl chloride (9.6 mmol, 0.76 ml in 2.33ml DCM ) was added dropwise at  $0^\circ\text{C}$  under nitrogen atmosphere and vigorous stirring. The reaction was then allowed to reach room temperature for overnight. after the reaction completion the reaction was quenched with ammonium chloride and washed with 20 ml ethyl acetate 3X. the organic layers were combined and washed with saturated sodium chloride and dried over sodium sulfate anhydrous. The product was purified using silica gel column chromatography hexane: ethyl acetate 9:1 1 to yield 2-chloro-N-phenylacetamide (**10**) 99%. The product was proved by  $^1\text{H}$ - $^{13}\text{C}$  NMR.

### 3.5.10. 2-chloro-1-(piperidin-1-yl)ethan-1-one (11)



To a solution of piperidine (**11A**) (6 mmol, 0.5 ml) dissolved 18 ml dichloromethane and triethylamine (12 mmol, 2 ml) chloroacetyl chloride (8.8 mmol, 0.76) was added dropwise at 0°C under nitrogen atmosphere and vigorous stirring. The reaction was then allowed to reach room temperature for overnight. After the reaction completion, the reaction was quenched with ammonium chloride and washed with 20 ml ethyl acetate 3X. the organic layers were combined and washed with saturated sodium chloride and dried over sodium sulfate anhydrous. The product was purified using silica gel column chromatography hexane: ethyl acetate 9:1 to yield 2-chloro-N-piperidin-2-ylacetamide (**11**) 99%

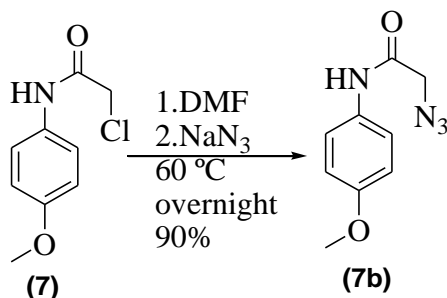
### 3.5.11. 2-chloro-1-(1H-indol-1-yl)ethan-1-one (**12**)



To a solution of indole (**12A**) (12.8 mmol, 1.5 g) dissolved 42 ml dichloromethane and triethylamine (12 mmol, 0.6 ml) chloroacetyl chloride (7.5 mmol, 1.7 ml) was added dropwise at 0°C under nitrogen atmosphere and vigorous stirring. The reaction was then allowed to reach room temperature for 24h. The reaction was quenched with ammonium chloride and washed with 20 ml ethyl acetate 3X. The organic layers were combined and washed with saturated sodium chloride and dried over sodium sulfate anhydrous. The

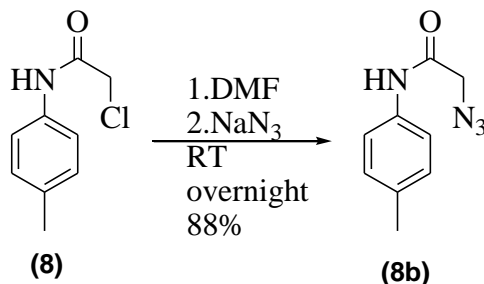
product was purified using silica gel column chromatography hexane: ethyl acetate 9:1 to yield 2-chloro-1-(1H-indol-1-yl)ethan-1-one (**12**) 33%. The product was proved by  $^1\text{H}$ - $^{13}\text{C}$  NMR.

### 3.5.12. 2-azido-N-phenylacetamide (7b)



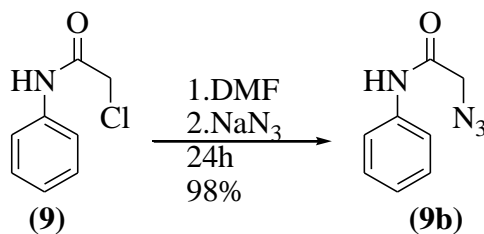
To a stirred solution of 2-chloro-N-(4-methoxyphenyl)acetamide (**7**) (1.22 mmol, 150 mg) in DMF (3ml) sodium azide (6.1 mmol, 400 mg) was added under nitrogen atmosphere. The reaction was heated gradually until it reaches 60 °C for overnight. After the reaction completion, the reaction was quenched with sodium bicarbonate and washed with ethyl acetate (20 ml × 3). The organic layers were combined and washed with saturated sodium chloride and dried over sodium sulfate anhydrous. The product was purified using silica gel column chromatography hexane: ethyl acetate 7:3 to yield 2-chloro-N-phenylacetamide (**7b**) 90%.

### 3.5.13. 2-azido-N-(p-tolyl)acetamide (8b)



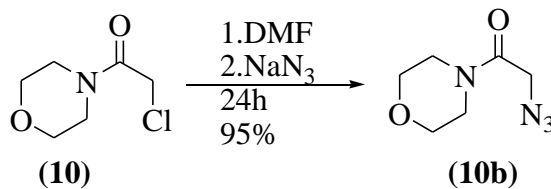
To a stirred solution of 2-chloro-N-(p-tolyl)acetamide (**8**) (0.55 mmol, 100 mg) in DMF (1.5 ml) sodium azide (2.8 mmol, 180 mg) was added under nitrogen atmosphere. After the reaction completion, the reaction was quenched with sodium bicarbonate and washed with ethyl acetate (20 ml  $\times$  3). The organic layers were combined and washed with saturated sodium chloride and dried over sodium sulfate anhydrous. The product was purified using silica gel column chromatography hexane: ethyl acetate 7:3 to yield 2-chloro-N-phenylacetamide (**8b**) 88%. The product was proved by  $^1\text{H}$ - $^{13}\text{C}$  NMR.

#### 3.5.14. 2-azido-N-(4-methoxyphenyl)acetamide (9b).



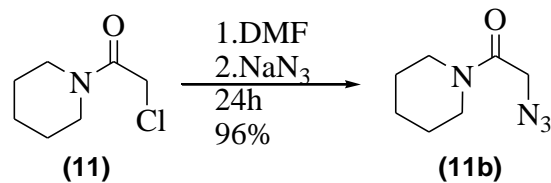
To a stirred solution of 2-chloro-N-phenylacetamide (**9**) divided on two round bottom flasks (16.385 mmol, 2.5 g) in DMF (32.75 ml) sodium azide (81.94 mmol, 5.3g) was added to each flask separately under nitrogen atmosphere. After the reaction completion, the reaction was quenched with sodium bicarbonate and washed with ethyl acetate (20 ml  $\times$  3). The organic layers were combined and washed with saturated sodium chloride and dried over sodium sulfate anhydrous. The product was purified using silica gel column chromatography hexane: ethyl acetate 7:3 to yield 2-chloro-N-phenylacetamide (**9b**) 98%. The product was proved by  $^1\text{H}$ - $^{13}\text{C}$  NMR.

#### 3.5.15. 2-azido-1-morpholinoethan-1-one (10b)



To a stirred solution of 2-chloro-1-morpholinoethan-1-one (**10**) (8.3 mmol, 1.35 g) in DMF (16.6 ml) sodium azide (41.5 mmol, 2.7g) was added under nitrogen atmosphere. After the reaction completion, the reaction was quenched with sodium bicarbonate and washed with ethyl acetate (20 ml  $\times$  3). The organic layers were combined and washed with saturated sodium chloride and dried over sodium sulfate anhydrous. The product was purified using silica gel column chromatography hexane: ethyl acetate 7:3 to yield 2-azido-1-morpholinoethan-1-one (**10b**) 95%. The product was proved by  $^1\text{H}$ - $^{13}\text{C}$  NMR.

#### 3.5.16 2-azido-1-(piperidin-1-yl)ethan-1-one (**11b**)

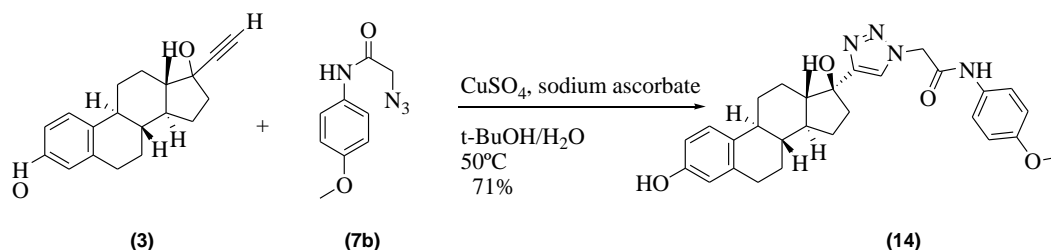


To a stirred solution of 2-chloro-1-(piperidin-1-yl)ethan-1-one (**11**) (5.8 mmol, 940 mg) in DMF (11.5 ml) sodium azide (29.2 mmol, 2.0 g) was added under nitrogen atmosphere. After the reaction completion, the reaction was quenched with sodium bicarbonate and washed with ethyl acetate (20 ml  $\times$  3). The organic layers were combined and washed with saturated sodium chloride and dried over sodium sulfate anhydrous. The product was purified using silica gel column chromatography hexane: ethyl acetate 7:3 to yield 2-azido-1-(piperidin-1-yl)ethan-1-one (**11b**) 96%. The product was proved by  $^1\text{H}$ - $^{13}\text{C}$  NMR.



with saturated sodium chloride and dried over sodium sulfate anhydrous. The product was purified using silica gel column chromatography ethyl acetate: hexane 8:2 to yield Estra-17-(1H-1,2,3-triazol-1-yl)-N-phenylacetamide)diol (**13**) 71%. <sup>1</sup>H NMR (400 MHz, Acetone-*d*<sub>6</sub>) δ 9.73 (s, 1H), 8.00 (s, 1H), 7.94 (s, 1H), 7.68 – 7.65 (m, 2H), 7.35 – 7.32 (m, 2H), 7.12 – 7.10 (m, 1H), 7.06 – 7.02 (m, 1H), 6.58 (m, 1H), 6.54 (d, *J* = 2.6 Hz, 1H), 5.38 (s, 2H), 2.78 – 2.67 (m, 3H), 2.43 – 1.93 (m, 4H), 1.87 – 1.65 (m, 6H), 0.94 (s, 3H), 0.86 (m, 2H). <sup>13</sup>C NMR (101 MHz, Acetone) δ 165.07, 162.99, 155.96, 155.15, 139.55, 138.45, 132.03, 129.72, 127.01, 124.83, 120.34, 115.98, 113.59, 82.70, 53.41, 48.98, 48.07, 44.51, 40.68, 38.57, 36.29, 33.83, 31.16, 28.38, 27.30, 24.50, 23.36, 14.94. HRMS Calcd. for 473.2547 found 473.25482

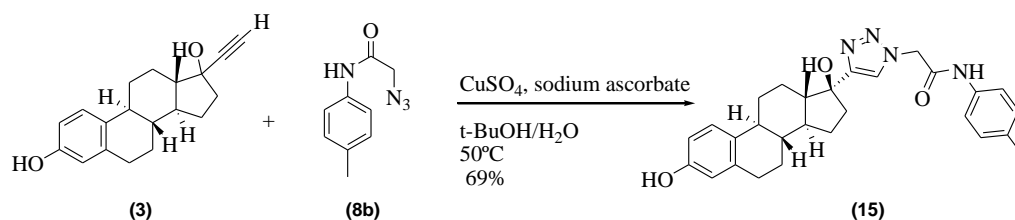
### 3.5.19. Estra-17-(1H-1,2,3-triazol-1-yl)-N-phenylacetamide)diol (**14**)(FZ300)



To a stirred solution of alkyne (**3**) (0.70 mmol) in t-BuOH/H<sub>2</sub>O (4mL), CuSO<sub>4</sub> 0.1 eq, sodium ascorbate 0.2 eq and azide (**7b**) (0.80 mmol) was added respectively. The reaction was stirred at 50°C for 24h. The reaction was quenched with ammonium chloride and washed with ethyl acetate (20 ml × 3). The organic layers were combined and washed with saturated sodium chloride and dried over sodium sulfate anhydrous. The product was purified using silica gel column chromatography ethyl acetate: hexane 8:2 to yield Estra-

17-(1H-1,2,3-triazol-1-yl)-N-phenylacetamide)diol (**14**) 71%. <sup>1</sup>HNMR (400 MHz, DMSO-*d*<sub>6</sub>) δ 10.25 (s, 1H), 8.83 (s, 1H), 7.74 (d, *J* = 2.4 Hz, 1H), 7.34 (d, *J* = 7.9 Hz, 2H), 6.97 (d, *J* = 8.0 Hz, 2H), 6.81 (d, *J* = 8.3 Hz, 1H), 6.34 (m, 1H), 6.29 (d, *J* = 2.6 Hz, 1H), 5.15 (s, 2H), 5.01 (s, 1H), 2.60 – 2.49 (m, 2H), 2.24 (m, 1H), 2.08 (m, 3H), 1.82 – 1.60 (m, 4H), 1.38 – 1.07 (m, 6H), 0.78 (s, 3H), 0.53 (m, 1H). <sup>13</sup>CNMR (101 MHz, DMSO) δ 170.27, 164.04, 154.86, 153.95, 137.11, 135.92, 132.66, 130.36, 129.22, 125.95, 124.22, 119.17, 114.88, 112.64, 81.13, 59.73, 52.09, 47.52, 46.75, 43.16, 37.17, 32.55, 29.26, 27.20, 26.07, 23.55, 20.41, 14.40. HRMS Calc. for 503.2653. found 503.26514.

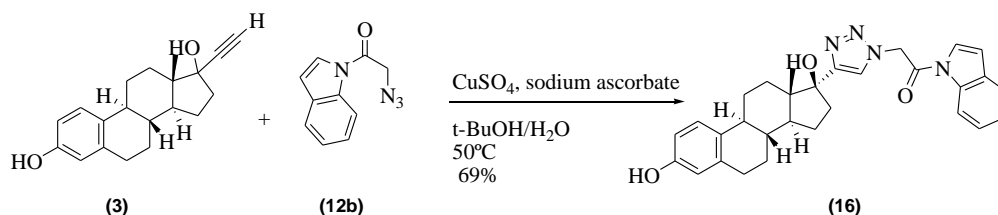
### 3.5.20. Estra-17-(1H-1,2,3-triazol-1-yl)-N-phenylacetamide)diol (**15**)(FZ313)



To a stirred solution of alkyne (**3**) (0.70 mmol) in t-BuOH/H<sub>2</sub>O (4mL), CuSO<sub>4</sub> 0.1 eq, sodium ascorbate 0.2 eq and azide (**8b**) (0.88 mmol) was added respectively. The reaction was stirred at 50°C for 24h. The reaction was quenched with ammonium chloride and washed with ethyl acetate (20 ml × 3). The organic layers were combined and washed with saturated sodium chloride and dried over sodium sulfate anhydrous. The product was purified using silica gel column chromatography ethyl acetate: hexane 8:2 to yield Estra-17-(1H-1,2,3-triazol-1-yl)-N-phenylacetamide)diol (**15**) 69 %. <sup>1</sup>HNMR (400 MHz, DMSO-*d*<sub>6</sub>) δ 10.36 (s, 1H), 9.00 (s, 1H), 7.89 (s, 1H), 7.54 – 7.49 (m, 2H), 6.99 – 6.92 (m, 2H), 6.90 (d, *J* = 2.2 Hz, 1H), 6.49 (dd, *J* = 8.3, 2.6 Hz, 1H), 6.44 (d, *J* = 2.6 Hz,

1H), 5.28 (s, 2H), 5.18 (s, 1H), 3.70 (s, 3H), 2.78 – 2.67 (m, 3H), 2.43 – 1.93 (m, 4H), 1.87 – 1.65 (m, 6H), 0.94 (s, 3H), 0.86 (m, 1H), 0.70 – 0.64 (m, 1H). <sup>13</sup>CNMR (101 MHz, DMSO) δ 163.77, 155.47, 154.83, 153.92, 137.12, 131.50, 130.36, 125.96, 124.20, 120.73, 114.86, 113.94, 112.62, 81.11, 59.74, 55.10, 52.02, 47.51, 46.73, 43.15, 37.13, 32.54, 29.25, 27.20, 26.05, 23.54, 20.70, 14.39, 14.04. HRMS Calc. for 487.2704. found 487.27104.

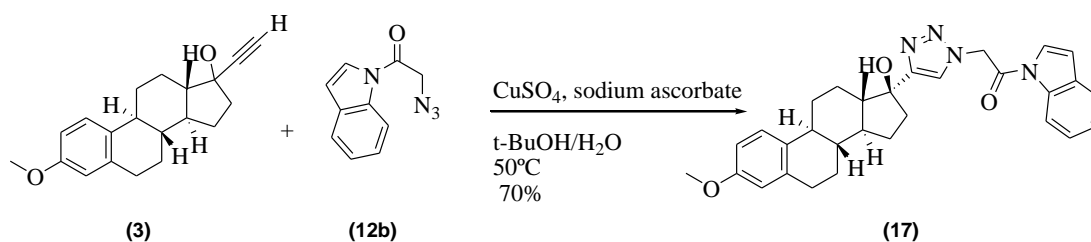
### 3.5.21. Estra-17-(1H-1,2,3-triazol-1-yl)-N-phenylacetamide)diol (16)(FZ518)



To a stirred solution of alkyne **(3)** (0.70 mmol) in t-BuOH/H<sub>2</sub>O (4mL), CuSO<sub>4</sub> 0.1 eq, sodium ascorbate 0.2 eq and azide **(12b)** (0.80 mmol) was added respectively. The reaction was stirred at 50°C for 24h. The reaction was quenched with ammonium chloride and washed with ethyl acetate (20 ml × 3). The organic layers were combined and washed with saturated sodium chloride and dried over sodium sulfate anhydrous. The product was purified using silica gel column chromatography ethyl acetate: hexane 8:2 to yield Estra-17-(1H-1,2,3-triazol-1-yl)-N-phenylacetamide)diol **(16)** 69%. <sup>1</sup>HNMR (400 MHz, DMSO-*d*<sub>6</sub>) δ 9.00 (s, 1H), 8.31 (d, *J* = 7.9 Hz, 1H), 8.02 (s, 1H), 7.97 (s, 1H), 7.67 (d, *J* = 7.4 Hz, 1H), 7.38 – 7.31 (m, 2H), 6.99 (s, 1H), 6.88 (d, *J* = 3.8 Hz, 1H), 6.50 (dd, *J* = 8.5, 2.6 Hz, 1H), 6.45 (s, 1H), 6.17 (s, 2H), 2.53 – 2.43 (m, 3H), 2.22 – 1.98 (m, 4H), 1.41 – 1.16 (m, 6H), 0.96 (s, 3H), 0.84 – 0.68 (m, 2H). <sup>13</sup>CNMR (101 MHz, DMSO) δ 165.68,

154.86, 154.26, 148.57, 137.14, 134.98, 130.37, 130.08, 125.99, 125.67, 124.97, 123.95, 121.10, 115.73, 114.89, 112.64, 109.42, 81.13, 52.20, 47.58, 43.21, 43.21, 37.23, 32.60, 29.27, 27.22, 26.10, 23.58, 14.41. **HRMS**. Cal. for 519.238216 found 519.236662

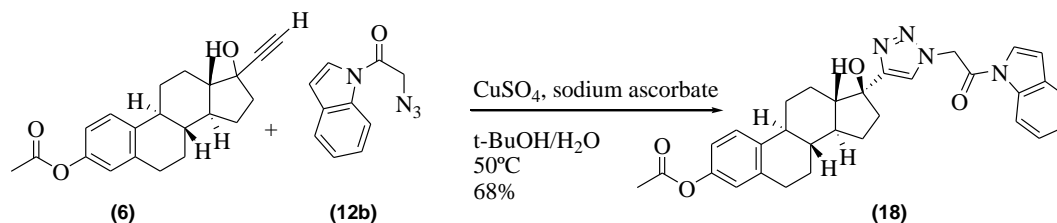
3.5.22. 3- Omethoxy estra-17-(1H-1,2,3-triazol-1-yl)-N-phenylacetamide)diol (**17**)(FZ 516)



To a stirred solution of alkyne (**4**) (0.70 mmol) in t-BuOH/H<sub>2</sub>O (4mL), CuSO<sub>4</sub> 0.1 eq, sodium ascorbate 0.2 eq and azide (**12b**) (0.80 mmol) was added respectively. The reaction was stirred at 50°C for 24h. The reaction was quenched with ammonium chloride and washed with ethyl acetate (20 ml × 3). The organic layers were combined and washed with saturated sodium chloride and dried over sodium sulfate anhydrous. The product was purified using silica gel column chromatography ethyl acetate: hexane 8:2 to yield 3-Omethoxy estra-17-(1H-1,2,3-triazol-1-yl)-N-phenylacetamide)diol (**17**) 70%. <sup>1</sup>H NMR (400 MHz, DMSO-d<sub>6</sub>) δ 8.31 (d, *J* = 7.9 Hz, 1H), 8.02 (d, *J* = 3.9 Hz, 1H), 7.96 (s, 1H), 7.70 – 7.65 (m, 1H), 7.39 – 7.30 (m, 2H), 7.11 (d, *J* = 8.7 Hz, 1H), 6.88 (d, *J* = 3.8 Hz, 1H), 6.65 (dd, *J* = 8.5, 2.7 Hz, 1H), 6.60 (d, *J* = 2.9 Hz, 1H), 6.18 (s, 2H), 5.26 (s, 1H) 3.69 (s, 3H). 2.53 – 2.43 (m, 3H), 2.22 – 1.98 (m, 4H), 1.41 – 1.16 (m, 6H), 0.96 (s, 3H), 0.84 – 0.68 (m, 2H). <sup>13</sup>C NMR (101 MHz, DMSO) δ 165.69, 156.96, 154.24, 137.40, 134.96,

132.08, 130.07, 126.11, 125.68, 124.96, 124.46, 123.95, 115.72, 113.36, 111.39, 109.41, 81.10, 54.80, 52.19, 47.55, 46.77, 43.20, 37.19, 32.57, 29.36, 28.21, 27.13, 26.01, 23.57, 14.39. **HRMS**. Calc. for 533.253636 found 533.252312.

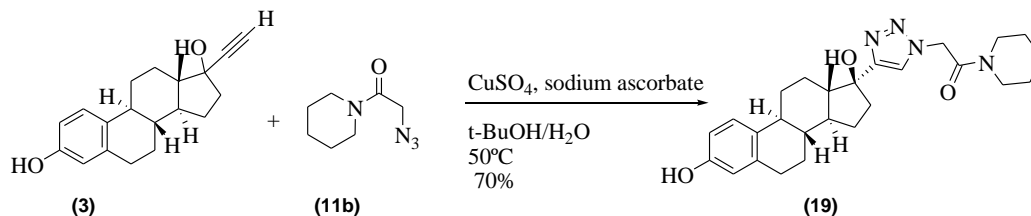
### 3.5.23. 3-Oacetate estra-17-(1H-1,2,3-triazol-1-yl)-N-phenylacetamide)diol (**18**)(FZ514)



To a stirred solution of alkyne (**6**) (0.70 mmol) in t-BuOH/H<sub>2</sub>O (4mL), CuSO<sub>4</sub> 0.1 eq, sodium ascorbate 0.2 eq and azide (**12b**) (0.80 mmol) was added respectively. The reaction was stirred at 50°C for 24h. The reaction was quenched with ammonium chloride and washed with ethyl acetate (20 ml × 3). The organic layers were combined and washed with saturated sodium chloride and dried over sodium sulfate anhydrous. The product was purified using silica gel column chromatography ethyl acetate: hexane 8:2 to yield 3-Oacetate estra-17-(1H-1,2,3-triazol-1-yl)-N-phenylacetamide)diol (**18**) 68%. **<sup>1</sup>H NMR (400 MHz, Acetone-*d*<sub>6</sub>)** δ 8.38 (dd, *J* = 8.2, 3.5 Hz, 1H), 7.95 – 7.91 (s, 1H), 7.65 (d, *J* = 7.4 Hz, 1H), 7.34 (t, *J* = 9.0 Hz, 1H), 7.22 (d, *J* = 8.3 Hz, 2H), 6.87 – 6.80 (m, 1H), 6.79 (s, 2H), 6.21 – 6.13 (m, 1H), 6.17 (s, 2H), 2.53 – 2.43 (m, 3H), 2.24 (s, 3H), 2.22 – 1.98 (m, 4H), 1.41 – 1.16 (m, 6H), 0.96 (s, 3H), 0.84 – 0.68 (m, 2H). **<sup>13</sup>C NMR (101 MHz, Acetone)** δ 169.91, 166.02, 155.37, 149.69, 138.85, 138.61, 136.54, 131.38, 127.03, 126.00, 125.69, 125.00, 122.44, 121.96, 119.62, 117.01, 110.69, 82.73, 60.62, 53.16,

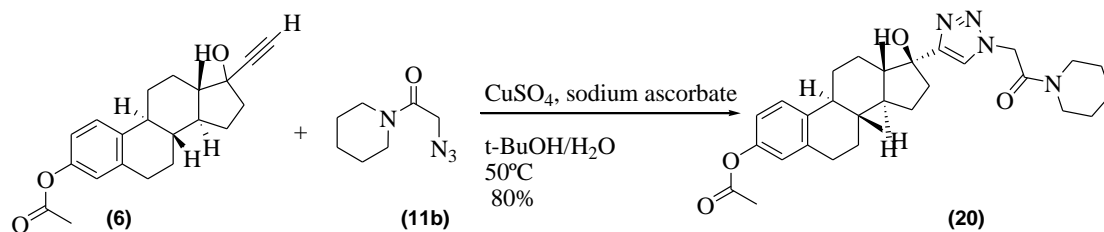
49.06, 48.07, 44.62, 40.19, 38.60, 33.82, 28.11, 27.09, 24.54, 21.09, 14.94. **HRMS** Calc. for 561.248732 found 561.247226.

3.5.24. Estra-17 1H-1,2,3-triazol-1-yl)-1-(piperidin-1-yl)ethanone (**29**)(FZ600)



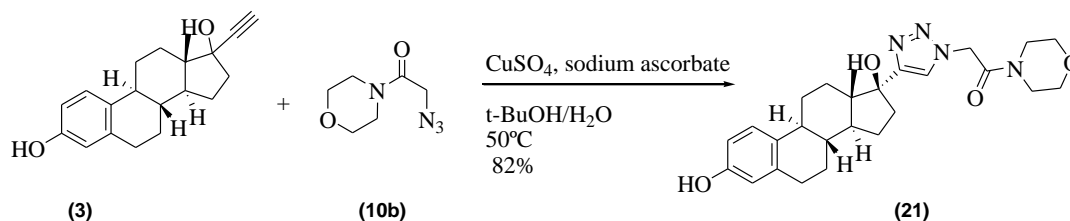
To a stirred solution of alkyne (**3**) (0.70 mmol) in t-BuOH/H<sub>2</sub>O (4mL), CuSO<sub>4</sub> 0.1 eq, sodium ascorbate 0.2 eq and azide (**11b**) (0.80 mmol) was added respectively. The reaction was stirred at 50°C for 24h. The reaction was quenched with ammonium chloride and washed with ethyl acetate (20 ml × 3). The organic layers were combined and washed with saturated sodium chloride and dried over sodium sulfate anhydrous. The product was purified using silica gel column chromatography ethyl acetate: hexane 8:2 to yield Estra-17-(1H-1,2,3-triazol-1-yl)-N-phenylacetamide diol (**19**) 70%. <sup>1</sup>H NMR (400 MHz, DMSO-*d*<sub>6</sub>) δ 8.94 (s, 1H), 7.74 (s, 1H), 6.97 (d, *J* = 8.5 Hz, 1H), 6.48 (dd, *J* = 8.4, 2.7 Hz, 1H), 6.43 (d, *J* = 2.6 Hz, 1H), 5.44 (s, 2H), 5.11 (s, 1H), 3.50 – 3.42 (m, 4H), 2.79 – 2.65 (m, 2H), 2.12–2.06 (m, 1H), 1.95–1.66 (m, 3H), 1.69 – 1.50 (m, 7H), 1.47– 1.16 (m, 6H), 0.94 (s, 3H), 0.68 (m 1H). <sup>13</sup>C NMR (101 MHz, DMSO) δ 163.86, 154.82, 153.65, 137.10, 130.35, 125.88, 124.19, 114.82, 112.58, 81.07, 50.46, 48.50, 47.48, 46.69, 45.20, 43.17, 42.42, 39.70, 39.56, 39.42, 39.28, 39.15, 39.01, 38.87, 37.04, 32.49, 29.21, 27.18, 26.03, 25.74, 25.09, 23.79, 23.45, 14.26. **HRMS**. Calc. for 465.2860. found 465.28653.

3.5.25. 3-OAcetate estra-17 1H-1,2,3-triazol-1-yl)-1-(piperidin-1-yl)ethanone  
(20)(Fz550)



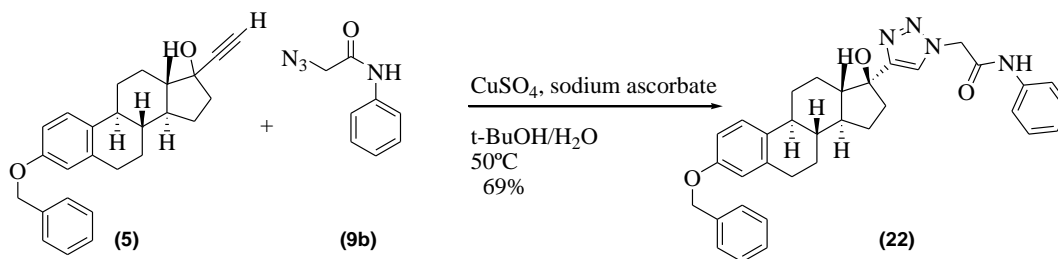
To a stirred solution of alkyne (**6**) (0.70 mmol) in t-BuOH/H<sub>2</sub>O (4mL), CuSO<sub>4</sub> 0.1 eq, sodium ascorbate 0.2 eq and azide (**11b**) (0.80 mmol) was added respectively. The reaction was stirred at 50°C for 24h. The reaction was quenched with ammonium chloride and washed with ethyl acetate (20 ml × 3). The organic layers were combined and washed with saturated sodium chloride and dried over sodium sulfate anhydrous. The product was purified using silica gel column chromatography ethyl acetate: hexane 8:2 to yield Estra-17-(1H-1,2,3-triazol-1-yl)-N-phenylacetamide)diol (**20**) 80%. <sup>1</sup>HNMR (400 MHz, Acetone-*d*<sub>6</sub>) δ 7.54 (s, 1H), 7.02 (d, *J* = 8.5 Hz, 1H), 6.61 – 6.60 (d, 1H), 5.19 (s, 2H), 3.32 (m, 4H), 2.22 (m, 2H), 2.02 (s, 3H) 1.98 – 1.84 (m, 4H) 1.63 – 1.38 (m, 6H), 1.43 – 1.11 (m, 6H), 0.88 (s, 3H), 0.88 (m, 1H), 0.74 – 0.58 (m, 2H). <sup>13</sup>CNMR (101 MHz, Acetone) δ 169.84, 164.61, 154.79, 149.68, 138.83, 138.59, 127.01, 124.75, 122.44, 119.62, 82.62, 51.64, 48.97, 47.97, 46.56, 44.66, 43.66, 40.21, 38.49, 33.76, 28.12, 27.12, 26.27, 25.09, 24.51, 21.08, 14.93. HRMS. Calc. for 507.296. found 507.29702.

## 3.5.26. Estra-17 1H-1,2,3-triazol-1-yl)-1-(morpholen-1-yl)ethanone (26)(FZ100)



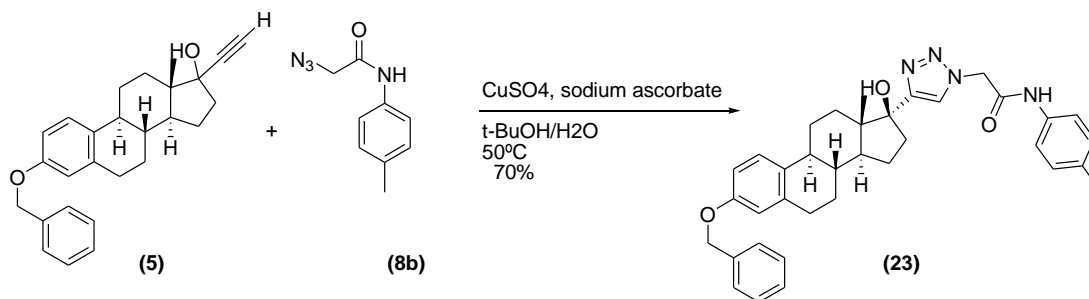
To a stirred solution of alkyne **(3)** (0.70 mmol) in t-BuOH/H<sub>2</sub>O (4mL), CuSO<sub>4</sub> 0.1 eq, sodium ascorbate 0.2 eq and azide **(10b)** (0.80 mmol) was added respectively. The reaction was stirred at 50°C for 24h. The reaction was quenched with ammonium chloride and washed with ethyl acetate (20 ml × 3). The organic layers were combined and washed with saturated sodium chloride and dried over sodium sulfate anhydrous. The product was purified using silica gel column chromatography ethyl acetate: hexane 8:2 to yield Estra-17 1H-1,2,3-triazol-1-yl)-1-(morpholen-1-yl)ethanone **(21)** 82%. <sup>1</sup>HNMR (400 MHz, DMSO-*d*<sub>6</sub>) δ 8.98 (s, 1H), 7.75 (s, 1H), 6.98 (d, *J* = 8.5 Hz, 1H), 6.48 (dd, *J* = 8.4, 2.7 Hz, 1H), 6.43 (d, *J* = 2.6 Hz, 1H), 5.45 (d, *J* = 2.7 Hz, 2H), 5.13 (s, 1H), 3.67 – 3.47 (m, 6H), 2.78 – 2.66 (m, 2H), 2.40 – 2.35 (m, 1H), 2.13 – 2.06 (m, 1H), 2.00 – 1.93 (m, 1H), 1.88 – 1.75 (m, 3H), 1.66 (m, 1H), 1.48 – 1.18 (m, 6H), 0.94 (s, 3H), 0.91 – 0.83 (m, 1H), 0.66 (m, 1H). <sup>13</sup>CNMR (101 MHz, DMSO) δ 164.59, 154.84, 153.74, 137.13, 130.35, 125.96, 124.25, 114.86, 112.62, 81.07, 65.93, 65.83, 50.37, 47.49, 46.73, 44.73, 43.18, 41.86, 37.08, 32.51, 29.25, 26.06, 23.53, 14.39. HRMS. Calc. for 467.2653. found 467.26496.

## 3.5.27. 3-Obenzyl Estra-17 (1H-1,2,3-triazol-1-yl)-N-phenylacetamide (22)(FZ57)



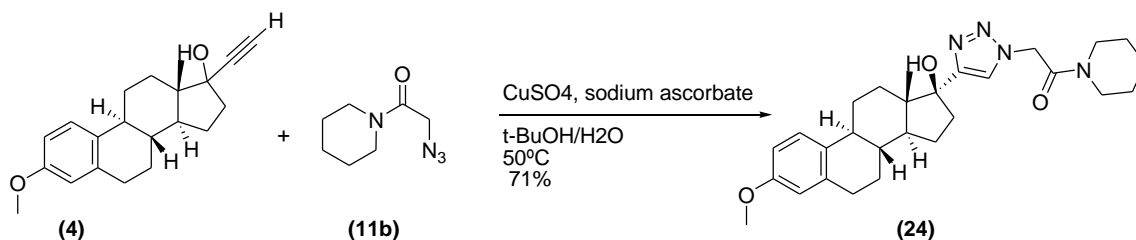
To a stirred solution of alkyne **(5)** (0.70 mmol) in t-BuOH/H<sub>2</sub>O (4mL), CuSO<sub>4</sub> 0.1 eq, sodium ascorbate 0.2 eq and azide **(9b)** (0.80 mmol) was added respectively. The reaction was stirred at 50°C for 24h. The reaction was quenched with ammonium chloride and washed with ethyl acetate (20 ml × 3). The organic layers were combined and washed with saturated sodium chloride and dried over sodium sulfate anhydrous. The product was purified using silica gel column chromatography ethyl acetate: hexane 8:2 to yield 3-Obenzyl Estra-17 (1H-1,2,3-triazol-1-yl)-N-phenylacetamide (**22**) 69%. <sup>1</sup>H NMR (400 MHz, Acetone-*d*<sub>6</sub>) δ 9.65 (s, 1H), 8.02 (s, 1H), 7.95 (s, 1H), 7.66 (d, *J* = 8.0 Hz, 2H), 7.32 (t, *J* = 7.9 Hz, 2H), 7.10 (t, *J* = 7.4 Hz, 1H), 7.01 (d, *J* = 8.4 Hz, 1H), 6.58 (dd, *J* = 8.4, 2.7 Hz, 1H), 6.53 (d, *J* = 2.6 Hz, 1H), 5.38 (s, 2H), 2.78 – 2.67 (m, 3H), 2.43 – 1.93 (m, 4H), 1.87 – 1.65 (m, 6H), 0.94 (s, 3H), 0.86 (m, 2H). <sup>13</sup>C NMR (151 MHz, Acetone) δ 165.10, 157.62, 155.16, 139.49, 138.78, 138.65, 133.65, 129.75, 129.26, 128.50, 128.33, 127.13, 124.90, 124.81, 120.43, 115.53, 113.09, 82.75, 70.27, 53.46, 49.03, 48.09, 44.48, 40.56, 38.62, 33.85, 29.59, 28.34, 27.24, 24.53, 14.99. HRMS. Calc. for 563.3017. found 563.30396.

## 3.5.28. 3-Obenzyl Estra-17 (-1H-1,2,3-triazol-1-yl)-N-p-tolylacetamide (23)(FZ400)



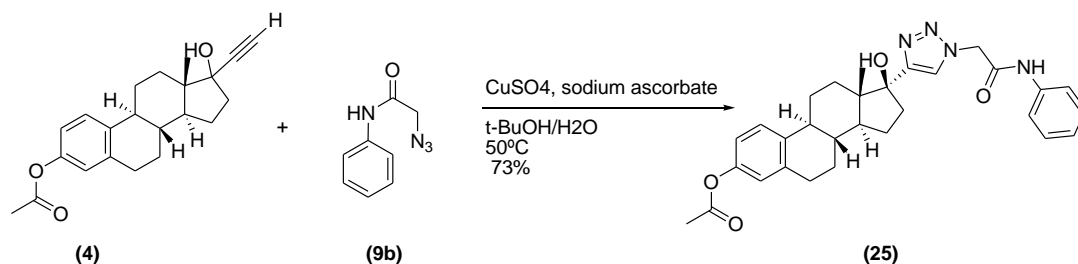
To a stirred solution of alkyne (**5**) (0.70 mmol) in t-BuOH/H<sub>2</sub>O (4mL), CuSO<sub>4</sub> 0.1 eq, sodium ascorbate 0.2 eq and azide (**8b**) (0.80 mmol) was added respectively. The reaction was stirred at 50°C for 24h. The reaction was quenched with ammonium chloride and washed with ethyl acetate (20 ml × 3). The organic layers were combined and washed with saturated sodium chloride and dried over sodium sulfate anhydrous. The product was purified using silica gel column chromatography ethyl acetate: hexane 8:2 to yield Obenzyl Estra-17 (-1H-1,2,3-triazol-1-yl)-N-p-tolylacetamide (**23**)(FZ400)70%. **<sup>1</sup>H NMR (400 MHz, DMSO-*d*<sub>6</sub>)** δ 10.25 (s, 1H), 8.83 (s, 1H), 7.74 (d, *J* = 2.4 Hz, 1H), 7.34 (d, *J* = 7.9 Hz, 2H), 6.97 (d, *J* = 8.0 Hz, 2H), 6.81 (d, *J* = 8.3 Hz, 1H), 6.34 (m, 1H), 6.29 (d, *J* = 2.6 Hz, 1H), 5.15 (s, 2H), 5.01 (s, 1H), 2.60 – 2.49 (m, 2H), 2.24 (m, 1H), 2.08 (m, 3H), 1.82 – 1.60 (m, 4H), 1.38 – 1.07 (m, 6H), 0.78 (s, 3H), 0.53 (m, 1H). **<sup>13</sup>C NMR (101 MHz, DMSO)** δ 170.27, 164.04, 154.86, 153.95, 137.11, 135.92, 132.66, 130.36, 129.22, 125.95, 124.22, 119.17, 114.88, 112.64, 81.13, 59.73, 52.09, 47.52, 46.75, 43.16, 37.17, 32.55, 29.26, 27.20, 26.07, 23.55, 20.41, 14.40. **HRMS**. Calc. for 577.3173 found 577.31846.

3.5.29. 3-methoxy estra-17 1H-1,2,3-triazol-1-yl)-1-(piperidin-1-yl)ethanone  
(24)(FZ552)



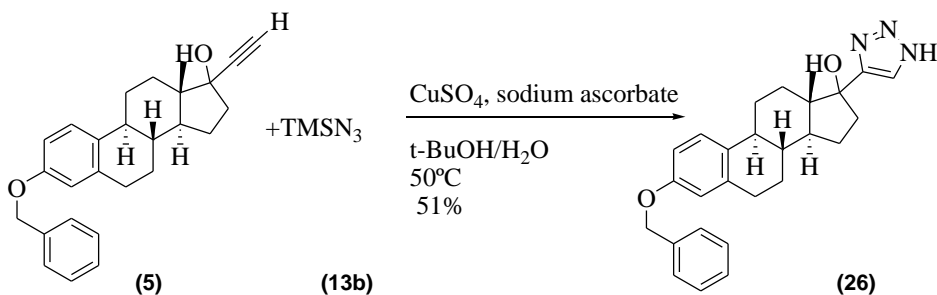
To a stirred solution of alkyne (**4**) (0.70 mmol) in t-BuOH/H<sub>2</sub>O (4mL), CuSO<sub>4</sub> 0.1 eq, sodium ascorbate 0.2 eq and azide (**11b**) (0.80 mmol) was added respectively. The reaction was stirred at 50°C for 24h. The reaction was quenched with ammonium chloride and washed with ethyl acetate (20 ml × 3). The organic layers were combined and washed with saturated sodium chloride and dried over sodium sulfate anhydrous. The product was purified using silica gel column chromatography ethyl acetate: hexane 8:2 to yield. 3-methoxy estra-17 1H-1,2,3-triazol-1-yl)-1-(piperidin-1-yl)ethanone (24)(FZ552) 71%. <sup>1</sup>HNMR (400 MHz, Chloroform-*d*) δ 7.63 (s, 1H), 7.13 (d, *J* = 8.5 Hz, 1H), 6.67 (m, 1H), 6.60 (d, *J* = 2.8 Hz, 1H), 5.21 (s, 2H), 3.15 (s, 3H), 3.58 – 3.46 (m, 4H), 2.41 – 2.22 (m, 2H), 1.93 – 1.86 (m, 4H), 1.67 – 1.57 (m, 6H), 1.43 – 1.25 (m, 6H), 1.04 (s, 3H), 0.90 – 0.68 (m, 2H). <sup>13</sup>CNMR (101 MHz, CDCl<sub>3</sub>) δ 163.20, 157.34, 153.95, 137.99, 132.67, 126.27, 123.17, 113.71, 111.40, 82.23, 55.18, 51.20, 47.33, 46.44, 43.52, 39.47, 37.83, 32.92, 29.90, 27.37, 26.29, 25.36, 24.22, 23.48, 19.60, 14.29. HRMS. Calc. for 479.3017. found 479.30139.

## 3.5.30. 3-OAcetate estra-17 (1H-1,2,3-triazol-1-yl)-N-phenylacetamide (25)(FZ200)



To a stirred solution of alkyne **(4)** (0.70 mmol) in t-BuOH/H<sub>2</sub>O (4mL), CuSO<sub>4</sub> 0.1 eq, sodium ascorbate 0.2 eq and azide **(9b)** (0.80 mmol) was added respectively. The reaction was stirred at 50°C for 24h. The reaction was quenched with ammonium chloride and washed with ethyl acetate (20 ml × 3). The organic layers were combined and washed with saturated sodium chloride and dried over sodium sulfate anhydrous. The product was purified using silica gel column chromatography ethyl acetate: hexane 8:2 to yield OAcetate estra-17 (1H-1,2,3-triazol-1-yl)-N-phenylacetamide (**25**)(FZ200). 73%. **<sup>1</sup>H NMR (400 MHz, Acetone-*d*<sub>6</sub>)** δ 9.74 (s, 1H), 7.98 (s, 1H), 7.66 (d, *J* = 8.0 Hz, 2H), 7.30 (t, *J* = 7.8 Hz, 2H), 7.19 (d, *J* = 8.5 Hz, 1H), 7.09 (t, *J* = 7.5 Hz, 1H), 6.83 (d, *J* = 8.9 Hz, 1H), 6.78 (s, 1H), 5.40 (s, 2H), 4.41 (s, 1H), 2.24 (s, 3H), 2.15 (m, 4H), 1.95 (m, 4H), 1.36 – 1.24 (m, 6H), 1.09 (s, 3H), 0.91 – 0.84 (m, 2H). **<sup>13</sup>C NMR (101 MHz, Acetone)** δ 170.05, 165.18, 155.14, 149.66, 139.43, 138.85, 138.63, 129.76, 127.08, 124.97, 122.44, 120.47, 119.61, 82.78, 53.46, 49.08, 48.05, 44.56, 40.16, 38.63, 33.83, 30.64, 28.09, 27.09, 24.55, 21.20, 14.65. **HRMS.** Calc. for 515.2653 found 515.26619.

## 3.5.31. 3-Obenzyl Estra-17 (-1H-1,2,3-triazol) (26) (FZ25)



To a stirred solution of alkyne (**5**) (0.70 mmol) in t-BuOH/H<sub>2</sub>O (4mL), CuSO<sub>4</sub> 0.1 eq, sodium ascorbate 0.2 eq and azide (**13b**) (0.80 mmol) was added respectively. The reaction was stirred at 50°C for 24h. The reaction was quenched with ammonium chloride and washed with ethyl acetate (20 ml × 3). The organic layers were combined and washed with saturated sodium chloride and dried over sodium sulfate anhydrous. The product was purified using silica gel column chromatography ethyl acetate: hexane 8:2 to yield 3-Obenzyl Estra-17 (-1H-1,2,3-triazol) (26) (FZ25) 51%. **<sup>1</sup>H NMR (400 MHz, Acetone-*d*<sub>6</sub>)**, δ 13.98 (s, 1H), 7.71 (s, 1H), 7.45 (d, *J* = 6.8 Hz, 2H), 7.37 (d, *J* = 7.5 Hz, 2H), 7.32 (d, *J* = 7.4 Hz, 1H), 7.10 (d, *J* = 8.5 Hz, 1H), 6.73 (d, *J* = 5.7 Hz, 1H), 6.70 (s, 1H) 5.04 (s, 2H), 2.84–2.61 (m, 2H), 2.52–2.42 (m, 1H), 2.12–1.92 (m, 3H), 1.95–1.66 (m, 3H), 1.59–1.27 (m, 6H), 1.08 (s, 3H), 0.70–0.66 (m, 1H). **<sup>13</sup>C NMR (101 MHz)** δ 157.61, 138.74, 138.58, 133.51, 129.24, 129.19, 128.48, 128.30, 127.08, 115.50, 113.07, 82.63, 70.22, 49.06, 48.09, 44.49, 40.47, 38.78, 33.89, 29.35, 28.32, 27.14, 24.38, 14.80. **HRMS**. Calc. for 430.2489 found 430.24895.

## 3.6. References

1. Mishra, B.B. and V.K. Tiwari, *Natural products: an evolving role in future drug discovery*. European journal of medicinal chemistry, 2011. **46**(10): p. 4769-4807.
2. Cragg, G.M. and D.J. Newman, *Natural products: a continuing source of novel drug leads*. Biochimica et Biophysica Acta (BBA)-General Subjects, 2013. **1830**(6): p. 3670-3695.
3. Harvey, A.L., *Natural products in drug discovery*. Drug discovery today, 2008. **13**(19): p. 894-901.
4. Mason, J., A. Good, and E. Martin, *3-D pharmacophores in drug discovery*. Current pharmaceutical design, 2001. **7**(7): p. 567-597.
5. Yang, S.-Y., *Pharmacophore modeling and applications in drug discovery: challenges and recent advances*. Drug discovery today, 2010. **15**(11): p. 444-450.
6. Zou, J., et al., *Towards more accurate pharmacophore modeling: Multicomplex-based comprehensive pharmacophore map and most-frequent-feature pharmacophore model of CDK2*. Journal of Molecular Graphics and Modelling, 2008. **27**(4): p. 430-438.
7. Brenk, R. and G. Klebe, *'Hot spot' analysis of protein-binding sites as a prerequisite for structure-based virtual screening and lead optimization*, in *Pharmacophores and pharmacophore searches*. 2006, Wiley-VCH. p. 171-192.
8. Rostovtsev, V.V., et al., *A stepwise Huisgen cycloaddition process: copper (I)-catalyzed regioselective "ligation" of azides and terminal alkynes*. Angewandte Chemie, 2002. **114**(14): p. 2708-2711.

9. Worrell, B., J. Malik, and V.V. Fokin, *Direct evidence of a dinuclear copper intermediate in Cu (I)-catalyzed azide-alkyne cycloadditions*. *Science*, 2013. **340**(6131): p. 457-460.
10. Liang, L. and D. Astruc, *The copper (I)-catalyzed alkyne-azide cycloaddition (CuAAC) "click" reaction and its applications. An overview*. *Coordination Chemistry Reviews*, 2011. **255**(23): p. 2933-2945.
11. Boren, B.C., et al., *Ruthenium-catalyzed azide-alkyne cycloaddition: Scope and mechanism*. *Journal of the American Chemical Society*, 2008. **130**(28): p. 8923-8930.
12. Cadelon, N., D. Lastòcou res, A. Khadri Diallo, J. Ruiz Aranzaes, D. Astruc, J.-M. Vincent. *Chem. Commun*, 2008. **7**: p. 41-43.
13. Kolb, H.C., M. Finn, and K.B. Sharpless, *Click chemistry: diverse chemical function from a few good reactions*. *Angewandte Chemie International Edition*, 2001. **40**(11): p. 2004-2021.
14. Tron, G.C., et al., *Click chemistry reactions in medicinal chemistry: Applications of the 1, 3-dipolar cycloaddition between azides and alkynes*. *Medicinal research reviews*, 2008. **28**(2): p. 278-308.
15. Miller, W.L. and R.J. Auchus, *The molecular biology, biochemistry, and physiology of human steroidogenesis and its disorders*. *Endocrine reviews*, 2010. **32**(1): p. 81-151.
16. Anstead, G.M., K.E. Carlson, and J.A. Katzenellenbogen, *The estradiol pharmacophore: ligand structure-estrogen receptor binding affinity relationships and a model for the receptor binding site*. *Steroids*, 1997. **62**(3): p. 268-303.

17. Ahmed, M.S., L.C. Kopel, and F.T. Halaweish, *Structural Optimization and Biological Screening of a Steroidal Scaffold Possessing Cucurbitacin-Like Functionalities as B-Raf Inhibitors*. ChemMedChem, 2014. **9**(7): p. 1361-1367.
18. Kopel, L.C., M.S. Ahmed, and F.T. Halaweish, *Synthesis of novel estrone analogs by incorporation of thiophenols via conjugate addition to an enone side chain*. Steroids, 2013. **78**(11): p. 1119-1125.
19. Solum, E.J., A. Vik, and T.V. Hansen, *Synthesis, cytotoxic effects and tubulin polymerization inhibition of 1, 4-disubstituted 1, 2, 3-triazole analogs of 2-methoxyestradiol*. Steroids, 2014. **87**: p. 46-53.
20. Clement, O.O., et al., *Three dimensional pharmacophore modeling of human CYP17 inhibitors. Potential agents for prostate cancer therapy*. Journal of medicinal chemistry, 2003. **46**(12): p. 2345-2351.
21. Dhyani, M.V., et al., *Preparation and preliminary bioevaluation of  $^{99m}\text{Tc}$  (CO)  $3\text{-}11\beta\text{-progesterone}$  derivative prepared via click chemistry route*. Nuclear medicine and biology, 2010. **37**(8): p. 997-1004.
22. Agalave, S.G., S.R. Maujan, and V.S. Pore, *Click Chemistry: 1, 2, 3-Triazoles as Pharmacophores*. Chemistry—An Asian Journal, 2011. **6**(10): p. 2696-2718.
23. Kharb, R., P.C. Sharma, and M.S. Yar, *Pharmacological significance of triazole scaffold*. Journal of enzyme inhibition and medicinal chemistry, 2011. **26**(1): p. 1-21.
24. Bohacek, R.S., C. McMartin, and W.C. Guida, *The art and practice of structure-based drug design: A molecular modeling perspective*. Medicinal research reviews, 1996. **16**(1): p. 3-50.

25. Csermely, P., et al., *Structure and dynamics of molecular networks: a novel paradigm of drug discovery: a comprehensive review*. *Pharmacology & therapeutics*, 2013. **138**(3): p. 333-408.
26. Ekins, S., J. Mestres, and B. Testa, *In silico pharmacology for drug discovery: applications to targets and beyond*. *British journal of pharmacology*, 2007. **152**(1): p. 21-37.
27. Kitchen, D.B., et al., *Docking and scoring in virtual screening for drug discovery: methods and applications*. *Nature reviews Drug discovery*, 2004. **3**(11): p. 935-949.
28. Charifson, P.S., et al., *Consensus scoring: A method for obtaining improved hit rates from docking databases of three-dimensional structures into proteins*. *Journal of medicinal chemistry*, 1999. **42**(25): p. 5100-5109.
29. Leach, A.R., *Ligand docking to proteins with discrete side-chain flexibility*. *Journal of molecular biology*, 1994. **235**(1): p. 345-356.
30. Brooijmans, N. and I.D. Kuntz, *Molecular recognition and docking algorithms*. *Annual review of biophysics and biomolecular structure*, 2003. **32**(1): p. 335-373.
31. Huang, S.-Y. and X. Zou, *Advances and challenges in protein-ligand docking*. *International journal of molecular sciences*, 2010. **11**(8): p. 3016-3034.
32. Kulkarni, S. and J.K. Savsaviya, *Study of a High-risk Group of Stage 2 Colon Cancer*.
33. Siegel, R.L., K.D. Miller, and A. Jemal, *Cancer statistics, 2016*. *CA: a cancer journal for clinicians*, 2016. **66**(1): p. 7-30.

34. Majumdar, S.R., R.H. Fletcher, and A.T. Evans, *How does colorectal cancer present? Symptoms, duration, and clues to location*. The American journal of gastroenterology, 1999. **94**(10): p. 3039-3045.
35. Cohen, S., *Isolation of a mouse submaxillary gland protein accelerating incisor eruption and eyelid opening in the new-born animal*. Journal of Biological Chemistry, 1962. **237**(5): p. 1555-1562.
36. Yarom, N. and D.J. Jonker, *The role of the epidermal growth factor receptor in the mechanism and treatment of colorectal cancer*. Discovery medicine, 2011. **11**(57): p. 95-105.
37. Alroy, I. and Y. Yarden, *The ErbB signaling network in embryogenesis and oncogenesis: signal diversification through combinatorial ligand-receptor interactions*. FEBS letters, 1997. **410**(1): p. 83-86.
38. Muthuswamy, S.K., M. Gilman, and J.S. Brugge, *Controlled dimerization of ErbB receptors provides evidence for differential signaling by homo- and heterodimers*. Molecular and cellular biology, 1999. **19**(10): p. 6845-6857.
39. Boudewijn, M. and P.J. Coffey, *Protein kinase B (c-Akt) in phosphatidylinositol-3-OH kinase signal transduction*. Nature, 1995. **376**(6541): p. 599.
40. Chan, T.O., S.E. Rittenhouse, and P.N. Tsichlis, *AKT/PKB and other D3 phosphoinositide-regulated kinases: kinase activation by phosphoinositide-dependent phosphorylation*. Annual review of biochemistry, 1999. **68**(1): p. 965-1014.
41. Petit, A., et al., *Neutralizing antibodies against epidermal growth factor and ErbB-2/neu receptor tyrosine kinases down-regulate vascular endothelial growth factor production by tumor cells in vitro and in vivo: angiogenic implications for signal*

*transduction therapy of solid tumors*. The American journal of pathology, 1997. **151**(6): p. 1523.

42. Engebraaten, O., et al., *Effects of EGF, BFGF, NGF and PDGF (bb) on cell proliferative, migratory and invasive capacities of human brain-tumour biopsies In Vitro*. International journal of cancer, 1993. **53**(2): p. 209-214.

43. Douillard, J.-Y., et al., *Randomized, phase III trial of panitumumab with infusional fluorouracil, leucovorin, and oxaliplatin (FOLFOX4) versus FOLFOX4 alone as first-line treatment in patients with previously untreated metastatic colorectal cancer: the PRIME study*. Journal of clinical oncology, 2010. **28**(31): p. 4697-4705.

44. Winawer, S., et al., *Colorectal cancer screening and surveillance: clinical guidelines and rationale—update based on new evidence*. Gastroenterology, 2003. **124**(2): p. 544-560.

45. Kroemer, R.T., *Structure-based drug design: docking and scoring*. Current protein and peptide science, 2007. **8**(4): p. 312-328.

46. Popat, S., R. Hubner, and R. Houlston, *Systematic review of microsatellite instability and colorectal cancer prognosis*. Journal of Clinical Oncology, 2005. **23**(3): p. 609-618.

47. Figueredo, A., et al., *Adjuvant therapy for stage II colon cancer: a systematic review from the Cancer Care Ontario Program in evidence-based care's gastrointestinal cancer disease site group*. Journal of clinical oncology, 2004. **22**(16): p. 3395-3407.

48. Raymond, E., et al., *Oxaliplatin: a review of preclinical and clinical studies*. Annals of Oncology, 1998. **9**(10): p. 1053-1071.

49. Longley, D.B., D.P. Harkin, and P.G. Johnston, *5-fluorouracil: mechanisms of action and clinical strategies*. Nature Reviews Cancer, 2003. **3**(5): p. 330-338.
50. Twelves, C., et al., *Capecitabine as adjuvant treatment for stage III colon cancer*. New England Journal of Medicine, 2005. **352**(26): p. 2696-2704.
51. Scoggins, C.R., et al., *Nonoperative management of primary colorectal cancer in patients with stage IV disease*. Annals of surgical oncology, 1999. **6**(7): p. 651-657.
52. August, D.A., R.T. Ottow, and P.H. Sugarbaker, *Clinical perspective of human colorectal cancer metastasis*. Cancer and metastasis reviews, 1984. **3**(4): p. 303-324.
53. Graham, M.A., et al., *Clinical pharmacokinetics of oxaliplatin: a critical review*. Clinical Cancer Research, 2000. **6**(4): p. 1205-1218.
54. Salonga, D., et al., *Colorectal tumors responding to 5-fluorouracil have low gene expression levels of dihydropyrimidine dehydrogenase, thymidylate synthase, and thymidine phosphorylase*. Clinical Cancer Research, 2000. **6**(4): p. 1322-1327.
55. Hezel, A., et al., *Phase II study of gemcitabine, oxaliplatin in combination with panitumumab in KRAS wild-type unresectable or metastatic biliary tract and gallbladder cancer*. British journal of cancer, 2014. **111**(3): p. 430-436.
56. Heggie, G.D., et al., *Clinical pharmacokinetics of 5-fluorouracil and its metabolites in plasma, urine, and bile*. Cancer research, 1987. **47**(8): p. 2203-2206.
57. Raymond, E., et al. *Oxaliplatin: mechanism of action and antineoplastic activity*. in *Seminars in oncology*. 1998.
58. Woynarowski, J.M., et al., *Sequence-and region-specificity of oxaliplatin adducts in naked and cellular DNA*. Molecular pharmacology, 1998. **54**(5): p. 770-777.

59. Markman, B., et al., *EGFR and KRAS in colorectal cancer*. Advances in clinical chemistry, 2010. **51**: p. 72.
60. Kallander, L.S., et al., *4-Aryl-1, 2, 3-triazole: a novel template for a reversible methionine aminopeptidase 2 inhibitor, optimized to inhibit angiogenesis in vivo*. Journal of medicinal chemistry, 2005. **48**(18): p. 5644-5647.
61. Pagliai, F., et al., *Rapid synthesis of triazole-modified resveratrol analogues via click chemistry*. Journal of medicinal chemistry, 2006. **49**(2): p. 467-470.
62. Lee, T., et al., *Synthesis and evaluation of 1, 2, 3-triazole containing analogues of the immunostimulant  $\alpha$ -GalCer*. Journal of medicinal chemistry, 2007. **50**(3): p. 585-589.
63. Pisaneschi, F., et al., *Development of a new epidermal growth factor receptor positron emission tomography imaging agent based on the 3-cyanoquinoline core: synthesis and biological evaluation*. Bioorganic & medicinal chemistry, 2010. **18**(18): p. 6634-6645.
64. Whiting, M., et al., *Rapid discovery and structure– activity profiling of novel inhibitors of human immunodeficiency virus type 1 protease enabled by the copper (I)-catalyzed synthesis of 1, 2, 3-triazoles and their further functionalization*. Journal of medicinal chemistry, 2006. **49**(26): p. 7697-7710.
65. Costa, M.S., et al., *Synthesis, tuberculosis inhibitory activity, and SAR study of N-substituted-phenyl-1, 2, 3-triazole derivatives*. Bioorganic & medicinal chemistry, 2006. **14**(24): p. 8644-8653.
66. Somu, R.V., et al., *Rationally designed nucleoside antibiotics that inhibit siderophore biosynthesis of mycobacterium tuberculosis*. Journal of medicinal chemistry, 2006. **49**(1): p. 31-34.

67. Pore, V., *T etrahedron* 2006, 62, 11178–11186; b) NG Aher, VS Pore, NN Mishra, A. Kumar, PK Shukla, A. Sharma, MK Bhat. *Bioorg. Med. Chem. Lett*, 2009. **19**: p. 759-763.
68. Reck, F., et al., *Novel substituted (pyridin-3-yl) phenyloxazolidinones: antibacterial agents with reduced activity against monoamine oxidase A and increased solubility*. *Journal of medicinal chemistry*, 2007. **50**(20): p. 4868-4881.
69. Reck, F., et al., *Identification of 4-substituted 1, 2, 3-triazoles as novel oxazolidinone antibacterial agents with reduced activity against monoamine oxidase A*. *Journal of medicinal chemistry*, 2005. **48**(2): p. 499-506.
70. Sequist, L.V., et al., *Genotypic and histological evolution of lung cancers acquiring resistance to EGFR inhibitors*. *Science translational medicine*, 2011. **3**(75): p. 75ra26-75ra26.
71. Sartore-Bianchi, A., et al., *PIK3CA mutations in colorectal cancer are associated with clinical resistance to EGFR-targeted monoclonal antibodies*. *Cancer research*, 2009. **69**(5): p. 1851-1857.
72. Ryan, K.J., *Biochemistry of aromatase: significance to female reproductive physiology*. *Cancer research*, 1982. **42**(8 Supplement): p. 3342s-3344s.
73. Ejembi, D.O., *Comparative Study of the Effects of Aqueous Extracts of Moringa Oleifera and Vernonia Amygdalina Leaves on Some Biochemical Indices in Albino Rats*. 2014, UNIVERSITY OF NIGERIA NSUKKA.
74. Chen, G.G., Q. Zeng, and G.M. Tse, *Estrogen and its receptors in cancer*. *Medicinal research reviews*, 2008. **28**(6): p. 954-974.

75. Heldring, N., et al., *Estrogen receptors: how do they signal and what are their targets*. *Physiological reviews*, 2007. **87**(3): p. 905-931.
76. Yeung, Y.-Y., R.-J. Chein, and E. Corey, *Conversion of Torgov's synthesis of estrone into a highly enantioselective and efficient process*. *Journal of the American Chemical Society*, 2007. **129**(34): p. 10346-10347.
77. Ibrahim-Ouali, M., *Recent advances in oxasteroids chemistry*. *Steroids*, 2007. **72**(6): p. 475-508.
78. Leese, M.P., et al., *A-ring-substituted estrogen-3-O-sulfamates: potent multitargeted anticancer agents*. *Journal of medicinal chemistry*, 2005. **48**(16): p. 5243-5256.
79. Bodnár, B., et al., *Synthesis and Biological Evaluation of Triazolyl 13 $\alpha$ -Estrone-Nucleoside Bioconjugates*. *Molecules*, 2016. **21**(9): p. 1212.
80. McGann, M., *FRED pose prediction and virtual screening accuracy*. *Journal of chemical information and modeling*, 2011. **51**(3): p. 578-596.
81. Schulz-Gasch, T. and M. Stahl, *Binding site characteristics in structure-based virtual screening: evaluation of current docking tools*. *Journal of Molecular Modeling*, 2003. **9**(1): p. 47-57.
82. de la Torre, M.C., et al., *The Reversible Nicholas Reaction in the Synthesis of Highly Symmetric Natural-Product-Based Macrocycles*. *European Journal of Organic Chemistry*, 2015. **2015**(5): p. 1054-1067.
83. Boivin, R.P., et al., *Structure-Activity Relationships of 17 $\alpha$ -Derivatives of Estradiol as Inhibitors of Steroid Sulfatase*. *Journal of medicinal chemistry*, 2000. **43**(23): p. 4465-4478.

84. Kasiotis, K.M., et al., *High affinity 17 $\alpha$ -substituted estradiol derivatives: Synthesis and evaluation of estrogen receptor agonist activity*. *Steroids*, 2006. **71**(3): p. 249-255.
85. Proulx, G. and R.G. Bergman, *Synthesis, structures, and kinetics and mechanism of decomposition of terminal metal azide complexes: isolated intermediates in the formation of imidometal complexes from organic azides*. *Organometallics*, 1996. **15**(2): p. 684-692.
86. Wei, F., et al., *Cu/Pd-catalyzed, three-component click reaction of azide, alkyne, and aryl halide: One-pot strategy toward trisubstituted triazoles*. *Organic letters*, 2015. **17**(11): p. 2860-2863.
87. Vidal, C. and J. García-Álvarez, *Glycerol: a biorenewable solvent for base-free Cu (I)-catalyzed 1, 3-dipolar cycloaddition of azides with terminal and 1-iodoalkynes. Highly efficient transformations and catalyst recycling*. *Green Chemistry*, 2014. **16**(7): p. 3515-3521.
88. Torii, S., et al., *Pd (O)-CATALYZED ELECTROREDUCTIVE CARBOXYLATION OF ARYL HALIDES,  $\beta$ -BROMOSTYRENE, AND ALLYL ACETATES WITH CO<sub>2</sub>*. *Chemistry Letters*, 1986. **15**(2): p. 169-172.
89. Reddy, K.R., et al., *Mild and efficient oxy-iodination of alkynes and phenols with potassium iodide and tert-butyl hydroperoxide*. *Tetrahedron Letters*, 2010. **51**(16): p. 2170-2173.
90. Gómez-Herrera, A., et al., *Sequential Functionalization of Alkynes and Alkenes Catalyzed by Gold (I) and Palladium (II) N-Heterocyclic Carbene Complexes*. *ChemCatChem*, 2016. **8**(21): p. 3381-3388.

91. Korenm, A.O., *Acid-mediated regioselective alkylation of 1, 2, 3-triazole*. Journal of heterocyclic chemistry, 2002. **39**(5): p. 1111-1112.

**Appendix1: consensus scoring of the designed estradiol-triazole library.**

VIDA Name	VIDA ID	PLP	Chemgauss3	OEChemscore	Screenscore	Consensus Score
FZ518_13	2	-73.3132	-86.1279	-51.1893	-178.543	18
FZ516_6	3	-72.1143	-87.5822	-47.6696	-188.167	26
FZ514_4	4	-70.4834	-80.0671	-46.3446	-178.962	85
FZ30_23	5	-58.8637	-93.3865	-46.8942	-165.309	90
FZ300_25	6	-69.5338	-77.0692	-49.079	-171.085	103
FZ550_20	7	-69.5338	-77.0692	-49.079	-171.085	107
FZ600_9	8	-66.8985	-81.6767	-46.2577	-164.832	108
FZ58	9	-64.1959	-87.6477	-46.5056	-151.585	112
FZ313_6	10	-69.532	-79.9692	-44.8459	-183.069	118
FZ25_3	11	-61.4369	-84.4336	-45.8785	-160.62	121
FZ400_7	12	-70.8689	-76.568	-48.0036	-174.46	121
FZ520_1	13	-66.066	-76.8503	-48.7326	-173.602	124
FZ57_73	14	-57.1153	-94.853	-46.9535	-149.389	140
FZ60_73	15	-57.1153	-94.853	-46.9535	-149.389	144
FZ552_2	16	-57.2465	-85.7379	-44.8097	-160.104	160
FZ200_28	17	-59.0869	-79.3166	-48.5955	-154.281	161
FZ_14	18	-67.1425	-75.8671	-46.6518	-169.39	163
FZ_50	19	-56.3365	-85.2949	-48.8623	-143.625	170
FZ512_12	20	-60.4612	-76.0219	-48.6576	-160.667	179
FZ100_137	21	-65.3973	-81.2972	-45.3846	-147.381	184
FZ510_25	22	-75.6194	-72.6507	-47.2687	-166.48	189
FZ624_15	23	-57.9291	-79.969	-45.6426	-156.863	189
FZ26_10	24	-59.7195	-90.4294	-44.0541	-143.825	199
FZ319_6	25	-59.4693	-76.588	-47.066	-155.866	200
FZ108_13	26	-64.7915	-76.7299	-44.6994	-156.325	220
FZ486_11	27	-69.2441	-75.4287	-43.7607	-177.896	222
FZ553_151	28	-65.1019	-75.2149	-43.6038	-168.053	249
FZ10_2	29	-57.1703	-76.3912	-45.4281	-155.503	254
FZ520_12	30	-67.4681	-77.0751	-41.4539	-167.575	254
FZ522_12	31	-67.4681	-77.0751	-41.4539	-167.575	256
FZ9_2	32	-57.1703	-76.3912	-45.4281	-155.503	258
FZ15_6	33	-56.1002	-76.4524	-44.7101	-155.97	274
FZ316_16	34	-53.0662	-79.0499	-50.249	-138.496	283

FZ27_20	35	-60.4415	-70.7327	-46.1848	-161.25	283
FZ21_14	36	-56.2403	-75.807	-44.6871	-157.485	284
FZ534_14	37	-54.479	-85.008	-47.9752	-131.118	286
FZ423_66	38	-66.3172	-74.5348	-41.9802	-165.136	297
FZ32_22	39	-56.197	-81.4166	-40.6689	-159.166	307
FZ187_41	40	-64.1495	-72.274	-44.2427	-151.571	308
FZ542_4	41	-59.4147	-79.0647	-40.069	-161.998	311
FZ531_75	42	-52.9113	-81.414	-46.7845	-135.556	311
FZ425_85	43	-66.7068	-73.8693	-41.8687	-162.384	319
FZ93_123	44	-57.8861	-80.6319	-42.0667	-141.094	323
FZ536_8	45	-59.187	-84.4685	-41.9693	-136.725	323
FZ521_23	46	-65.7554	-71.2773	-42.4269	-162.385	325
FZ426_8	47	-68.4164	-77.7637	-38.5788	-168.715	338
FZ189_9	48	-61.6191	-77.2512	-40.4525	-149.913	340
FZ550_38	49	-59.6025	-74.6821	-42.171	-151.915	342
FZ301_36	50	-51.2222	-89.8414	-42.3273	-141.647	342
FZ427_83	51	-55.8815	-82.929	-40.3364	-147.842	345
FZ344_36	52	-51.2222	-89.8414	-42.3273	-141.647	346
FZ483_69	53	-55.899	-74.5997	-46.3261	-137.317	348
FZ6_2	54	-54.6022	-83.6764	-40.2275	-148.306	357
FZ549_66	55	-58.5657	-71.5585	-42.9567	-151.947	365
FZ66_8	56	-53.1843	-87.3745	-44.0261	-129.948	368
FZ313_27	57	-55.7391	-75.6516	-48.2593	-131.303	368
FZ94_12	58	-61.2277	-64.4345	-44.9911	-158.554	371
FZ106_14	59	-66.2786	-58.6268	-46.6788	-173.449	372
FZ535_145	60	-55.8566	-84.2235	-43.4835	-127.312	377
FZ504_22	61	-63.8195	-61.6453	-47.3391	-152.536	378
FZ554_14	62	-56.0613	-85.474	-43.3396	-125.749	382
FZ173_4	63	-64.017	-76.6261	-38.4207	-166.499	390
FZ512_6	64	-57.0364	-64.373	-50.0677	-145.631	390
FZ462_15	65	-66.1707	-69.3401	-40.4907	-178.753	390
FZ332_6	66	-53.339	-74.5492	-46.3364	-135.733	390
FZ82_1	67	-58.2301	-69.683	-42.8953	-152.573	394
FZ338_6	68	-53.339	-74.5492	-46.3364	-135.733	394
FZ422_15	69	-48.1169	-89.8582	-42.7562	-138.058	396
FZ314_108	70	-57.6926	-67.3758	-46.321	-141.291	396
FZ317_23	71	-59.3166	-70.6389	-42.2461	-155.071	396
FZ4	72	-51.0426	-79.6693	-43.1015	-137.74	400
FZ14_41	73	-52.806	-89.6845	-39.0092	-148.346	405
FZ551_20	74	-63.7104	-62.6699	-44.2464	-159.173	407
FZ538_8	75	-54.368	-76.6625	-44.4028	-131.665	416

FZ169_9	76	-58.4367	-73.2288	-43.9397	-135.357	419
FZ3_1	77	-55.2294	-75.0907	-41.0444	-149.581	423
FZ580_176	78	-60.983	-66.2589	-42.4146	-143.643	452
FZ374_15	79	-52.6968	-88.3208	-38.6831	-138.7	471
FZ494_8	80	-49.8408	-84.0711	-42.1401	-129.893	473
FZ518_15	81	-53.2346	-71.8274	-41.9556	-143.965	479
FZ307_24	82	-53.7231	-75.3257	-44.4604	-127.181	480
FZ8	83	-50.1803	-80.6981	-38.8152	-149.937	482
FZ315_14	84	-50.6828	-71.6078	-45.2301	-136.921	482
FZ431_41	85	-49.6693	-76.4473	-44.2425	-133.601	483
FZ456_77	86	-50.8035	-77.5208	-41.9273	-135.479	483
FZ190_100	87	-62.2544	-70.9163	-41.4225	-136.029	484
FZ330_24	88	-52.1738	-82.2491	-38.9689	-139.804	484
FZ529_45	89	-49.7968	-72.0599	-45.0824	-137.278	486
FZ487_195	90	-49.3031	-70.9413	-44.2193	-146.51	487
FZ336_24	91	-52.1738	-82.2491	-38.9689	-139.804	488
FZ327_63	92	-50.7437	-74.5071	-47.1175	-126.058	489
FZ269_28	93	-51.4848	-63.7386	-44.9218	-155.514	489
FZ333_63	94	-50.7437	-74.5071	-47.1175	-126.058	491
FZ477_85	95	-51.7231	-79.7431	-42.7499	-124.466	496
FZ105_101	96	-52.9786	-85.2176	-36.5323	-145.623	505
FZ20_8	97	-52.2562	-78.8198	-37.99	-151.175	508
FZ434_8	98	-50.5304	-77.2186	-40.4328	-137.863	511
FZ541_71	99	-54.5524	-73.0937	-43.5393	-128.382	513
FZ117_98	100	-56.9721	-78.0642	-35.4338	-154.786	518
FZ492_36	101	-49.7351	-83.5182	-38.8129	-139.101	518
FZ532_18	102	-50.0234	-77.9756	-45.7259	-119.492	523
FZ577_8	103	-58.5273	-61.1629	-44.1364	-139.034	524
FZ433_153	104	-51.0308	-81.3242	-39.0244	-135.705	529
FZ115_97	105	-42.8039	-75.446	-46.2053	-140.204	531
FZ540_15	106	-54.6099	-74.1463	-42.6208	-125.825	535
FZ186_77	107	-55.0326	-66.9057	-42.7416	-135.567	539
FZ17_87	108	-52.4773	-74.3351	-40.1841	-138.681	545
FZ490_41	109	-52.8837	-76.2838	-39.9146	-135.296	545
FZ25_11	110	-54.7285	-71.5795	-37.993	-159.322	548
FZ481_113	111	-59.7038	-69.472	-40.2941	-135.626	548
FZ48_3	112	-50.9832	-63.66	-53.497	-133.658	549
FZ318_111	113	-46.4294	-79.5465	-42.2599	-129.909	552
Erlotinibe	114	-53.0708	-68.6377	-46.0952	-126.378	553
FZ586_144	115	-46.0233	-72.2362	-45.6576	-134.795	554
FZ203_4	116	-46.3201	-64.716	-44.2448	-158.286	559

FZ172_77	117	-50.1122	-79.3797	-40.3506	-128.252	564
FZ472_26	118	-53.5756	-70.3264	-41.8316	-134.544	565
FZ24_18	119	-47.4784	-85.81	-44.8088	-115.236	570
FZ103_154	120	-54.5255	-74.4842	-37.3395	-146.631	577
FZ558_79	121	-47.1733	-76.4278	-45.4625	-122.399	579
FZ79_19	122	-53.7281	-76.8795	-36.1868	-144.081	579
FZ560_52	123	-53.0893	-71.9352	-44.5425	-121.596	583
FZ60_10	124	-52.0772	-77.7409	-42.2566	-119.047	583
FZ58_96	125	-49.2885	-77.0423	-40.9826	-128.437	590
FZ552_13	126	-54.9522	-74.2293	-44.1723	-116.591	592
FZ116_11	127	-54.9882	-68.1269	-38.8106	-147.954	594
FZ432_38	128	-45.7587	-78.4969	-42.2136	-126.422	602
FZ118_4	129	-61.7841	-63.6335	-38.0071	-153.391	607
FZ136_15	130	-55.1783	-65.6744	-39.4549	-141.712	610
FZ171_16	131	-55.85	-66.0513	-39.7641	-137.456	613
FZ165_15	132	-55.1783	-65.6744	-39.4549	-141.712	614
FZ480_5	133	-46.7094	-82.357	-38.7838	-134.161	615
FZ500_42	134	-59.5782	-64.5943	-36.4289	-164.68	618
FZ127_7	135	-57.105	-73.291	-35.6735	-143.225	624
FZ559_32	136	-49.2088	-76.3734	-41.9903	-123.103	625
FZ479_79	137	-52.7706	-70.4433	-43.8667	-122.221	625
FZ582_39	138	-43.3893	-78.6451	-46.3119	-119.196	628
FZ498_19	139	-54.2919	-59.3219	-44.6215	-132.29	628
5-FU	140	-55.5727	-54.8646	-43.1139	-141.268	630
FZ257_23	141	-47.5053	-64.0215	-41.1439	-157.818	630
FZ513_39	142	-50.4467	-63.961	-42.5521	-137.282	630
FZ148_26	143	-54.4994	-63.4126	-40.7375	-138.303	633
FZ509_90	144	-44.0762	-71.5874	-46.0283	-128.587	639
FZ463_52	145	-46.8705	-65.7609	-42.4497	-141.165	639
FZ380_8	146	-48.7137	-74.9015	-43.1453	-121.23	639
FZ36_19	147	-47.4472	-82.5125	-41.1931	-118.846	641
FZ430_76	148	-46.9413	-76.2327	-39.5431	-134.169	646
FZ72_9	149	-54.1929	-70.08	-38.7277	-136.849	647
FZ428_16	150	-51.6182	-76.6126	-42.3294	-115.193	651
FZ81_68	151	-56.7351	-70.6795	-35.6215	-145.728	654
FZ263_26	152	-47.6572	-60.1107	-48.6035	-130.361	660
FZ533_46	153	-44.9673	-74.258	-45.8021	-119.869	662
FZ459_54	154	-53.3378	-73.5966	-35.5733	-145.256	663
FZ561_25	155	-44.7079	-77.0534	-41.667	-125.842	666
FZ168_15	156	-48.6946	-70.8621	-42.0445	-127.253	667
FZ563_15	157	-44.882	-77.9197	-41.2912	-124.29	667

FZ41	158	-43.727	-70.1728	-45.7686	-129.336	668
FZ579_15	159	-60.4661	-68.7032	-33.7143	-157.689	669
FZ392_26	160	-49.6535	-77.7823	-40.4742	-118.524	670
FZ16_37	161	-48.8529	-82.465	-38.8858	-121.854	671
FZ458_2	162	-43.2067	-79.8468	-46.5486	-114.331	671
FZ129_68	163	-39.8432	-78.3691	-39.005	-142.602	678
FZ562_179	164	-46.7052	-71.8105	-43.5114	-123.181	680
FZ11_1	165	-49.3853	-76.999	-37.2774	-133.771	682
FZ130_1	166	-48.4138	-62.6614	-41.3671	-142.935	682
FZ474_22	167	-47.4474	-73.2447	-39.311	-134.442	689
FZ22_3	168	-48.9253	-76.5025	-39.5064	-122.791	697
FZ360_105	169	-45.17	-85.4817	-37.4929	-128.109	701
FZ91_54	170	-41.6573	-79.604	-42.0886	-122.3	704
FZ468_16	171	-53.864	-51.8196	-43.8364	-135.199	717
FZ275_14	172	-55.7727	-55.7709	-42.2779	-130.069	720
FZ515_62	173	-55.8525	-49.9883	-40.4879	-151.544	721
FZ429_54	174	-45.0877	-72.1443	-47.5132	-113.622	725
FZ133_126	175	-39.9426	-80.3338	-43.9071	-115.79	734
FZ510_38	176	-51.1832	-62.0726	-45.8952	-117.912	734
FZ162_126	177	-39.9426	-80.3338	-43.9071	-115.79	736
FZ493_54	178	-46.6011	-64.8241	-44.4203	-123.45	737
FZ489_82	179	-48.0442	-65.203	-44.8804	-119.332	740
FZ460_14	180	-42.0548	-69.179	-42.3889	-134.087	741
FZ567	181	-56.3761	-57.7373	-41.7274	-125.975	742
FZ188_18	182	-44.1373	-63.2861	-44.2957	-132.449	747
FZ322_26	183	-59.4378	-68.8417	-34.8685	-133.792	749
FZ475_178	184	-48.24	-71.1915	-39.0567	-128.305	749
FZ23_19	185	-47.0728	-71.4721	-39.107	-129.688	751
FZ537_11	186	-52.5568	-65.8534	-38.4068	-131.63	764
FZ457_166	187	-48.7491	-64.2757	-41.351	-126.534	766
FZ356_7	188	-49.2912	-65.8328	-42.4211	-119.688	766
FZ83_55	189	-52.6777	-66.2751	-34.0063	-151.538	780
oxaliplatin	190	-46.3484	-75.9761	-40.3616	-116.602	782
FZ329_10	191	-53.3589	-62.8697	-39.793	-124.057	782
FZ335_10	192	-53.3589	-62.8697	-39.793	-124.057	786
FZ585_3	193	-50.9504	-76.7475	-36.765	-119.473	791
FZ439_113	194	-44.5164	-75.9586	-35.0554	-142.352	791
FZ35_38	195	-47.9601	-73.1731	-36.3992	-133.092	792
FZ530	196	-44.9604	-63.1227	-39.4025	-140.395	805
FZ470_11	197	-43.5045	-64.301	-39.0462	-145.459	810
FZ469_181	198	-49.6557	-58.3445	-40.8798	-130.489	811

ligand_cape	199	-42.2222	-76.7647	-44.842	-107.74	814
FZ575_4	200	-48.519	-60.7935	-38.8183	-137.05	818
FZ584_46	201	-51.0159	-63.1794	-41.9883	-116.8	823
FZ227_6	202	-44.8917	-61.439	-40.677	-135.149	825
FZ34_17	203	-48.2722	-73.935	-41.5231	-109.021	831
FZ80_14	204	-40.4293	-72.0242	-37.9366	-138.592	837
FZ455_92	205	-49.486	-67.5978	-36.9827	-129.388	841
FZ267_38	206	-44.6439	-56.0757	-41.1159	-140.89	845
FZ438_11	207	-51.9036	-65.9592	-40.0229	-115.314	846
FZ326_21	208	-50.5792	-65.9952	-39.9352	-116.425	850
FZ416_28	209	-43.893	-71.5772	-43.6843	-112.854	852
FZ5_2	210	-45.4403	-80.1369	-36.0777	-118.914	852
FZ55_2	211	-47.8711	-56.4229	-38.958	-138.697	862
FZ408_23	212	-36.8364	-84.0451	-37.6048	-123.357	865
FZ453_196	213	-46.521	-68.729	-38.1936	-125.349	873
FZ145_77	214	-47.7712	-71.3023	-33.508	-136.944	878
FZ583_25	215	-43.792	-79.2503	-38.6241	-114.622	879
FZ514_50	216	-48.0719	-60.4508	-37.4501	-136.997	880
FZ128_26	217	-38.7313	-71.2069	-37.0844	-141.232	881
FZ237_4	218	-39.2417	-59.2067	-39.9151	-147.569	882
FZ478_7	219	-41.1512	-77.1592	-40.6945	-111.525	884
FZ516_28	220	-45.8452	-64.662	-39.4623	-124.047	885
FZ239_4	221	-39.2417	-59.2067	-39.9151	-147.569	886
FZ328_9	222	-46.2232	-77.3189	-38.7114	-109.934	891
FZ71_109	223	-48.5416	-62.7043	-36.828	-133.315	894
FZ517_106	224	-45.487	-64.0227	-41.8861	-117.303	894
FZ334_9	225	-46.2232	-77.3189	-38.7114	-109.934	895
FZ325_123	226	-57.4422	-65.8603	-33.834	-123.454	898
FZ221_1	227	-51.4395	-57.0398	-39.0556	-124.826	901
FZ62_52	228	-46.7179	-70.8055	-39.5216	-113.813	907
FZ144_24	229	-44.1647	-52.2494	-46.2223	-122.891	908
FZ546_7	230	-50.0063	-58.928	-38.1361	-128.62	908
FZ406_31	231	-35.6517	-84.4236	-35.9731	-124.157	908
FZ289_13	232	-48.3987	-58.0493	-38.9847	-127.809	915
FZ454_85	233	-44.6444	-70.073	-37.9187	-123.129	926
FZ471_54	234	-47.3357	-62.6253	-39.8536	-118.801	927
FZ331_78	235	-44.4897	-75.5143	-39.1211	-110.934	929
FZ337_78	236	-44.4897	-75.5143	-39.1211	-110.934	933
FZ528_4	237	-43.4562	-72.1116	-38.4684	-118.61	941
FZ149_108	238	-50.0326	-65.7149	-30.5995	-142.279	945
FZ28_14	239	-44.9504	-71.4026	-41.8688	-102.936	945

FZ170_13	240	-47.5649	-43.25	-45.7437	-122.15	947
FZ68_16	241	-52.1429	-58.9173	-33.0097	-141.56	952
FZ1_2	242	-44.8158	-77.6807	-34.6806	-117.142	959
FZ508_88	243	-34.5897	-74.4449	-44.8138	-105.298	959
FZ295_6	244	-41.9537	-57.8144	-37.5147	-145.772	967
FZ245_1	245	-47.002	-55.8539	-39.8472	-122.438	973
FZ40_25	246	-31.9322	-63.5351	-45.0871	-120.501	974
FZ409_153	247	-41.8659	-81.9202	-33.1834	-122.103	978
FZ543_33	248	-46.7278	-49.8442	-40.4285	-127.077	986
FZ7_3	249	-45.1929	-68.7474	-33.156	-134.399	989
FZ440_6	250	-41.0932	-66.7045	-42.3877	-109.687	998
FZ209_3	251	-38.2045	-60.4962	-42.7609	-118.074	1001
FZ445_190	252	-50.3296	-50.4866	-35.6983	-138.543	1002
FZ539_40	253	-46.3987	-48.4243	-42.5667	-119.421	1006
FZ281_24	254	-44.8991	-67.7505	-38.8118	-113.334	1011
FZ294_176	255	-46.2614	-52.8373	-38.7804	-127.605	1016
FZ410_32	256	-37.3808	-74.172	-37.09	-121.037	1017
FZ321_47	257	-52.9849	-68.699	-33.2602	-116.186	1025
FZ233_22	258	-45.7985	-54.3489	-41.0509	-117.177	1025
FZ525_16	259	-36.6747	-73.9267	-39.5976	-111.313	1034
FZ215_14	260	-37.8774	-66.4134	-39.3351	-117.686	1039
FZ225_28	261	-37.0705	-57.3343	-40.3444	-127.589	1041
FZ197_9	262	-47.8068	-56.9415	-41.362	-109.836	1044
FZ568_37	263	-42.695	-55.9584	-41.127	-119.199	1045
FZ107_44	264	-46.9371	-65.5777	-29.4264	-136.896	1052
FZ95_9	265	-36.521	-69.1691	-34.7177	-132.274	1063
FZ544_13	266	-45.9768	-58.0994	-39.3196	-114.409	1073
FZ420_20	267	-31.1817	-83.1956	-35.5684	-115.818	1080
FZ131_2	268	-32.7742	-65.155	-35.8651	-136.779	1086
FZ261_9	269	-43.211	-50.5039	-39.1078	-126.792	1089
FZ384_41	270	-32.5393	-82.1186	-35.3548	-115.019	1092
FZ312_16	271	-44.9723	-53.5297	-35.8187	-129.863	1102
FZ251_4	272	-37.2004	-54.6575	-36.1711	-141.295	1107
FZ466_27	273	-29.7377	-74.0284	-35.7165	-125.21	1107
FZ59	274	-41.1157	-60.8047	-34.4636	-131.859	1114
FZ496_32	275	-35.8217	-69.9758	-34.6484	-125.066	1114
FZ524	276	-38.6544	-75.2374	-37.1257	-107.925	1114
FZ526	277	-39.6189	-70.9901	-35.4773	-116.637	1114
FZ573_13	278	-45.8242	-57.7967	-38.2529	-115.352	1117
FZ396_41	279	-36.2193	-77.0613	-35.937	-109.848	1121
FZ398_22	280	-46.5019	-63.6208	-35.4463	-114.984	1121

FZ65_110	281	-44.9259	-64.5173	-36.8888	-111.894	1122
FZ436	282	-42.568	-61.3442	-39.7154	-109.809	1130
FZ507_123	283	-30.6159	-73.817	-41.5958	-100.495	1131
FZ473_17	284	-48.488	-69.6347	-27.1173	-121.929	1131
FZ547_65	285	-44.0195	-61.1269	-37.6134	-114.76	1140
FZ291_36	286	-45.2656	-52.1485	-39.864	-113.303	1140
FZ397_150	287	-41.9164	-71.1072	-36.1984	-109.538	1143
FZ378_4	288	-44.8379	-62.8356	-34.9532	-117.665	1144
FZ348_118	289	-44.624	-57.3338	-33.5246	-130.256	1150
FZ249_8	290	-34.0012	-55.8967	-37.9615	-132.844	1152
FZ366_118	291	-44.624	-57.3338	-33.5246	-130.256	1154
FZ147_70	292	-39.4635	-45.9821	-41.0912	-122.926	1156
FZ282_11	293	-45.0899	-47.1925	-42.8319	-104.975	1165
FZ372_20	294	-38.4698	-75.7592	-32.5807	-116.223	1166
FZ320_192	295	-51.622	-66.9011	-31.4056	-110.304	1168
FZ370_36	296	-37.2021	-73.2502	-32.0719	-122.049	1171
FZ506_19	297	-39.328	-53.2074	-43.7437	-105.812	1174
FZ362_73	298	-34.3053	-77.446	-33.6488	-113.233	1178
FZ154_11	299	-54.1293	-43.4159	-40.2917	-99.7111	1180
FZ135_93	300	-43.6698	-50.3894	-38.3547	-121.264	1181
FZ140_15	301	-42.4516	-47.7492	-39.0372	-121.794	1182
FZ164_93	302	-43.6698	-50.3894	-38.3547	-121.264	1185
FZ574_62	303	-43.1815	-52.8051	-38.2518	-118.494	1190
FZ499_135	304	-31.5581	-69.7833	-35.6043	-121.224	1190
FZ349_43	305	-43.2044	-54.0016	-33.6422	-131.62	1194
FZ414_66	306	-36.8869	-70.0233	-37.5427	-106.436	1198
FZ367_43	307	-43.2044	-54.0016	-33.6422	-131.62	1198
FZ123_40	308	-41.1568	-45.6667	-40.5258	-117.871	1199
FZ578_42	309	-46.9812	-37.284	-40.8833	-113.493	1199
FZ576_23	310	-35.12	-67.3973	-37.894	-110.63	1203
FZ255_16	311	-34.8723	-46.8517	-42.7693	-115.326	1221
FZ56	312	-39.5071	-58.2274	-33.2117	-130.226	1223
FZ297_79	313	-31.477	-82.9266	-32.8528	-110.353	1228
FZ421_119	314	-37.6103	-66.6822	-34.9369	-114.19	1230
FZ324_31	315	-43.3725	-75.7399	-28.3504	-112.088	1230
FZ340_79	316	-31.477	-82.9266	-32.8528	-110.353	1232
FZ214_57	317	-32.6035	-63.7053	-33.1949	-131.328	1234
FZ305_5	318	-41.4709	-62.3352	-38.2902	-103.286	1234
FZ548_3	319	-42.2487	-58.5106	-36.0727	-114.784	1237
FZ352_71	320	-43.4798	-51.7231	-37.5739	-116.105	1239
FZ43_3	321	-44.4734	-51.4384	-41.4677	-97.801	1240

FZ44	322	-44.4734	-51.4384	-41.4677	-97.801	1241
FZ13_3	323	-34.2362	-83.2646	-31.2292	-107.938	1243
FZ461_31	324	-38.4204	-67.0331	-27.4475	-127.588	1243
FZ45	325	-44.4734	-51.4384	-41.4677	-97.801	1245
FZ382_28	326	-33.2015	-69.5455	-35.4399	-114.359	1246
FZ435_28	327	-33.71	-61.6696	-38.5278	-112.592	1253
FZ119_98	328	-30.8457	-69.7841	-36.3863	-112.909	1258
FZ31_2	329	-39.8396	-69.4792	-34.1183	-108.787	1259
FZ19_2	330	-35.1371	-71.1997	-36.4842	-101.127	1261
FZ311_25	331	-37.3277	-60.2544	-39.9132	-98.2437	1264
FZ78_1	332	-35.203	-51.5818	-42.7872	-104.121	1267
FZ142_28	333	-35.3372	-50.4499	-37.182	-124.272	1271
FZ273_60	334	-39.5571	-55.3043	-33.656	-124.621	1273
FZ160_28	335	-35.3372	-50.4499	-37.182	-124.272	1275
FZ207_7	336	-34.6604	-48.7488	-37.8323	-125.081	1276
FZ571_13	337	-41.0405	-51.0419	-38.3534	-114.409	1279
FZ92_25	338	-31.8874	-66.4673	-35.6996	-113.748	1280
FZ134_84	339	-40.8923	-64.6984	-31.15	-117.719	1284
FZ446	340	-32.3981	-61.0569	-39.65	-104.924	1287
FZ163_84	341	-40.8923	-64.6984	-31.15	-117.719	1288
FZ183_7	342	-38.0499	-54.2062	-35.0438	-121.597	1289
FZ309_44	343	-37.5113	-60.038	-38.5923	-102.856	1291
FZ231_1	344	-44.3101	-50.2817	-33.8257	-122.446	1293
FZ156_10	345	-44.7208	-54.7835	-33.8806	-115.047	1296
FZ293_13	346	-44.5482	-45.4263	-37.7746	-114.979	1298
FZ195_5	347	-42.434	-49.553	-34.703	-121.559	1312
FZ386_23	348	-25.9926	-78.993	-31.9583	-112.629	1313
FZ124_1	349	-44.7944	-41.8839	-33.8739	-124.996	1319
FZ212_58	350	-40.1901	-29.285	-39.4533	-118.005	1325
FZ418_39	351	-31.3408	-75.8692	-33.0012	-108.016	1326
FZ444	352	-39.6729	-51.5869	-37.4587	-113.089	1328
FZ152_8	353	-40.3345	-44.3947	-36.9684	-119.419	1329
FZ146_43	354	-43.1999	-51.7144	-31.7918	-124.85	1330
FZ137_145	355	-32.8998	-65.8813	-29.5069	-122.593	1342
FZ185_9	356	-35.3525	-48.7122	-37.3385	-118.163	1343
FZ166_145	357	-32.8998	-65.8813	-29.5069	-122.593	1344
FZ70_15	358	-31.832	-58.8537	-33.628	-122.425	1357
FZ57_97	359	-36.5682	-60.0324	-37.122	-101.644	1361
FZ412_76	360	-39.4392	-53.4916	-34.5425	-115.576	1361
FZ303_86	361	-36.3366	-61.6552	-36.0036	-102.721	1363
FZ256_59	362	-26.7682	-61.2824	-34.7709	-119.826	1363

FZ104_19	363	-25.3263	-71.0893	-38.0498	-97.1249	1364
FZ114_3	364	-41.509	-51.0122	-37.1443	-108.022	1364
FZ394_54	365	-30.4171	-77.6759	-30.495	-104.926	1368
FZ566_62	366	-37.782	-40.3939	-38.5228	-116.174	1370
FZ179_2	367	-39.1212	-47.9954	-35.9169	-116.454	1371
FZ223_23	368	-28.9696	-61.5643	-34.7574	-116.663	1373
FZ90_27	369	-45.9229	-53.0118	-34.6331	-102.03	1379
FZ201_6	370	-31.5145	-60.0804	-33.7628	-117.975	1382
FZ177_2	371	-33.235	-57.9382	-34.667	-116.024	1384
FZ226_163	372	-23.9617	-62.421	-33.4994	-123.925	1384
FZ402_51	373	-35.2015	-65.916	-34.2301	-99.9832	1393
FZ379_1	374	-39.7761	-54.3377	-29.3066	-122.84	1395
FZ306_161	375	-41.1411	-58.4108	-35.3753	-98.2495	1398
FZ390_65	376	-37.7577	-58.3009	-36.3313	-97.1333	1419
FZ495_12	377	-36.8595	-43.9055	-38.87	-107.461	1430
FZ194_45	378	-33.9292	-37.4858	-38.5707	-116.12	1432
FZ211_22	379	-28.4449	-60.8023	-35.4385	-111.068	1432
FZ102_1	380	-40.4049	-53.5851	-33.7121	-109.838	1433
FZ385_150	381	-36.6268	-69.0918	-28.2152	-107.47	1439
FZ202_55	382	-20.2418	-66.1502	-29.2334	-124.076	1442
FZ373_187	383	-34.897	-73.7263	-27.3177	-102.319	1443
FZ143_175	384	-34.8621	-38.1469	-38.4302	-113.615	1446
FZ161_175	385	-34.8621	-38.1469	-38.4302	-113.615	1450
FZ76_1	386	-44.2702	-37.823	-38.3419	-98.1844	1456
FZ238_151	387	-19.4303	-64.371	-28.2002	-126.621	1465
FZ565_11	388	-25.4717	-59.723	-36.5024	-107.512	1466
FZ354_12	389	-37.5993	-59.944	-35.5053	-87.9659	1467
FZ265_74	390	-26.9817	-60.0747	-34.2515	-113.342	1470
FZ393_114	391	-45.8693	-33.3426	-38.1086	-94.8204	1474
FZ302_134	392	-39.593	-48.3383	-32.9655	-115.094	1476
FZ465_54	393	-33.2367	-58.5659	-35.2568	-99.8413	1482
FZ350_57	394	-40.9095	-53.0699	-34.6978	-97.7567	1483
FZ247_19	395	-18.8427	-56.925	-35.7371	-115.427	1491
FZ369_111	396	-30.7655	-49.584	-40.9313	-88.6669	1493
FZ417_112	397	-33.3354	-58.0276	-34.2635	-104.258	1495
FZ110_10	398	-36.9814	-41.3916	-34.0999	-117.33	1496
FZ413_191	399	-26.6037	-67.0269	-34.9639	-89.9041	1514
FZ285_22	400	-33.3566	-44.1744	-36.2143	-111.564	1514
FZ497_64	401	-35.6762	-42.1455	-36.8534	-107.752	1516
FZ63_55	402	-33.1308	-48.9748	-38.8542	-92.607	1518
FZ415_183	403	-32.8555	-58.234	-31.4165	-112.824	1518

FZ304_93	404	-33.1311	-43.261	-39.1198	-97.2842	1527
FZ368_57	405	-34.1671	-54.311	-36.954	-87.987	1529
FZ564_70	406	-31.6784	-53.2595	-35.3281	-104.364	1530
FZ485_62	407	-27.0591	-54.1653	-31.7661	-119.805	1530
FZ268_177	408	-25.9117	-55.0753	-32.2721	-118.589	1535
FZ151_44	409	-31.6917	-50.6284	-37.3963	-98.4155	1538
FZ347_185	410	-27.4368	-63.7684	-33.1669	-98.9506	1556
FZ365_185	411	-27.4368	-63.7684	-33.1669	-98.9506	1560
FZ252_134	412	-35.0592	-34.5236	-38.998	-97.5306	1562
FZ235_18	413	-23.4838	-59.3654	-34.3259	-104.44	1571
FZ388_74	414	-34.1064	-56.422	-30.7645	-108.175	1572
FZ346_155	415	-35.3077	-51.784	-32.7539	-107.331	1573
FZ355_29	416	-34.3752	-53.585	-29.7976	-111.848	1576
FZ442_37	417	-21.0116	-59.7734	-36.4612	-94.9385	1580
FZ219_2	418	-38.6289	-45.9491	-32.3028	-110.472	1581
FZ276_12	419	-44.0935	-37.3454	-33.635	-101.953	1582
FZ310_99	420	-24.0543	-67.9188	-33.4186	-89.621	1583
FZ74_2	421	-35.8625	-42.7286	-38.1449	-87.1284	1587
FZ199_24	422	-24.2361	-52.9606	-35.3747	-106.553	1593
FZ61_67	423	-29.7047	-48.0374	-35.86	-105.102	1593
FZ400_2	424	-41.6797	-59.4722	-23.8943	-96.2511	1597
FZ505_186	425	-25.8798	-55.2611	-32.6693	-112.423	1599
FZ403_44	426	-35.6221	-55.5452	-25.7326	-110.559	1601
FZ253_62	427	-21.5251	-55.7045	-35.096	-104.243	1604
FZ200_25	428	-33.9235	-27.2133	-35.0726	-113.328	1609
FZ286_193	429	-37.4824	-49.7306	-32.2972	-102.556	1610
FZ351_118	430	-29.7458	-58.8799	-33.8371	-89.1292	1624
FZ411_1	431	-29.7871	-56.0346	-34.8533	-87.1611	1632
FZ570_40	432	-32.8219	-45.3731	-36.4407	-92.5546	1637
FZ98_33	433	-32.5791	-51.7952	-30.4359	-108.427	1645
FZ46_6	434	-31.5969	-46.8411	-33.4675	-105.912	1656
FZ77_16	435	-28.0873	-51.6949	-33.8984	-99.8702	1658
FZ49_7	436	-31.6339	-46.6503	-34.3255	-98.8495	1666
FZ126_1	437	-29.2737	-52.6074	-29.0805	-111.993	1667
FZ50_7	438	-31.6339	-46.6503	-34.3255	-98.8495	1668
FZ222_120	439	28.9789	-56.1568	-39.1981	-54.9358	1670
FZ51	440	-31.6339	-46.6503	-34.3255	-98.8495	1670
FZ101_63	441	-38.999	-37.8429	-26.4664	-114.636	1671
FZ100_1	442	-29.1862	-48.0991	-31.9717	-111.393	1671
FZ437_25	443	-21.3135	-58.7727	-33.4733	-97.309	1674
FZ243_9	444	-34.9253	-48.2624	-29.755	-105.664	1676

FZ353_172	445	-23.8071	-62.0729	-33.4275	-84.0948	1677
FZ401_187	446	-25.7342	-59.8765	-33.2931	-86.5069	1683
FZ174_73	447	-33.3242	-46.7217	-33.7986	-95.7373	1685
FZ125_30	448	-27.2786	-49.2021	-32.014	-110.072	1691
FZ75_48	449	-23.5351	-34.8028	-39.5657	-91.0807	1691
FZ491_87	450	-27.7122	-46.2172	-36.7221	-89.6014	1691
FZ361_176	451	-22.0287	-62.8178	-32.2173	-88.067	1703
FZ208_129	452	-32.7053	-42.0095	-30.7957	-111.311	1704
FZ181_24	453	-30.5609	-45.9342	-32.7536	-106.472	1705
FZ175_30	454	-28.642	-53.2471	-30.3041	-102.73	1709
FZ205_67	455	-26.8526	-36.8895	-34.6892	-108.888	1711
FZ184_170	456	-27.4163	-57.759	-29.5101	-98.6405	1712
FZ283_13	457	-40.6989	-42.0248	-31.109	-95.5748	1712
FZ358_64	458	-29.9578	-56.7276	-26.9154	-101.717	1716
FZ279_19	459	-27.665	-52.6355	-33.3497	-92.1784	1721
FZ502_57	460	-30.312	-48.2263	-34.9679	-83.7578	1721
FZ113_3	461	-30.2127	-51.8767	-24.3417	-110.521	1722
FZ111_73	462	-34.2144	-32.853	-31.3524	-110.774	1724
FZ377_99	463	-19.0043	-63.9901	-32.3793	-80.2572	1724
FZ89_124	464	-24.4164	-58.5383	-27.5954	-101.643	1734
FZ389_166	465	-23.6352	-61.7273	-31.2712	-82.1809	1737
FZ391_3	466	-28.8572	-58.8969	-28.2389	-91.7048	1742
FZ345_88	467	-28.4723	-43.1094	-35.9023	-85.9025	1744
FZ176_23	468	-32.2155	-51.13	-27.3868	-101.379	1747
FZ363_88	469	-28.4723	-43.1094	-35.9023	-85.9025	1748
FZ419_86	470	-26.1678	-52.7501	-33.2123	-88.6007	1749
FZ47_6	471	-22.5302	-57.4264	-31.4613	-91.5073	1768
FZ178_155	472	-27.4095	-52.6625	-31.4853	-91.9513	1772
FZ399_151	473	-25.4992	-50.1635	-32.8577	-89.935	1795
FZ67_2	474	-21.499	-45.65	-36.5109	-73.4211	1798
FZ122_32	475	-25.7122	-52.6715	-32.1852	-84.6651	1802
FZ155_124	476	-28.3205	-46.5324	-29.472	-102.138	1807
FZ139_139	477	-24.5988	-35.6313	-34.4862	-96.9801	1821
FZ97_125	478	-30.9754	-42.783	-31.4795	-92.81	1822
FZ158_139	479	-24.5988	-35.6313	-34.4862	-96.9801	1825
FZ180_12	480	-23.8243	-37.5738	-36.1302	-72.7804	1840
FZ259_86	481	-23.2802	-33.7651	-28.6724	-114.398	1840
FZ284_62	482	-22.6186	-47.2	-31.6565	-96.7682	1841
FZ501_94	483	-18.6842	-53.6811	-29.4737	-92.9293	1845
FZ112_29	484	-30.5805	-40.4975	-31.5627	-91.633	1850
FZ88_1	485	-31.7226	-47.0655	-28.4738	-86.5441	1850

FZ196_71	486	-21.3918	-46.4914	-28.7891	-104.589	1852
FZ271_7	487	-29.2458	-30.3572	-29.2537	-106.213	1860
FZ220_186	488	-23.4159	-30.7713	-33.2005	-100.828	1861
FZ405_177	489	-34.4357	-29.8605	-32.7998	-74.1393	1865
FZ300_152	490	-30.3435	-41.1029	-24.1569	-103.817	1865
FZ545_25	491	-19.1277	-47.9433	-30.1601	-98.6303	1869
FZ343_152	492	-30.3435	-41.1029	-24.1569	-103.817	1869
FZ236_80	493	-22.912	-47.0839	-30.3401	-95.818	1872
FZ277_63	494	-30.6286	-41.6657	-30.3418	-88.8158	1874
FZ308_2	495	-23.0287	-51.1283	-31.0031	-82.5385	1874
FZ86_11	496	-26.8238	-42.4095	-32.7629	-85.1708	1876
FZ387_33	497	-21.3723	-52.0476	-30.8457	-80.4135	1878
FZ296_103	498	-17.1055	-60.6637	-26.8012	-69.6969	1882
FZ339_103	499	-17.1055	-60.6637	-26.8012	-69.6969	1884
FZ38_81	500	-24.6501	-47.2201	-26.6136	-97.1876	1894
FZ87_79	501	-20.1576	-31.8557	-34.1943	-91.7674	1898
FZ69_39	502	-18.2702	-36.8643	-33.6003	-93.7077	1899
FZ441_117	503	-13.9469	-53.9478	-25.9321	-93.2628	1900
FZ244_71	504	-27.5175	-45.1804	-19.9053	-97.8568	1915
FZ527_15	505	-19.435	-45.762	-32.5331	-80.7078	1921
FZ467_66	506	-25.0082	-27.8283	-34.4992	-69.6031	1924
FZ182_21	507	-34.2856	-39.3592	-24.5953	-79.7568	1931
FZ234_66	508	-22.0905	-35.0688	-32.9947	-87.0834	1939
FZ381_100	509	-24.665	-36.4613	-30.4152	-92.4078	1942
FZ216_54	510	-29.9698	-23.0091	-31.5367	-81.8006	1949
FZ229_57	511	-24.3778	-37.3781	-28.3272	-96.7757	1949
FZ280_119	512	-13.5357	-49.1043	-22.5562	-97.2638	1956
FZ242_45	513	-19.7199	-21.9025	-32.4898	-96.0584	1959
FZ274_49	514	-24.6936	-16.4915	-31.239	-92.2562	1966
FZ232_123	515	-22.5439	-36.7762	-27.2586	-98.5505	1967
FZ73_2	516	-21.2503	-30.8421	-32.8064	-84.9697	1968
FZ375_78	517	-29.6168	-46.8118	-22.0266	-72.622	1968
FZ198_8	518	-18.1633	-39.774	-32.2415	-82.1756	1970
FZ39_81	519	-14.9927	-52.1614	-26.6684	-63.4149	1988
FZ37_81	520	-14.9927	-52.1614	-26.6684	-63.4149	1990
FZ248_25	521	-7.9712	-38.0529	-30.04	-92.2688	2003
FZ224_73	522	-20.165	-23.8228	-31.6146	-86.8725	2007
FZ266_140	523	-10.8849	-25.2824	-27.54	-103.371	2012
FZ357_184	524	-14.6281	-43.5498	-30.4452	-70.4016	2014
FZ241_34	525	-6.79	-53.0992	-16.6205	-56.6215	2030
FZ109_6	526	-11.7372	-46.0078	-28.3089	-73.8141	2032

FZ264_108	527	-14.05	-33.0316	-32.7658	-65.8112	2032
FZ278_30	528	-27.9333	-24.1971	-24.0809	-87.1119	2036
FZ217_57	529	-20.1654	-36.9792	-20.6847	-93.155	2041
FZ230_72	530	-12.6319	-26.1485	-32.4006	-75.5063	2044
FZ141_107	531	-17.7467	-42.4182	-27.6534	-73.5287	2045
FZ99_73	532	-3.5744	-50.7137	-26.3127	-50.18	2046
FZ159_107	533	-17.7467	-42.4182	-27.6534	-73.5288	2047
FZ503_76	534	-17.6386	-12.6714	-29.951	-90.5476	2048
FZ572_8	535	-15.7649	-30.3051	-31.0922	-78.998	2053
FZ85_99	536	-19.7383	-29.2458	-30.2603	-72.1816	2066
FZ210_17	537	-6.6913	-44.8938	-25.5962	-80.1002	2068
FZ228_75	538	-22.272	-19.4072	-29.6353	-73.5714	2068
FZ359_141	539	-18.6487	-29.8224	-28.399	-80.7928	2072
FZ395_59	540	-12.4824	-37.2107	-30.2284	-59.4375	2073
FZ121_27	541	-12.3243	-39.99	-26.4031	-80.3355	2081
FZ371_97	542	-4.8427	-45.3257	-26.735	-56.8396	2085
FZ246_7	543	-11.2734	-41.2011	-21.3921	-84.1058	2090
FZ443_78	544	2.5388	-48.1488	-21.5059	-49.6692	2096
FZ53	545	2.8121	-46.9778	-23.0059	-56.0433	2098
FZ192_40	546	-17.7954	-24.5921	-27.504	-77.0325	2108
FZ204_90	547	-12.4338	-23.1862	-28.7417	-77.5642	2112
FZ240_2	548	-12.4411	-21.0854	-28.5603	-79.1328	2113
FZ54_8	549	13.4665	-45.9557	-25.4055	-43.9675	2115
FZ42_25	550	0.0071	-41.0787	-27.7095	-37.1522	2123
FZ407_64	551	-17.5384	-34.7329	-21.009	-75.5743	2129
FZ153_90	552	-4.8267	-44.4343	-21.2669	-40.6413	2130
FZ292_25	553	-3.4152	-35.3264	-23.893	-77.7538	2144
FZ383_104	554	-7.0944	-34.686	-26.0843	-64.1516	2146
FZ262_21	555	-12.0473	-27.9951	-22.2009	-79.3365	2149
FZ52_8	556	-12.0031	-27.823	-27.4021	-52.6416	2152
FZ260_107	557	-1.2291	-41.4326	-17.9254	-47.3465	2160
FZ298_79	558	-3.778	-36.5102	-24.9363	-49.6273	2161
FZ341_79	559	-3.778	-36.5102	-24.9363	-49.6273	2163
FZ206_89	560	-1.2592	-37.7996	-19.195	-52.3302	2168
FZ218_81	561	2.8746	-38.1175	-14.6371	-48.0451	2179
FZ272_82	562	-0.2856	-37.0467	-12.2068	-53.0586	2180
FZ258_51	563	9.4193	-23.7001	-18.132	-38.2578	2230
FZ270_75	564	43.1607	-14.6264	-5.9986	-1.2922	2247

FZ229_57	565	-24.3778	-37.3781	-28.3272	-96.7757	1949
FZ280_119	567	-13.5357	-49.1043	-22.5562	-97.2638	1956
FZ242_45	568	-19.7199	-21.9025	-32.4898	-96.0584	1959
FZ274_49	569	-24.6936	-16.4915	-31.239	-92.2562	1966
FZ232_123	600	-22.5439	-36.7762	-27.2586	-98.5505	1967
FZ73_2	601	-21.2503	-30.8421	-32.8064	-84.9697	1968
FZ375_78	602	-29.6168	-46.8118	-22.0266	-72.622	1968
FZ198_8	603	-18.1633	-39.774	-32.2415	-82.1756	1970
FZ39_81	604	-14.9927	-52.1614	-26.6684	-63.4149	1988
FZ37_81	605	-14.9927	-52.1614	-26.6684	-63.4149	1990
FZ248_25	606	-7.9712	-38.0529	-30.04	-92.2688	2003
FZ224_73	607	-20.165	-23.8228	-31.6146	-86.8725	2007
FZ266_140	608	-10.8849	-25.2824	-27.54	-103.371	2012
FZ357_184	609	-14.6281	-43.5498	-30.4452	-70.4016	2014
FZ241_34	610	-6.79	-53.0992	-16.6205	-56.6215	2030
FZ109_6	611	-11.7372	-46.0078	-28.3089	-73.8141	2032
FZ264_108	612	-14.05	-33.0316	-32.7658	-65.8112	2032
FZ278_30	613	-27.9333	-24.1971	-24.0809	-87.1119	2036
FZ217_57	614	-20.1654	-36.9792	-20.6847	-93.155	2041

FZ230_72	615	-12.6319	-26.1485	-32.4006	-75.5063	2044
FZ141_107	616	-17.7467	-42.4182	-27.6534	-73.5287	2045
FZ99_73	617	-3.5744	-50.7137	-26.3127	-50.18	2046
FZ159_107	618	-17.7467	-42.4182	-27.6534	-73.5288	2047
FZ503_76	619	-17.6386	-12.6714	-29.951	-90.5476	2048
FZ572_8	620	-15.7649	-30.3051	-31.0922	-78.998	2053
FZ85_99	621	-19.7383	-29.2458	-30.2603	-72.1816	2066
FZ210_17	622	-6.6913	-44.8938	-25.5962	-80.1002	2068
FZ228_75	623	-22.272	-19.4072	-29.6353	-73.5714	2068
FZ359_141	624	-18.6487	-29.8224	-28.399	-80.7928	2072
FZ395_59	625	-12.4824	-37.2107	-30.2284	-59.4375	2073
FZ121_27	626	-12.3243	-39.99	-26.4031	-80.3355	2081
FZ371_97	627	-4.8427	-45.3257	-26.735	-56.8396	2085
FZ246_7	628	-11.2734	-41.2011	-21.3921	-84.1058	2090
FZ443_78	629	2.5388	-48.1488	-21.5059	-49.6692	2096
FZ53	630	2.8121	-46.9778	-23.0059	-56.0433	2098
FZ192_40	631	-17.7954	-24.5921	-27.504	-77.0325	2108
FZ204_90	632	-12.4338	-23.1862	-28.7417	-77.5642	2112
FZ240_2	633	-12.4411	-21.0854	-28.5603	-79.1328	2113
FZ54_8	634	13.4665	-45.9557	-25.4055	-43.9675	2115
FZ42_25	635	0.0071	-41.0787	-27.7095	-37.1522	2123
FZ407_64	636	-17.5384	-34.7329	-21.009	-75.5743	2129
FZ153_90	637	-4.8267	-44.4343	-21.2669	-40.6413	2130

FZ292_25	638	-3.4152	-35.3264	-23.893	-77.7538	2144
FZ383_104	639	-7.0944	-34.686	-26.0843	-64.1516	2146
FZ262_21	789	-12.0473	-27.9951	-22.2009	-79.3365	2149
FZ52_8	791	-12.0031	-27.823	-27.4021	-52.6416	2152
FZ260_107	792	-1.2291	-41.4326	-17.9254	-47.3465	2160
FZ298_79	793	-3.778	-36.5102	-24.9363	-49.6273	2161
FZ341_79	794	-3.778	-36.5102	-24.9363	-49.6273	2163
FZ206_89	795	-1.2592	-37.7996	-19.195	-52.3302	2168
FZ218_81	796	2.8746	-38.1175	-14.6371	-48.0451	2179
FZ272_82	798	-0.2856	-37.0467	-12.2068	-53.0586	2180
FZ258_51	799	9.4193	-23.7001	-18.132	-38.2578	2230
FZ270_75	800	43.1607	-14.6264	-5.9986	-1.2922	2247